Validation of a Noninvasive Blood Perfusion Measurement Sensor

by

Alex V. Cardinali, B.S.

Thesis submitted to the Faculty of the Virginia Polytechnic Institute and State University in partial fulfillment of the requirements for the degree of

Master of Science
In
Mechanical Engineering

Dr. Thomas E. Diller, Co-advisor
Dr. Elaine P. Scott, Co-advisor
Dr. Otto Lanz

July 2002
Blacksburg, VA

Validation of a Noninvasive Blood Perfusion Measurement Sensor

Alex V. Cardinali, B.S.
Virginia Polytechnic Institute and State University, 2002
Supervisor: Dr. Thomas E. Diller/Dr. Elaine P. Scott

Abstract

This work represents the next step in the ongoing development of a system to noninvasively estimate blood perfusion using thermal methods. A combination thermocouple/thermopile sensor records heat flux and temperature measurements on the tissue of interest (in this case skin) for a given period of time. These data, in combination with other experimental parameters, are read into a computer program that compares them to a biothermal finite difference model of the system. The program uses an iterative process incorporating Gauss Minimization to adjust parameters in the biothermal model until the predicted system behavior satisfactorily approximates the real world data. The result is an estimation of blood perfusion in the tissue being measured, as well as an estimate of the thermal contact resistance between the probe and tissue. The system is tested on human forearms, canine legs during laparoscopic spay surgery, and on a canine medial saphenous fasciocutaneous free tissue flap model. Experimental measurements, especially those performed on the tissue flap model, show distinct correlation between blood perfusion and bioprobe output. This research demonstrates the accuracy of the biothermal model and the parameter estimation technique, as well as the usability of the system in a clinical setting.

Acknowledgments

I would like to thank Dr. Tom Diller and Dr. Elaine Scott for the countless hours of guidance and repeated moments of insight that helped me during the exploration presented in this work. I would also like to specially thank Dr. Diller for providing a warm spot to rest my head during hurried trips into Blacksburg. Thanks to Dr. Otto Lanz for serving on my committee, providing medical expertise in designing and performing experiments, arranging for the use of the Vet School's equipment, and for bringing an all around good nature and fun atmosphere to the project.

I would also like to thank various staff of the Mechanical Engineering Department at Virginia Tech who helped me through computer problems, graduation requirements, equipment malfunctions, and a variety of other concerns. While this is by no means a complete list, the following individuals were always willing to help, and what's better, they did it with a smile: Randy Smith, Ben Poe, Jamie Archual, Johnny Cox, Cathy Hill, Eloise McCoy.

Thank you to the Vatell Corporation for providing quick response to last minute manufacturing requests, without which the most interesting findings presented here would not have been found at all. I must thank those other souls haunting the Heat Transfer lab with me and generally putting up with me – thank you Wu, Pang, Marie, Scott and Will. And finally, a most important thank you goes out to my family and my wonderful roommates who have helped me more than they know.

Contents

List of Figures

List of Tables

Nomenclature

A,B,C,D,E	coefficients for heat flux smoothing functions
b	parameter estimates; **b**(i) = [ω_b(i), R_c(i)]
c	specific heat
h	convective heat transfer coefficient
k	thermal conductivity, counter variable
n	total number of data points
q	heat generatio
q”	heat flux
R	thermal resistance
s	sample variance
s(x)	standard deviation of a data set x
SSY	sum of the squares of the residuals between two data sets
T	temperature
$\bar{x}$	sample mean
α	confidence level
ρ	density
ω	blood perfusion

Subscripts

a	arterial
v	vein
t	tissue
b	blood
p	probe
m	metabolic
c	contact

Chapter 1 Introduction

Advances in medical diagnostic equipment have improved the ability of medical professionals to detect and treat various forms of illness and disease. Through this ongoing research and the continual improvement of patient care, the lives of many people are enhanced. Much of this progress has been localized in the development of pharmaceuticals, biomedical implants, imaging techniques, information transfer ability, remote diagnostic procedures and even robotic surgical assistance. The research outlined in this work focuses on a lesser well publicized, however important, advance in medical equipment that is expected to fill some holes left by current technology as well as open up new avenues of exploration.

The advancements presented here represent the next step in the ongoing development of a noninvasive blood perfusion sensor, referred to throughout this document as the bioprobe, at Virginia Polytechnic Institute & State University (Virginia Tech). Blood perfusion refers to the local, multidirectional blood flow through the capillaries and intracellular space of living tissue. The bulk flow of blood through the major blood vessels of the body, such as arteries and veins, is not included in this definition. Blood perfusion is a measure of the blood volume exchange per volume of tissue over time and has the units of ml/ml/s. Due to the convoluted nature of the capillaries and intracellular pathways through which this blood flow moves, blood perfusion is considered to be a directionless quantity at the macroscopic level.

Blood perfusion is an extremely important component of human physiology. Capillary and intracellular space blood flow is responsible for providing the oxygen and nutrients required by cells of the body to fuel life processes. It is also responsible for removing waste products generated by those same processes, which must be discarded to maintain the health of the system. In addition, this blood flow, and the control of it, is a chief component in the thermo-regulatory system of the human body.

The significance of blood perfusion in the normal operation of the human body makes it a useful diagnostic in many areas of medical practice. Even at the current level of development, the use of blood perfusion sensors has been explored in many arenas. Some of the more specific fields of interest are the healing of burns and skin grafts, cerebral blood perfusion in head trauma patients, prediction of organ transplantation success before closure of the body cavity,

and the detection of tumors. In each instance, researchers look for blood perfusion that differs from normal levels to determine areas of tissue damage, regions of elevated healing response, or inconsistencies in expected function.

All of the currently employed methods of measuring blood perfusion are either invasive in nature, do not produce quantifiable results, or are difficult and time consuming to use. Furthermore, the accuracy and repeatability of some of the measurement techniques are widely disputed. The development of a reliable, accurate, and quantifiable measurement system that minimally effects the tissue being measured is of prime benefit to those sciences that could use blood perfusion measurements.

The design the Virginia Tech bioprobe is centered on a combination thermocouple - thermopile sensor produced to our specifications by Vatell Corporation. The sensor, and the data acquisition equipment associated with it, records data controlled by the heat transfer characteristics of the tissue being measured. This information is then compared to a mathematical model representing the sensor and the tissue, and using Gauss Minimization, an estimate for the blood perfusion is calculated. The operation of the probe does not compromise the structural integrity of the tissue being measured, nor does it require a chemical marker of any kind. It is completely noninvasive.

The ultimate goal of the bioprobe research program is a fully functional and production ready diagnostic sensor capable of measuring blood perfusion on a continuous time scale. At the outset of the work presented here several hurdles existed in the realization of this goal. While the basic principles of operation used in the design of the probe have been proven sound, reliable and repeatable execution of the parameter estimation routine on real world data was lacking. The theoretical operation of the bioprobe lacked a significant 'proof of concept' experiment. The ability of the bioprobe to discern different levels of blood perfusion in varying conditions was in question. In addition, the bioprobe was never tested on a controllable, living environment or in a surgical setting to determine its performance in these situations. The work presented here sought to answer some of these questions.

1.1 Objectives

The main underlying goal of this research was to validate the blood perfusion measurement method employed by the Virginia Tech bioprobe. There were other secondary goals such as streamlining the parameter estimation code, determining and improving upon the measurement accuracy, development of experimental protocols, and exploring the operation of the probe in different experimental environments. However, all of these goals merely supported the desire to prove the bioprobe concept.

This document describes in detail the methods and means by which these objectives were pursued. First, background covering the wide and varied field of blood perfusion

measurement is provided for a historical, as well as consumer, perspective. This is followed by a description of the bioprobe and its associated parameter estimation routine. Next the experiments conducted during the course of this research are explained in detail. Results of these experiments, analysis of the data, and discussion of the findings follow. Finally, conclusions and recommendations based on the research conducted here are discussed.

Chapter 2 Literature Review

The significance of this research and its goals can be made most evident through comparison with other work in the field. Of prime importance are the methods of measurement employed by a variety of other blood perfusion measurement devices, the successes and advancements guiding today's research, as well as the limitations displayed by current technology.

In this chapter, a summary of the work performed at Virginia Tech is provided. This is intended to provide a historical perspective of the research performed at Virginia Tech as it relates to the bioprobe. Further details regarding the operation of the probe itself and the parameter estimation routine are included in later chapters as needed.

This literature review is intended to provide the reader with an understanding of the methods of measuring blood perfusion available at the writing of this document. A detailed and complete history of blood perfusion measurement efforts through 1998 can be found in Robinson [1]. This document focuses on advancements made since 1998 and an overall understanding of the operation and limitations of each measurement method.

2.1 Virginia Tech Bioprobe History

The first application of heat flux sensors to the blood perfusion measurement problem, and the inaugural research for the bioprobe, is described in Michener [2]. This work describes the mathematical model incorporating the Pennes bioheat equation that is the basis of operation for the sensor. Additional research and development reported by Fouquet et al. [3] and O'Reilly et al. [4] resulted in a fully functional sensor prototype.

The most recent developments are described in Robinson [1] and Scott et al. [5], from which the research presented in this document builds. Robinson explores a new sensor design as well as several variations on the parameter estimation scheme. Detailed assessment of the parameter estimation program sensitivity to different variables is included.

2.2 Other Blood Perfusion Measurement Efforts

The importance of blood perfusion measurement to medical and other scientific communities is best illustrated by the number and variety of systems currently being researched. The large

number of measurement schemes also points to the difficulties found in the field. Each of the current technologies has at least one aspect that prevent it from being the ideal blood perfusion measurement system. The main areas where problems are encountered are measurement accuracy, invasiveness, ease of use, and the ability to make continuous measurements.

Laser-Doppler Flowmetry (LDF)

LDF makes estimates of blood perfusion by measuring the Doppler shift in a laser source directed into perfuse tissue. The laser light is reflected off of moving red blood cells and observed by a detector. The probe measures the change in frequency of the reflected laser light and determines a corresponding blood velocity. Two methods for measuring tissue are available. A single site measurement technique continually monitors the same skin area for the desired amount of time. In LDF perfusion mapping, multiple single point measurements are made over an area of tissue and a two dimensional map of perfusion is made. This method is also known as Laser Doppler Imaging (LDI).

The main benefit of LDF based measurements systems is that they are generally noninvasive and, in fact, do not alter the environment that they are measuring. One exception to this is a technique proposed by Scalise et al [6] that uses a self-mixing laser diode to measure the velocity of blood in an artery or vein. A catheter specially fitted with the self-mixing laser diode is inserted directly into the desired blood vessel for measurement. This method greatly reduces the invasiveness typically associated with making these kinds of measurements using ultrasonic or electromagnetic sensors applied directly to the blood vessel.

However, there are many difficulties associated with LDF technology. By its nature, LDF makes velocity measurements in only one direction. If the direction of flow is not in line with the measurement direction, something that is impractical to determine, then absolute and quantifiable measurements cannot be made. Another problem is that LDF is highly sensitive to the optical properties of the tissue being measured. These properties vary both from patient to patient as well as directionally within the same tissue. For these reasons, LDF is used only to make relative measurements of changes in blood flow in the tissue it is measuring. Other issues such as a high sensitivity to movement, a high operational cost, a lack of portability, and susceptibility to interference with other equipment [7] make the method less than ideal.

There is ongoing research attempting to improve the usability of LDF systems. Forrester et al. made measurement of tissue properties in conjunction with LDF measurement that could make it possible to accurately compare LDF output from two different test subjects [8]. A method for determining penetration depth of the system was proposed and explored by Liebert et al. using a multi-channel laser probe [9].

Doppler Ultrasound (DU)

DU measurement systems operate similarly to LDF systems. However, DU uses the Doppler shift in an acoustic wave to determine the perfusion level in the tissue being measured. And although there are advantages to using DU such as deeper tissue penetration and insensitivity to the optical properties of skin, the DU method has other problems such as a high sensitivity to measurement artifacts (wave interference, small muscle twitches, variations in blood pressure, probe movement) that prevent it from becoming a clinically useful tool.

Thermal Diffusion Probe (TDP) Measurement

Pioneered by Valvano et al. [10] and Bowman [11], a TDP uses a self-heated thermistor to measure perfusion in real time. The probe is inserted into the tissue being measured and is heated to a prescribed level above the local tissue temp (typically about 0.2 ºC). The probe then monitors how much power is required to keep its temperature at the prescribed offset. The theory is that for higher levels of blood perfusion, more power will be required to maintain the temperature difference. This method works very well and is capable of making accurate measurements of tissue perfusion, although it is more successful at higher flow rates.

The two main drawbacks that currently plague these systems are their inability to respond accurately to low flow rates and the invasive nature of the probe.

Positron Emission Tomography (PET)

PET scans can be used to make measurements of blood perfusion, but requires the introduction of a radioactive tracer into the blood supply. As the tracer travels through the tissue of interest it emits radiation as part of its normal decay. Detectors located around the area of interest measure these radioactive particles. While accurate measurements can be made with PET, this method is time consuming, requires the injection of a foreign substance into the body, and is incapable of making continuous measurements.

Magnetic Resonance Imaging (MRI)

MRI methods can make measurements of blood perfusion in a fashion similar to PET. Instead of using a radioactive tracer however, MRI 'marks' the blood by magnetizing it with an external magnetic field before it enters the tissue of interest. The magnetization in the tissue of interest in measured and compared to a control area that is not magnetized to determine the amount of blood flowing through the tissue.

This method of measuring blood perfusion is capable of accurate measurements, however it requires the use of very expensive and bulky equipment.

Chapter 3 Bioprobe and Parameter Estimation

This chapter outlines the design of the Virginia Tech bioprobe as it was used in this research. The fully functional blood perfusion bioprobe consists of two main components: a sensor with its related data acquisition equipment used to gather information and a parameter estimation code written in FORTRAN that analyzes the recorded data and predicts the blood perfusion.

The physical design of the probe (shown in Figure 3.1) and the data acquisition set up remain largely unchanged as they are presented in Robinson [1]. Therefore, it is introduced here for the record but without the historical decisions involved in the design. Any changes made to the design that cause it to differ from that presented in Robinson, such as the use of a new thermocouple -thermopile sensor, are noted and explained in more detail.

There have been, however, extensive changes to the parameter estimation routine during the course of this research. These changes and the reasons for their implementation are discussed in this chapter. Also provided is a summary of new programs that were written to aid in the preparation of raw data for the parameter estimation routine and the presentation of output in a graphic format. All of the computer programs discussed here can be found in Appendix A included at the end of this work.

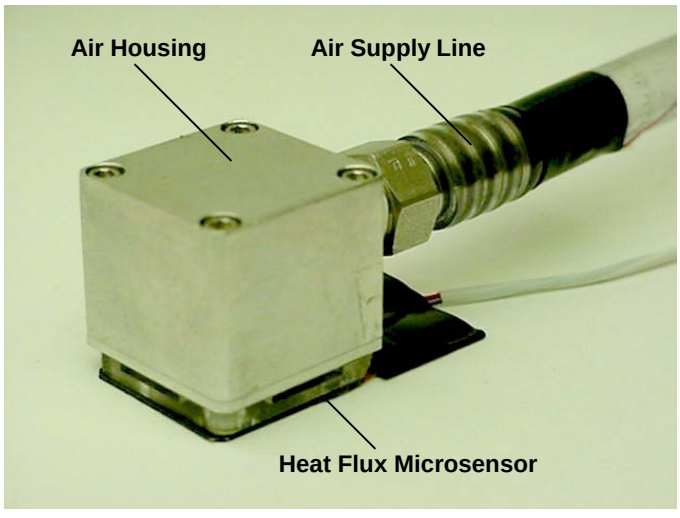

Figure 3.1: The bioprobe showing the major physical components

3.1 Bioprobe

Sensor A

Sensor A denotes the exact sensor used in Robinson [1] as it was found at the beginning of this research. It's design centers around a 206-junction thermopile manufactured by Vatell Corporation. This nickel and copper thermopile is arranged in a circular pattern, 1.91 centimeters in diameter, on an anodized aluminum substrate base. The overall dimensions of the sensor are 2.97 by 2.95 by 0.006 centimeters.

Modifications were made to the Vatell thermopile to create the bioprobe sensor. A thin piece of aluminum foil was attached to one side of the sensor with high conductivity paste to create an isothermal layer over the thermopile. A type E thin-foil thermocouple was also mounted on the surface of the sensor on the same side as the aluminum foil. This allows the sensor to make temperature measurements of the skin during experiments.

Throughout the course of this research problems were encountered with Sensor A shorting out and producing useless output. Some of these problems were solved with reinforcement of the connection of the sensor leads to the isothermal junction box (see data acquisition setup). In other instances, the wires near the sensor were adjusted manually until a usable signal appeared. The returning signal never contained a detectable offset or distortion in sensitivity, so accurate measurements were always possible when the sensor was working. In retrospect, it was concluded that the thermopile was beyond its predicted lifetime and a separation of the layers comprising the thermopile were probably to blame for the problems encountered. In spite of these difficulties, Sensor A was used successfully in a number of the experiments included in this work.

Near the end of the experimentation phase, Sensor A failed completely and was determined unfixable. In order to continue taking measurements, a new sensor was contracted from Vatell. Unfortunately, the thermopile sensor that acted as the foundation for Sensor A is several generations behind the current sensors available through Vatell. Therefore an exact reproduction could not be made.

Sensor B

The replacement sensor (Vatell 1040 Episensor B04X), referred to as Sensor B, is similar in shape and size to the previous one but does retain slightly different physical and performance characteristics. A comparison of the physical properties of both sensors is shown in Table 3.1. A schematic of the two sensors is provided in Figure 3.2.

Due to the smaller size of the new sensor, care is needed in positioning the sensor under the air housing. Also, the thermopile is not centered on the substrate of the sensor. In fact, it is located nearer to the edge opposite the leads requiring an offset position relative to the air housing.

Table 3.1: Comparison of Sensor Properties

Property	Sensor A	Sensor B
Length (cm)	2.96	2.55
Width (cm)	2.94	2.53
Thickness (cm)	0.06	0.05
Sensitivity ($mV/W/cm^2$)	6.33	1.18

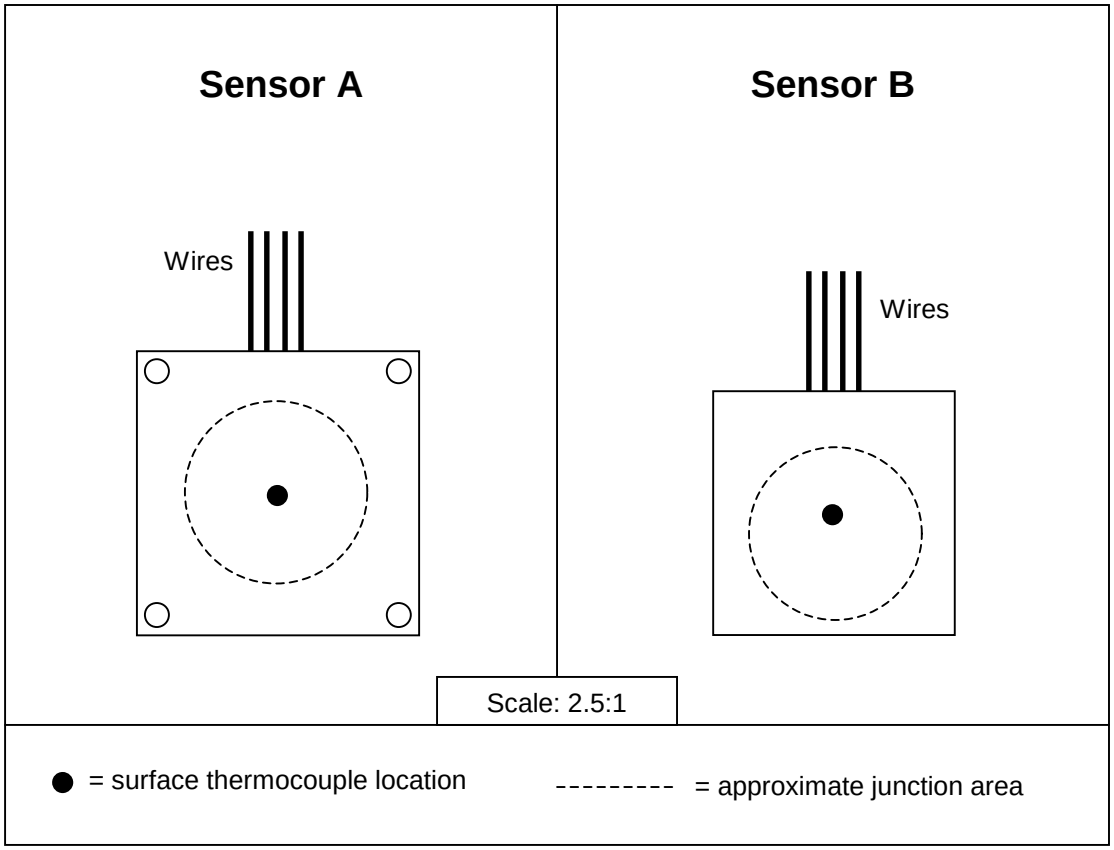

Figure 3.2: Comparison schematic showing the two sensors on an equal scale. The size difference is evident. It can also be seen how the junction layout in sensor B is off center and not aligned with the surface thermocouple.

Air Housing

The air housing delivers room temperature air to the back of the sensor with a carefully designed air-jet plenum. The plenum creates impinging jets that improve the heat transfer coefficient on the back of the sensor, and therefore increases overall heat transfer through the system. This effectively improves the sensitivity of the bioprobe to temperature disturbances in the tissue below.

The air supply provided to the air housing was maintained at 138 kPa throughout all tests reported in this work. Air pressure was controlled with the in-wall pressure valve connected to the building air system in Randolph Hall during the human forearm tests. Unfortunately, there was no air system in the surgical suite used for the dog experiments. Therefore, in all the dog tests, a two-stage regulator (Airco model 806 8454) connected to a nitrogen tank provided the required airflow.

Data Acquisition

A Pentium Pro Dual processor computer serves as the base for the DAQ system. A Keithley DAS-TC board is installed to condition and convert the heat flux and temperature signal output by the bioprobe. The board performs the required A/D conversion of the incoming signal as well as the cold junction linearization of the thermocouple output. The thermopile and surface thermocouple of the bioprobe wire directly into an isothermal junction box that is then connected to the DAS-TC board with a shielded ribbon cable.

Test Point software is installed on the computer to control the data acquisition process. The DAS-TC board outputs a temperature in Celsius and a voltage signal representing the heat flux measured by the thermopile. Test Point converts the voltage signal into a heat flux value according to the sensor's sensitivity coefficient and records it with the temperature signal in an ASCII file. It also provides real time graphs of the bioprobe output.

Air and Arterial Temperature Measurement

The temperature of the cooling air was monitored using a type-T thermocouple connected to a Doric Trendicator 410A thermocouple reader. During tests with sensor A, the thermocouple was located inside the air housing. However, when shorting problems arose with the switch to sensor B, the thermocouple was moved into the air supply line just in front of the air housing.

Arterial temperature measurements made during the human forearm tests were made with another type-T thermocouple inserted under the subject's tongue. During canine tests the subject core temperature was monitored with an oral temperature probe.

3.2 Biomodel

The biomodel that represents the tissue-probe system was first developed by Michener [2] and later expanded by Robinson [1]. The code, written in FORTRAN, consists of a semi-infinite finite difference model of the probe and underlying tissue that uses an alternating direction implicit method of solution.

The key aspect of this program is the use of the Pennes bioheat equation to represent the energy balance of the tissue. This equation (3.1), and in the reduced form used in the code (3.2), has a transient term that accounts for blood flow into the tissue:

$$\left(\rho c_p\right)_t \frac{\partial T_t}{\partial t} = k_t \nabla^2 T_t + \left(\rho c_p \omega\right)_b \left(T_a - T_v\right) + q_m \qquad \text{Eq. 3.1}$$

$$\left(\rho c_p\right)_t \frac{\partial T_t}{\partial t} = k_t \nabla^2 T_t + \left(\rho c_p \omega\right)_b \left(T_a - T_t\right) \qquad \text{Eq. 3.2}$$

where T_t is the temperature of the tissue, T_a and T_v are arterial and venous temperatures, respectively, q_m symbolizes metabolic heat generation, ω_b is the blood perfusion rate and $(\rho c_p k)_t$ and $(\rho c_p)_b$ are the respective thermal properties of tissue and blood. The reduced equation assumes that metabolic heat generation in the tissue is negligible and that the tissue temperature reasonably approximates the venous temperature.

This equation is a 'rough estimate' of the actual environment it represents. It does not take into account nonhomogeneities in tissue properties or the effects of nearby major blood vessels. However, it is this very characteristic of the equation that makes the Pennes bioheat equation applicable to a variety of situations without the need for detailed information about the tissue being measured.

The sensor is modeled as homogenous flat plate with constant physical properties. The representative equation is similar to the Pennes equation but without the heat generation and perfusion terms:

$$\left(\rho c_p\right)_p \frac{\partial T_p}{\partial t} = k_p \nabla^2 T_p \qquad \text{Eq. 3.3}$$

where T_p is the probe temperature, and $(\rho c_p k)_p$ are the thermal properties of the probe.

The model contains two independent unknown variables. The first is the blood perfusion term, ω_b, included in the Pennes bioheat equation. The second is the thermal contact resistance, R_c, between the probe and underlying tissue. This contact resistance will vary from test to test according to the amount of pressure applied to the bioprobe, the presence of air between the sensor and tissue, the amount of hair underneath the probe, and a variety of other factors. The

other variables required to solve the model (air temperature, skin temperature, arterial temperature) are recorded during experimentation.

Thermal Constants

The model requires thermal physical properties of the tissue being measured (in the case presented here, skin). Instead of requiring further experiments to determine properties for each test subject, reported averages were taken from literature for skin tissue conductivity and thermal diffusivity [12] and specific heat [13] as reported in Robinson [1]. The property values used in this research are summarized in Table 3.2.

Also required are the thermal properties of the sensor. Those determined by Robinson [1] are still in use and are listed in Table 3.3 below. These properties were kept when analyzing data gathered with Sensor B. It was assumed that the two sensors had similar properties.

Table 3.2: Thermal Tissue Properties

Property	Value
Blood Density (kg/m$^{3)}$	1000.0
Blood Specific Heat (Jkg/K)	4000.0
Skin Conductivity (W/mK)	0.50
Skin Diffusivity (m^2/s)	1.5 x 10^{-7}

Table 3.3: Probe Thermal Properties

Property	Value
Density (kg/m^3)	2021.6
Conductivity (W/mK)	177.0
Specific Heat (J/kgK)	875.0
Diffusivity (m^2/s)	1.00 x 10^{-4}

3.3 Parameter Estimation Routine

The parameter estimation code compares the recorded heat flux data to an estimate predicted by the biomodel to solve for blood perfusion term in the Pennes bioheat equation. A flow chart describing the process is shown in Figure 3.3. The model is initially solved using guesses for the two driving unknown parameters, blood perfusion and contact resistance. This numerical solution is then compared to the data set gathered using the sensor. The code determines how closely correlated the estimated solution is to the experimental data and then, if it is not satisfactorily accurate, makes changes to the initial parameter estimates and repeats the solution. This continues until the system behavior predicted by the biomodel accurately matches the recorded data set.

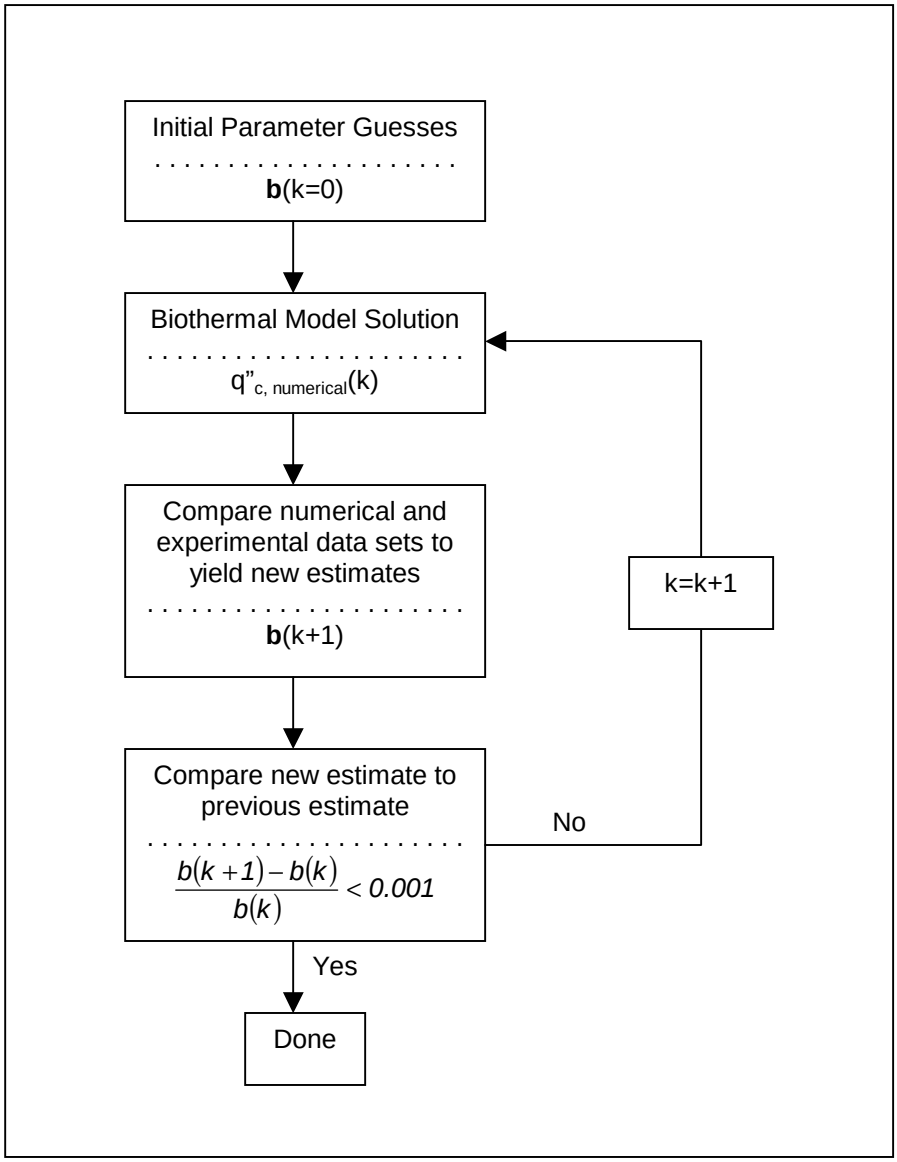

Figure 3.3: Flowchart of the parameter estimation process. The model is first solved using the guessed values for blood perfusion and contact resistance (**b**(0)= [ω_b(0), R_c(0)]). The solution continues until two sequential parameter estimates are sufficiently close.

Heat Flux Curve Characteristics

The heat flux curves (experimental and numerical) have a very distinct shape that is governed by effects of the two unknown parameters. There is an initial peak at the beginning of the data set when the cooling air is first turned on. This peak heat flux gradually decays as the system approaches steady state. Contact resistance dominates the first few seconds of system response [1]. Different values of blood perfusion show little effect to the timing, size, or shape of the heat flux spike. Conversely, after the first few seconds of data (>20 s), the system is insensitive to changes in contact resistance and the blood perfusion value dominates the response [1]. These trends become important when analyzing the data, as will be explained in Chapter 5.

3.3.1 Alterations and New Code

Box Kanemasu Modification

Experiments outlined in Robinson [1] showed that the Box-Kanemasu modification to the Gauss minimization process did not positively affect the accuracy of the solution. Due to its superfluous nature and the increased computation time it necessitated, the modification was removed from the program.

Heat Flux Calculation

One major modification to the existing code was related to the calculation of the heat flux used in the parameter estimation procedure. The heat flux in the finite difference model can be calculated between any two nodes in the mesh when the temperature is known at the two nodes in question. There are three specific calculations of heat flux that are interesting in observation; convective heat flux at the surface of the probe (q''_c), conductive heat flux through the thermopile (q''_p), conductive heat flux across the contact resistance between the surface of the tissue and the probe (q''_{Rc}). These are depicted graphically in Figure 3.4.

In the program left by Robinson, q''_{Rc} was used as the calculated heat flux in the parameter estimation routine. It is theorized that this is not an accurate representation of what the thermopile in the bioprobe is measuring. This heat flux drastically under predicts the magnitude of the initial spike in the heat flux curve and maintains some offset over the typical experimental data set time (60 s). While somewhat accurate solutions can be found by weighting out the influence of the beginning data, using this heat flux adds error into the blood perfusion estimate.

Changes were made to the code so that the heat flux used in the parameter estimation procedure is calculated using the top and bottom nodes in the sensor. This effectively calculates q''_p, which is a more accurate representation of the thermopile output. However, heat flux

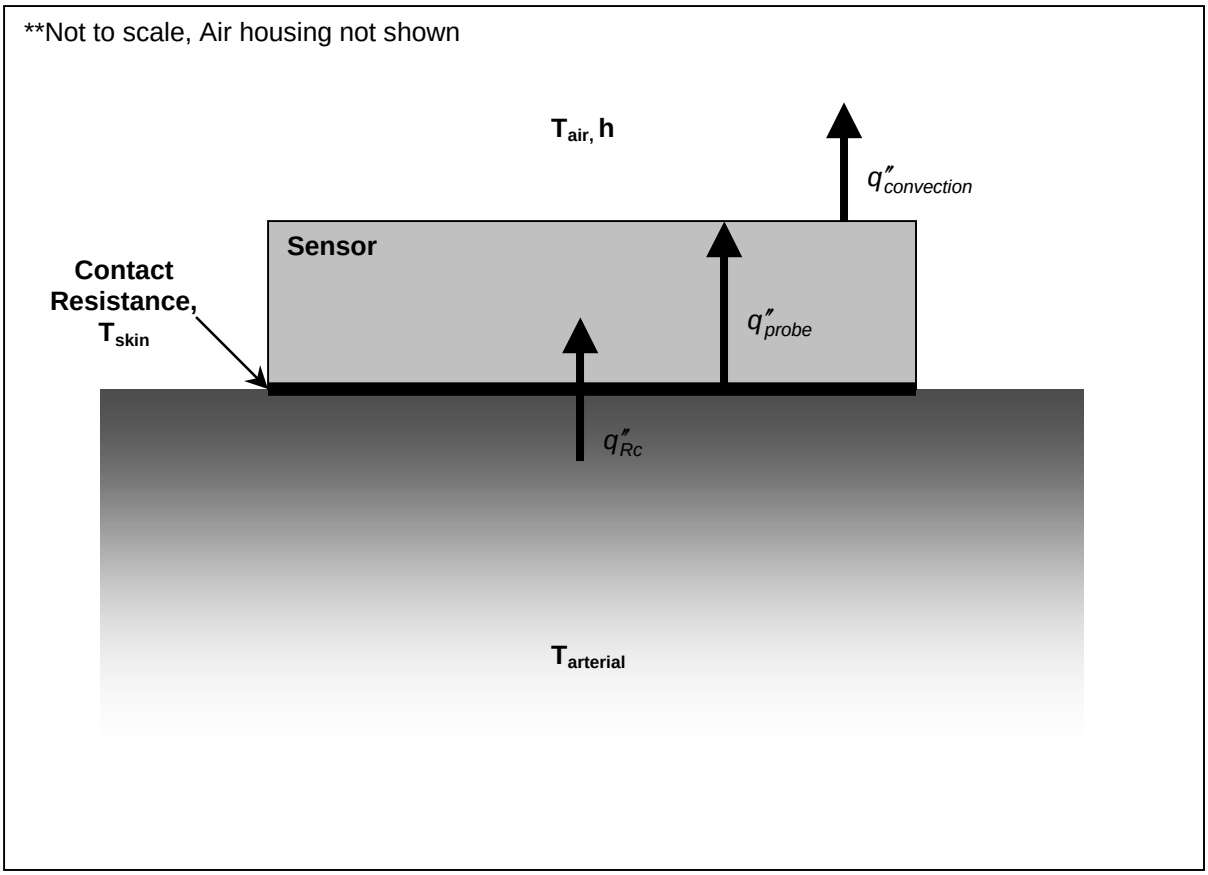

Figure 3.4: Schematic depicting the three different ways to calculate heat flux in the system.

calculated in this way shows damped oscillatory effects that eventually die out completely over time. Expectedly, this oscillation associated with q''_p is contained within bounds represented by q''_c and q''_{Rc} as shown in Figure 3.5.

An explanation of this unstable behavior can be found in Robinson [1]. The oscillatory nature of the semi-implicit finite difference method is dependent on the ratio of thermopile sensor model thickness to the size of the time step used. Since the sensor thickness is fixed, a non-oscillatory solution can be determined by lowering the time step size. Robinson showed that the time step would need to be reduced to 1/400 s to achieve such a solution. This very small time step would require increased computation time (about 40x) for a model solution that is already time intensive. In order to use q''_p convergence in the parameter estimation routine, another method of removing the unstable oscillations was needed. It was decided to smooth the heat flux by mathematical manipulation using a time-averaging routine.

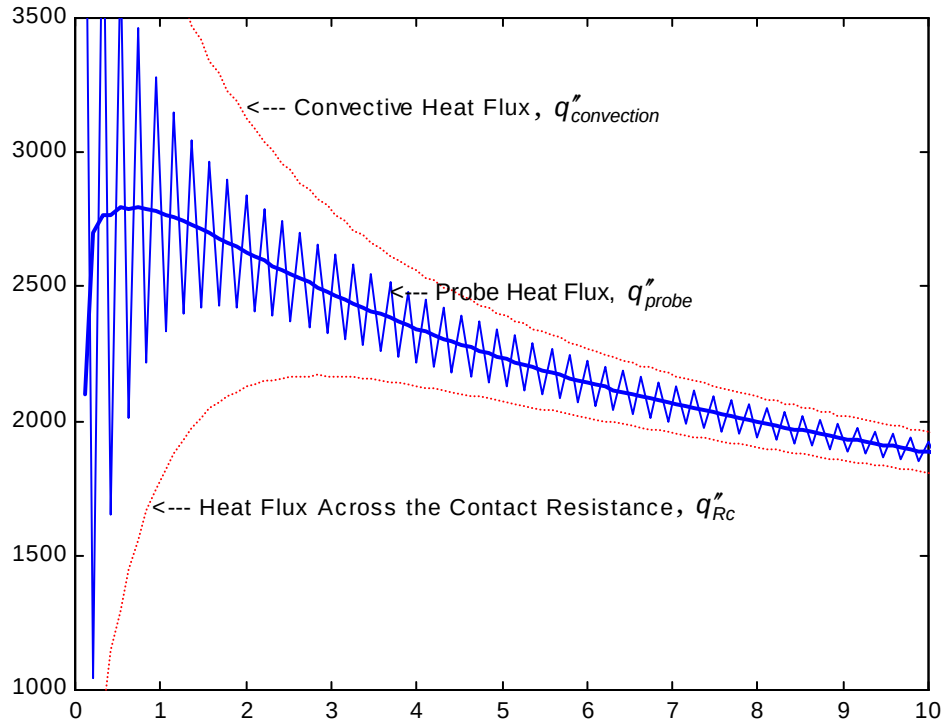

Figure 3.5: Close up of the predicted heat flux curve as calculated at three different points in the biomodel. This figure clearly illustrates the oscillatory nature of the thru-probe heat flux before smoothing and the shape produced after smoothing.

Code Restructuring and Heat Flux Averaging

In order to employ a smoothing routine, it was necessary to modify the order of solution in the original parameter estimation routine. The old code solved the biomodel simultaneously as the parameter estimates were being calculated. That is to say, for every iteration of the estimation routine the temperature field of the biomodel was solved for each time step. At the end of each time step, the desired heat flux was calculated and then compared to the recorded data set to find the residual. These residuals were added up for the entire time domain and the magnitude of the sum determined how much the parameter estimates are altered before the next iteration of the biomodel is solved. Once the residual for that particular time step was calculated, the heat flux was output to a data file but not stored within the program. The variable was simply overwritten during the next time step. The problem that this scheme created was that it prevented the use of a time based smoothing function as desired. The program cannot smooth data with respect to time without having the heat flux over the whole domain (or the number of time steps used in the smoothing function) available. More importantly, accurate residuals cannot be calculated until the oscillations have been removed from the heat flux being explored.

The solution was to rearrange the code so that for each iteration of the parameter estimation routine the biomodel was solved for the whole time domain. The calculated heat flux was stored in a new array representing the entire domain, the data set was smoothed, and finally the residuals are calculated before the new parameter estimates are determined. This resulted in vast reorganization of the existing code, including the addition of some new elements, however it retains the original model coded by Michener [2] and improved by Robinson [1].

The method of smoothing q''_p was a five-point time averaging of the data set. The averaging equations are shown below:

$$q''_s(1) = \frac{C * q''(1) + D * q''(2) + E * q''(3)}{(A + B + C + D + E)}$$

$$q''_s(2) = \frac{B * q''(1) + C * q''(2) + D * q''(3) + E * q''(4)}{(A + B + C + D + E)}$$

$$q''_s(i) = \frac{A * q''(i-2) + B * q''(i-1) + C * q''(i) + D * q''(i+1) + E * q''(i+2)}{(A + B + C + D + E)} \qquad \text{Eq. 3.4}$$

$$q''_s(n-1) = \frac{A * q''(n-3) + B * q''(n-2) + C * q''(n-1) + D * q''(n)}{(A + B + C + D)}$$

$$q''_s(n) = \frac{A * q''(n-2) + B * q''(n-1) + C * q''(n)}{(A + B + C)}$$

where $q''_s(i)$ is the ith term in the smoothed heat flux array, $q''(i)$ is the ith term in the oscillating data set, n is the total number of data points, and A,B,C,D,E are coefficients with the values shown in Table 3.4.

Table 3.4: Finalized Smoothing Function Coefficients

Coefficient	Value
A	0.10
B	0.25
C	0.30
D	0.25
E	0.10

The best coefficients were chosen through trial and error. A non-oscillating 20 s heat flux data set was calculated using a time step of 1/408.5 s as described by Robinson [1]. An oscillating 20 s data set using the same input parameters and a time step of 1/9.5 s was

calculated and compared to the non-oscillating data set. Test smoothing functions were applied to the oscillating set and then the result was compared to the non-oscillating set both visually and by calculating the correlation coefficient between the two sets of data (every 408.5/9.5=43rd data point in the non-oscillating set was used). Seven-point and three-point averaging solutions were also tried, but the five-point solution was found to be the most accurate.

A comparison of the non-oscillating set with the smoothed oscillating set using the finalized coefficients is shown in Figure 3.6. The graph clearly shows that the smoothed set closely matches the non-oscillating data set (correlation coefficient = 0.969). There is still a bit of oscillation present in the smoothed data set, but it has been greatly reduced. There is also some error in the first and last data points, but this is to be expected using time-averaged data and does not have a significant effect on the operation of the parameter estimation code.

Code Variations for Experimental Air Supply Conditions

Two versions of the biomodel and parameter estimation routine are available. One routine (Airflow_Parameter_Estimation) contains an added DO loop to vary the convection coefficient at the beginning of the test. This is required because tests conducted in the Heat Transfer Laboratory use the Randolph Hall building air supply. The response of this air pressure when turned on at the beginning of a test is not instantaneous. In fact, there is a lag between 0.5-1.5 seconds for each test. Since the airflow does not begin at it's steady state rate, it is theorized that a similar lag in the convection coefficient is created. Varying the convection coefficient in the biomodel allows for a more accurate representation of the real world phenomena.

In addition to the added DO loop, there is a slight restructuring in the code. The convection coefficient at the top of the probe is included in some of the matrix coefficients used in the non-dimensional finite difference model. A stable convection coefficient allows the matrix coefficients to be calculated once and used for all time steps. A convection coefficient that changes with time, however, requires that the matrix coefficients be recalculated for every time step. This adds to the total computation time of the model, but it does result in more accurate performance of the estimation routine.

By comparison, tests in the Virginia-Maryland Regional School of Veterinary Medicine used nitrogen tanks to supply the cooling 'air' to the sensor. These tanks did not have the air pressure lag associated with the Randolph Hall building air supply. Therefore, the model used to predict the blood perfusion and contact resistance in these tests (Parameter_Estimation) has a steady convection coefficient and steady matrix coefficients. This model performs well and is a bit quicker in operation than that found in Airflow_Parameter_Estimation.

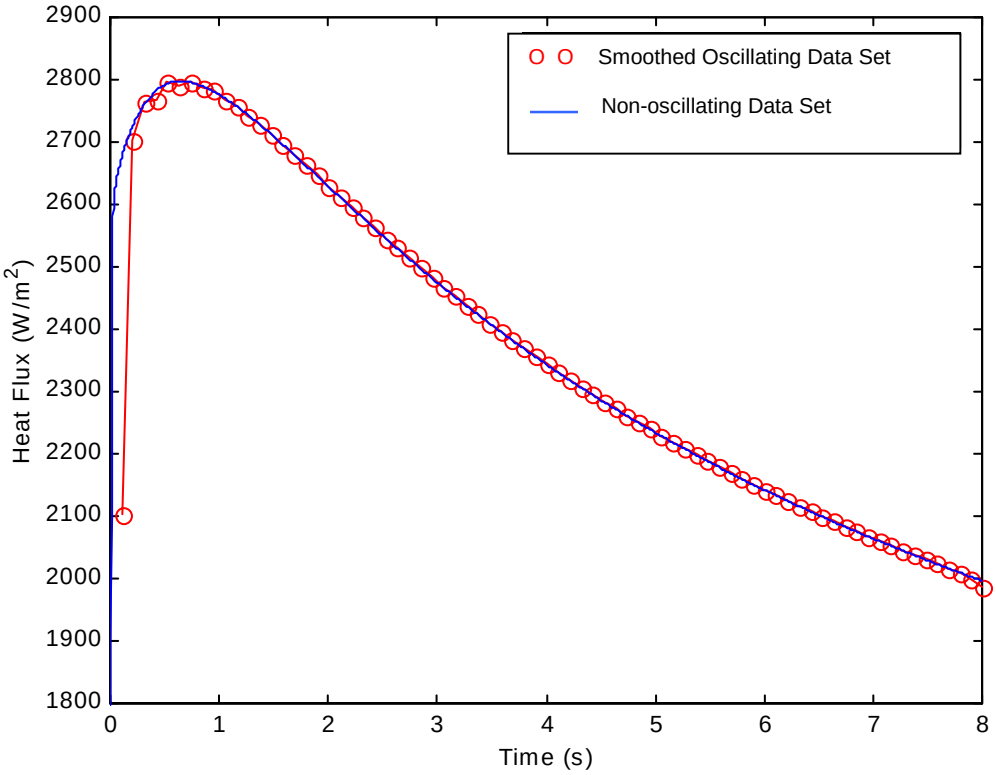

Figure 3.6: Comparison of a non-oscillating data set (time step < 1/400 s) to a smoothed oscillating set (time step = 1/9.5 s). The oscillations that were removed can be seen clearly in Figure 3.1.

Input and Output Files

Alterations were made to the input files used with the parameter estimation routine to allow for greater control over the model without making changes to the actual code. Each input file contains a header that contains information relevant to the biomodel. While the structure of this header file is similar to that presented in Robinson [1], some additions to the model input were made. In previous versions of the biomodel, the arterial temperature was assumed to be a constant 37.0 °C. As it was discovered that an accurate measure of arterial temperature was integral to good performance of the biomodel (and thus, the parameter estimation routine) it was deemed a necessary input into the code. Also, it was desired to test different size variations of the finite difference mesh of the biomodel. To simplify this process, the parameters controlling mesh size are also included in the input header. These tests revealed no need to change the standard values used in Robinson [1]. However, it is anticipated that different size sensors will be used with the parameter estimation routine in the future and the optimization of the finite difference mesh will need to be repeated so this aspect of the code remains in tact.

An example of a standard input file with a description of the header format and required values is included with this work in Appendix C.

Data Output and Processing

Several subprograms were written in Matlab to handle the processing of the parameter estimation output and the creation of the input data files. All of the plots presented in this document were made using these Matlab programs. Short descriptions are included below in Table 3.5, however, the fully commented programs are available in Appendix A. All of these m-files were written to be compatible with Matlab versions 5 or newer.

Table 3.5: Helpful Matlab programs

File Name	Description
Datasort.m	Reads in the ASCII file generated by Test Point and formats it into an input file readable by the parameter estimation program. Asks for experimental and model variables to be defined and trims away excess data before the beginning of the desired data set.
Estcomp.m	Reads the output file generated by the parameter estimation routine and plots a comparison of the converged biomodel solution with the experimentally recorded data.
Smoothitcomp.m	Reads in two output files generated by the parameter estimation routine and plots them together. Also calculates ssy for the two data sets as well as a correlation coefficient.
Oscillationcomp.m	Reads a biomodel simulation output file and generates graphs showing all four calculated heat fluxes (convective, unsmoothed thru-probe, smoothed thru-probe, contact resistance) on the same set of axes.

Chapter 4 Experiments and Procedures

During the course of this research, many tests were executed to explore different aspects of the parameter estimation program in an effort to improve its performance. These exploratory tests are far too numerous to be explained in detail. The experimental procedures that follow are the result of many trial and error experiments seeking to determine the format that provides the most repeatable and accurate method. The procedures outlined here are similar to those implemented by Robinson [1].

The experiments presented in this work can be divided into two major categories: human forearm tests and dog tests. The human forearm tests can be further subdivided into restricted blood flow, normal blood flow, and increased flow tests, while the dog experiments include uncontrolled and controlled perfusion experiments.

This chapter includes a discussion of the methods and procedures used during each of the experiments conducted as well as the expected significance of each type of test.

4.1 Experimental Procedures

4.1.1 Human Forearm Experiments

All experiments conducted on live human subjects were performed according to the same procedure as outlined here. In some experiments, attempts were made to affect changes to the subject's skin perfusion rate through normal physiologic processes without invasively interacting with the test subject. The goal of these experiments was to show that the bioprobe could in fact measure a change from normal blood flow in a given subject and do it with sufficient repeatability. Therefore, measurements of resting or unaffected blood perfusion were made before the perfusion change was attempted.

General Experimental Procedure

All of the human tests were performed on the subject's forearm. The placement of the bioprobe was chosen on a relatively flat part of the forearm away from excessive hair and any major visible blood vessels. The probe was held in place by hand with enough pressure to assure good contact with the tissue beneath but light enough that the skin was not indented.

After the probe was placed, it was allowed to reach equilibrium with the tissue. This was determined by observing the real-time heat flux and temperature curves output by Test Point and waiting until the curves leveled off. In most cases, equilibrium was achieved in one or two minutes. Waiting for equilibrium ensures an accurate measure of the skin temperature below the probe. When the values were reasonably constant over time, data logging was initiated and then the cooling air turned on. For approximately one minute the temperature and heat flux signals were recorded by the data acquisition system. Data logging was then terminated and the cooling air shut off.

The temperature of the cooling air was measured by a type-T thermocouple located in the air housing connected to a Doric Trendicator 410A thermocouple reader. Since a time-based signal of this measurement was not recorded, air temperature at the beginning and end of the experiment were noted. The subject's core temperature was measured in similar fashion with a thermocouple inserted under the tongue just before each experiment.

Restricted Flow Measurements

Several tests were attempted using an inflated blood pressure cuff to restrict blood flow to the subject's forearm. This was intended to simulate a low perfusion situation. The only change to the experimental procedure was the addition of cuff placement and inflation before the general procedure outlined above. For a subject with normal systolic and diastolic blood pressure, an inflation pressure of 160 mm Hg was used.

One of the main experimental problems with this test arrangement is that restricting blood flow to a limb for the amount of time needed to accurately perform these tests becomes painful for the test subject. Including setup and waiting for the system to reach equilibrium with the actual test time means that the subject is required to endure in excess of 3 minutes of restricted blood flow. Due to the painful nature of these tests, they were abandoned early in the testing phase, before the final experimental procedure was developed. Therefore, no results from these tests are presented in this work.

Increased Flow Measurements

The method chosen for creating an increased blood flow environment in the test subject was light exercise aimed at the muscles under the chosen measurement site (forearm). Before beginning the general test procedure, the test subject performed several sets of push-ups and then squeezed a spring loaded grip exerciser for approximately five minutes. The grip exerciser was then continually used on the test arm while the system reached equilibrium, but use was terminated before data logging began. It is theorized that the increased muscle activity in the upper body, and specifically the forearm being tested, would increase the blood flow to the area.

The goal of this experiment is to determine if the bioprobe can measure a difference in blood perfusion before and after exercise.

4.1.2 Canine Experimental Procedure

The canine experiments performed during the course of this research were intended to provide another venue to test the ability of the bioprobe to detect different levels of blood perfusion. This area of the research was performed in conjunction with the Virginia-Maryland Regional School of Veterinary Medicine and Dr. Otto Lanz.

In the first three groups of tests, I was allowed to record data during three laparoscopic spay surgeries already scheduled by the Vet School. The fourth and fifth test sets (skin flap experiments) were designed specifically to test the bioprobe under different blood flow conditions. All of the tests were performed on the rear leg of the test subject. All of the dogs were fully anesthetized during the surgeries and were completely unconscious before bioprobe testing began.

Spay Tests

Similar tests during laparoscopic spays were performed on three separate occasions in the Vet School on subjects already scheduled for surgery. The goal of these tests was to gain experience with the bioprobe in a surgical setting and record data. However, it should be noted that no attempts to control or affect perfusion were made.

The probe was placed on the surface of the inside rear leg to record data on a site that had been shaved clean. In these tests, the sterile boundary enveloped the area on the subject's leg where the probe was placed. Only fully sterilized personnel are allowed to intrude on the sterile boundary, so it was required that the bioprobe be set up and left undisturbed during the course of the surgery.

To preserve the orientation of the bioprobe housing with the sensor, the sensor was attached using plastic adhesive tape. The tape was applied in such a way as to create an even layer across the surface of the probe in contact with the skin. Then the sensor and housing were placed on the chosen test site and held in place using surgical cloth tape. The surgical tape was wrapped around the subject's leg with care being taken to apply just enough pressure to hold the probe in place.

This is a small departure from the standard procedure where the bioprobe is held in place by hand, however, it was necessary given the situation and was expected to add little distortion to the data recorded. It was expected that the contact resistance estimate would absorb the thermal effect of the plastic adhesive tape.

Data sets were recorded at intervals of seven minutes from the beginning of one test to the next. The three surgeries lasted approximately 50-60 minutes each and resulted in six or seven data sets.

Skin Flap Experiments

Two sets of experiments, designed in conjunction with Dr. Otto Lanz and the Virginia-Maryland Regional School of Veterinary Medicine, were performed using a canine medial saphenous fasciocutaneous free tissue flap model. The tissue flap is a method of harvesting skin to replace damaged or removed skin on another part of the patient's body. In the experiments described here, the flap was excised to the point that its only vascular connection to the body was the single artery and vein in the medial saphenous neurovascular bundle. The flap is then reattached to the body leaving the artery and vein exposed. This set up allows for experimental control of the perfusion to the area of skin being measured by 'shutting off' with microvascular clamps. The method of harvesting the skin flap presented below is a standard medical procedure. The description that follows was adapted from Lanz [14].

Preparation of the Skin Flap [14]

Approval for the use of the dogs in this study was obtained from the Virginia Tech Animal Care Committee. The dogs were considered to be healthy based on physical examination, complete blood count, biochemical profile, and urinalysis.

Each dog was premedicated with acepromazine (0.02 mg/kg, IM) and morphine sulfate (0.25 mg/kg, IM). After placement of an indwelling cephalic catheter, anesthesia was induced with propofol (6 mg/kg, IV). Dogs were intubated and anesthesia was maintained with isoflurane in 100% oxygen. Lactated Ringer's solution was administered IV at a rate of 10 ml/kg/hr. A 20-gauge catheter was then placed in a lingual artery for direct arterial blood pressure measurement. All animals were ventilated with a volume-controlled ventilator (Ohmeda, 4700 Oxicap Monitor, Louisville, CO). Tidal volume was kept at 10 ml/kg and the respiratory rate was adjusted to maintain the end tidal (ET) CO_2 between 34 and 41 mmHg. Heart rate, respiratory rate, direct arterial pressure, ET CO_2 levels, and body temperature were monitored throughout the entire procedure.

The right pelvic limb was clipped and prepared for sterile surgery. Each dog was placed in right lateral recumbency to allow surgical access to the medial femorotibial area of the right pelvic limb. A sterile marker was used to outline the proposed dimensions of the medial saphenous fasciocutaneous flap. The anatomic borders of the flap were the proximal 1/3 of the right medial thigh to the proximal 1/3 of the medial tibia and from the patella to the popliteal lymph node.

Baseline measurements of the undisturbed tissue were taken at this point. A surgical technician held the bioprobe in place and several sets of data were taken at prescribed intervals. After completion of the baseline readings the flap was dissected. During flap elevation a deep plane of dissection at the level of the sartorius and gracilis muscles was maintained to preserve the small cutaneous vascular branches that arborize from the larger saphenous vessels. The medial saphenous neurovascular bundle was identified and isolated proximally to the level of the femoral artery and vein. Vascular branches from the medial saphenous vessels were ligated and divided as they entered the sartorius and gracilis muscles. Care was taken to preserve the tissues immediately surrounding the medial saphenous neurovascular bundle. At the distal aspect of the flap the cranial and caudal branches of the medial saphenous artery, vein, and nerve were ligated and divided. After elevation of the island flap the flap was sutured back to the adjacent skin edges with 3-0 glycomer 60 (B. Braun Surgical Ltd., Neuhausen, Germany) in a simple interrupted intradermal pattern followed by skin staples for skin closure. The proximal aspect of the flap was left open to allow access to the proximal portion of the medial saphenous neurovascular bundle.

With the flap reattached, several more measurements of the skin flap were taken. The flap was then occluded using microvascular clamps. Two clamps were applied to the exposed femoral artery leaving the femoral vein open to drain the flap. The femoral vein was then blocked with a clamp. The bioprobe was applied to the skin flap and several measurements were made.

Next, the clamps were removed to restore blood flow to the flap. In the first skin flap experiment, measurements were begun after the flap was reperfused. In the second flap experiment, data were recorded as the blood supply to the skin flap was opened, to determine if the bioprobe would be able to detect the immediate change in tissue perfusion. In both cases, after several measurements were taken, the flap was fully sutured back in its original position and stapled. Several more data sets were recorded on the reattached flap. The surgical site was then protectively dressed and the dog brought out from the effects of the anesthesia.

Chapter 5 Results and Discussion

The method of data reduction presented in this chapter is the result of an untold number of trial experiments performed using the bioprobe. During the course of becoming familiar with the operation of the probe and testing improvements to the parameter estimation routine, as outlined in Chapter 3, many variations on solution method were experimented with. Nearing the end of the research presented here, the most reliable method of solution was applied to previous data sets so that all results are attained in the same manner. This allows the comparison of trends in different data sets without adding the unknowns associated with using different methods of solution.

It is important to point out that the only data recorded with Sensor B are those taken during the second flap study. Unfortunately there is no direct or controlled method of comparing the responses of Sensors A and B to the same conditions. However, the analyses presented in this chapter are more geared towards trends in the data sets rather than absolute measurements or the accuracy of the measurements themselves.

It is necessary to understand that there was no quantified measure of blood perfusion available during the experimentation phase. Without the availability of another blood perfusion measurement system making accurate results, there is no way to know the real value of blood perfusion being measured. Therefore, it is impossible to make any claims as to the repeatability of measurements from test to test, or to even argue for or against measurement accuracy, without making large and non-verifiable assumptions. In spite of these difficulties, it is still possible to glean very convincing evidence of the sensitivity of the Virginia Tech bioprobe to blood perfusion.

This chapter first explains some of the discoveries encountered during research and testing that resulted in changes to experimental procedure and data analysis, followed by the details of the final analysis scheme. The remainder of the chapter is dedicated to the analysis and discussion of the experimental data for each group of tests.

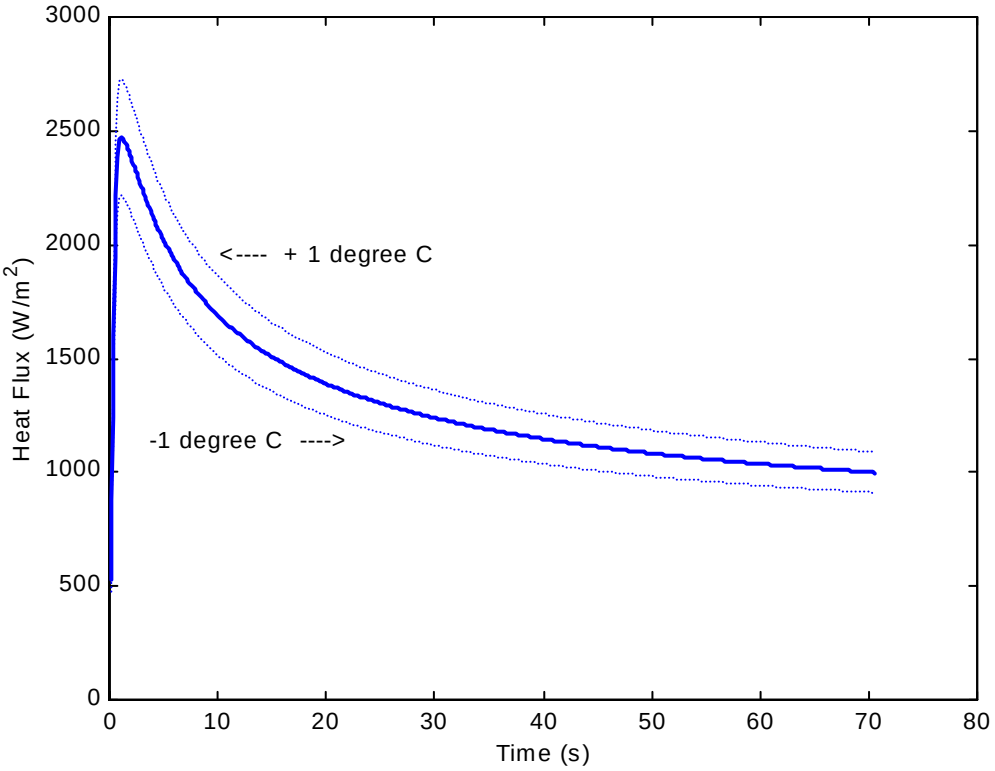

Figure 5.1: Variation of biomodel output with input skin temperature. One degree of variation in skin temperature has a profound effect on the heat flux predicted by the biomodel.

5.1 Procedural Discoveries

Temperature Measurements

The discussion presented in Robinson [1] on sensitivity of the biomodel to different variables dealt with previous versions of the biomodel and bioprobe. While the general trends that were observed remain true for the current version, the magnitude of a given parameter's influence on model output is somewhat different.

The sensitivity of the biomodel to the initial skin temperature and air temperature is tremendous. Slight inaccuracies in these measurements create an offset in the predicted response of the biomodel. Figure 5.1 shows a typical heat flux signal created with ordinary parameter values. Two other heat flux signals are shown for comparison. They were created using the same input parameters as the first data set, however the skin temperature was increased by 1 °C for one data set and decreased by 1 °C in the other. It is clearly evident that a large bias is created. Decreasing air temperature by 1 °C and increasing it by 1 °C has exactly the same effect on output. This error translates directly to the accuracy of the estimates

generated by the parameter estimation routine. If the measurement error is large enough, the biomodel will not be able to find a satisfactory solution.

For this reason, ensuring the accuracy of the air and skin temperature measurements is extremely important. It is necessary to wait for the bioprobe to reach equilibrium with the tissue being measured. The skin temperatures presented with the data in this document are considered accurate. There is, however, some inaccuracy in the air temperature measurements. During every experiment reported here, air temperature varied with time. While constant values for air temperature were used during the analyses presented here, it would be worthwhile to mathematically approximate the variation of air temperature for these experiments and re-estimate blood perfusion and contact resistance in each case. There are three different reasons why variation in air temperature was observed.

In the Heat Transfer Laboratory in Randolph Hall, the design of the building's pressurized air supply will inevitably lead to temperature variations in the air. The building system is very large and is continually renewing/maintaining its pressure. It draws ambient air in from the outdoor environment. Simple things such as nuances in the operation of the system and, to an extent, usage and outdoor temperature will create disturbances in the temperature of the output air from day to day and even during the span of several tests.

The experimental setup of the dog test leads to a different problem. The use of a sealed nitrogen tank as the air supply creates severe temperature changes as the tank is emptied and the internal pressure changes. Variations in output temperature of more than 10 °C in the air stream were not uncommon.

The third cause is common to all tests. In between tests, the air in the supply line leading to the air housing has a chance to increase in temperature as it is exposed to the ambient environment or is heated by the test subject. On some of the recorded data sets, a second rise after the initial heat flux peak is clearly evident. An example of this is shown in Figure 5.2. It was determined that this second rise correlated to the time when the air line was cleared of the warmed up stagnant air and the pressurized air (from the building or nitrogen tank) finally reached the sensor.

In all of the data analysis presented here, the air temperature at the end of the experiment was used as the input to the parameter estimation routine. Since accuracy is desired in the blood perfusion estimate, and this is achieved best by accurately fitting the final portion of the heat flux curve, using the final air temperature was decided as the best option.

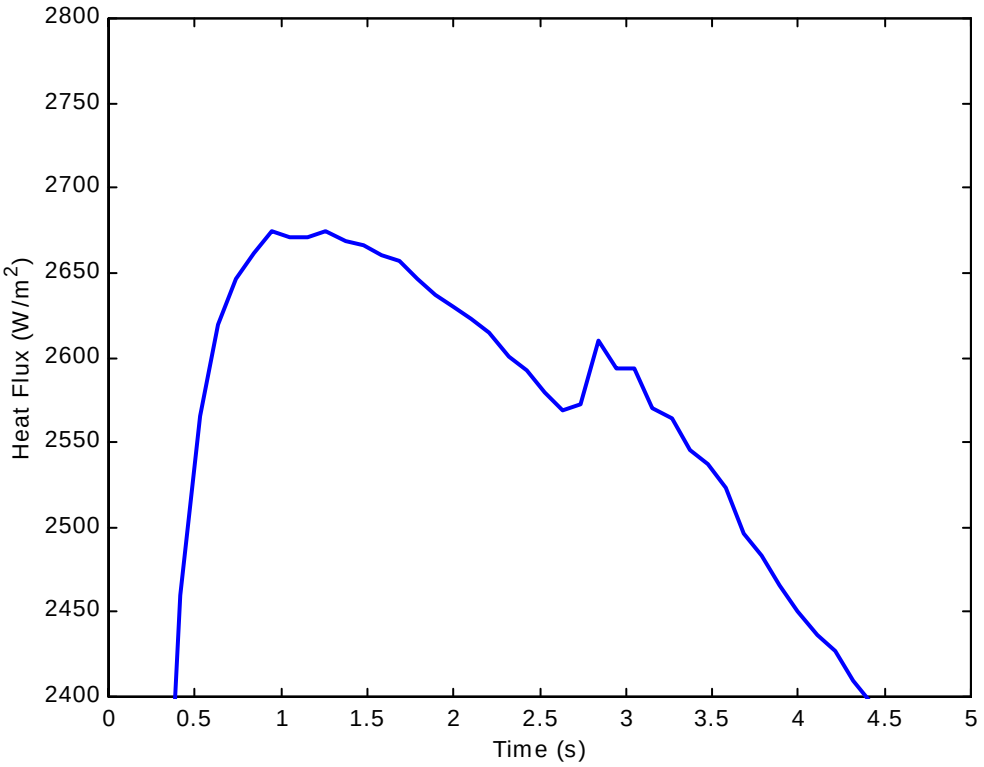

Figure 5.2: Close up of experimental data recorded in the Heat Transfer Laboratory in Randolph Hall using the building air supply to cool the probe. A second spike in the data set resulting from cooler air hitting the bioprobe is clearly visible.

Weighting of the Heat Flux Data

Analysis for many of the data sets resulted in adequate convergence of the parameter estimation routine, but with a model output that did not adequately predict the heat flux curve recorded during experimentation. This resulted in confusing trends in predicted blood perfusion values in experiments that were not expected to have much variation. The estimation program is designed to find the best fit to the experimental data based on both of the independent parameters, blood perfusion and contact resistance. Since the biomodel is an approximation of the system being measured, there are bound to be differences when comparing recorded data to the estimated data. The problem is that these residuals are minimized over the entire time domain. Since the beginning of the curve is effected most by contact resistance and the final seconds of the response are dictated by blood perfusion, the error in estimation is spread equally between both parameters.

In order to maximize the accuracy of the blood perfusion estimate, the parameter estimation routine can be made to favor correlation with the second half of the heat flux curve. In

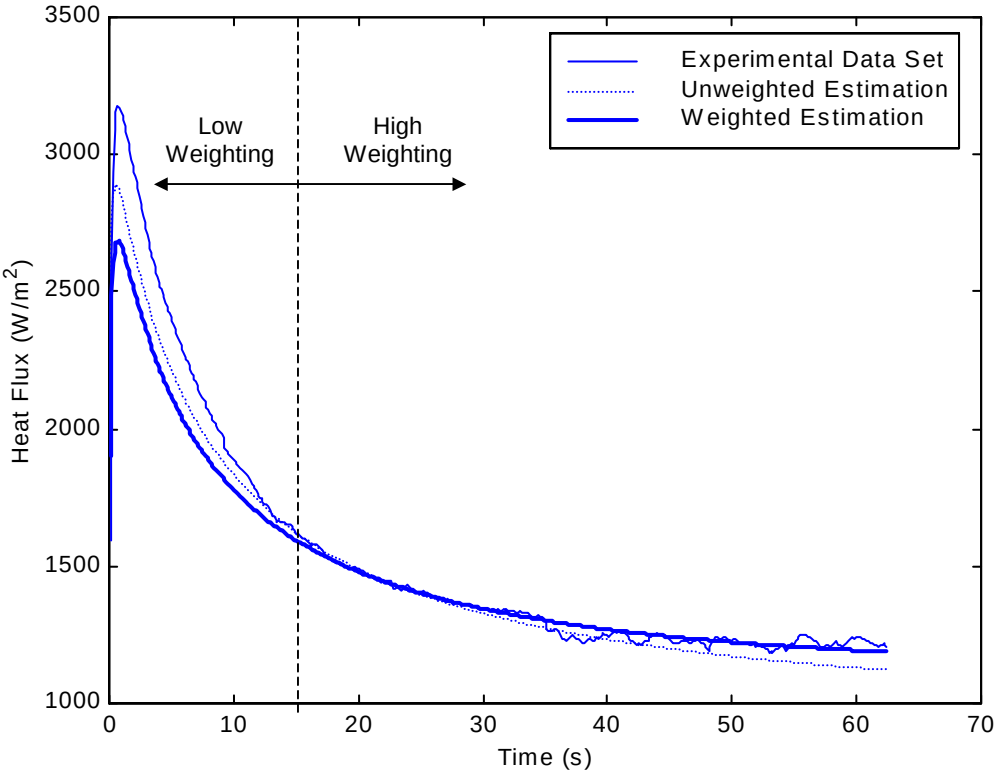

Figure 5.3: Comparison of weighted vs. non-weighted estimation. It can be seen that a model using parameters estimated with a weighted variance better estimates the final 25 seconds of the experimental data set.

the parameter estimation routine, the program determines how far away the estimated curve is from the recorded curve by calculating the following sum:

$$SSY = \sum_{i=1}^{n} \frac{\left(q''_{experimental} - q''_{calculated}\right)_i^2}{s\left(q''_{experimental}\right)} \qquad \text{Eq. 5.1}$$

where $q''_{experimental}$ is the experimentally recorded heat flux data, $q''_{calculated}$ is the numerically approximated heat flux, $s\left(q''_{experimental}\right)$ is the variance of the experimental heat flux data set, and n is the total number of data points.

The magnitude of the SSY variable at the end of each iteration of the parameter estimation routine determines how much the parameter estimates are altered for the next iteration. By decreasing the variance after a desired i-th data point, the SSY sum becomes more sensitive to changes in the latter portion of the heat flux curve. In the research presented here, the variance was weighted after 15 seconds by a factor of 1000. This effectively makes the

second half of the curve 'more important' and pushes the parameter estimation code towards a more accurate blood perfusion estimate. A graphic comparison of weighted vs. non-weighted estimation can be found in Figure 5.3. While the weighted estimate produces more error than the non-weighted estimate in the first part of the curve, the negative effect is constrained to the accuracy of the contact resistance estimate. The trade off is closer correlation with the experimental data during the final 25 seconds of the heat flux curve, as is clearly visible in the comparison plot. It is theorized that this results in a more accurate prediction of blood perfusion by sacrificing accuracy in the contact resistance estimate.

Uncertainty Analysis

It is important to understand how uncertainty in the recorded data affects the parameter estimates. All measurements inherently contain some level of error. Any solution based on those measurements must thereby have some uncertainty in it. In a case where multiple variables are used in the solution, the influence of the uncertainty in each must be accounted for. In the case presented here, it is assumed that there is an uncertainty of ±2°C for each of the three temperature measurements (air temperature, skin temperature, arterial temperature) and a ±5% uncertainty in the heat flux measurement. These values are based on the collective experience of the heat transfer group at Virginia Tech.

The cumulative effect on the parameter estimates for blood perfusion and contact resistance can be estimated mathematically [15]

$$u_y = \left[\sum_{i=1}^{n} \left(\frac{\partial y}{\partial x_i} u_{x_i} \right)^2 \right]^{1/2} \qquad \text{Eq. 5.2}$$

where y is the estimated parameter, x_i are the measured variables, n is the number of measured variables, u_{x_i} are the measurement uncertainties in the measured variables, $\frac{\partial y}{\partial x_i}$ are the sensitivities of the blood perfusion estimate to each of the measured variables, and u_y is the approximated uncertainty in the blood perfusion value.

The uncertainty in the parameter estimates can be approximated by estimating the sensitivities in Eq. 5.2

$$\frac{\partial y}{\partial x_i} \cong \frac{\Delta y}{\Delta x_i} \qquad \text{Eq. 5.3}$$

where Δx_i are the changes in the measured variables and Δy are the resulting changes to the estimated parameters.

The idea is to create a baseline data set using known values for the measured variables. Then each of the input variables are individually perturbed (the others remain at the baseline values) and the parameter estimation routine is run compared to the baseline data. This generates new parameter estimates that are compared to the baseline inputs to determine Δy for both blood perfusion and contact resistance. In this way, the amount of change to the parameter estimates caused by fluctuations in each input parameter can be approximated

This scheme was carried out using a baseline data set created using the input parameters ω_b = 0.001 ml/ml/s and R_c = 0.001 m^2K/W and the variable values listed in Table 5.1. Perturbation values equal to a 0.5% disturbance were applied to each variable and new parameter estimates generated. In the case of the heat flux value, the entire data set was multiplied by 1.005 before re-estimating the parameters. This analysis uses values from the end of the heat flux curve for calculation.

Results of the analysis are also shown in Table 5.1. The majority of the uncertainty in the parameter estimates comes from the heat flux measurement. We are most concerned with accuracy in the blood perfusion estimate. With the baseline blood perfusion value chosen as 0.001 ml/ml/s, the total estimated uncertainty of 3.23×10^{-4} ml/ml/s represents a 32% uncertainty in the blood perfusion estimate. This may seem high, but because the uncertainty is a weak function of the blood perfusion value, the percentage of uncertainty decreases proportionately with larger values of blood perfusion. Longer measurement times or better heat flux measurements would also decrease uncertainty.

Table 5.1: Uncertainty Analysis Summary

Variable x	Baseline Value	u_x	Δx	$\omega_b(x+\Delta x)$	$R_c(x+\Delta x)$	$\Delta\omega_b$	ΔR_c	$(\Delta\omega b/\Delta x*u_x)^2$	$(\Delta Rc/\Delta x*u_x)^2$
q''	NA	5%	0.5%	0.00103	0.00096	0.00003	-0.00004	9.00E-08	1.60E-07
T_{skin}	32 °C	0.2 °C	0.16	0.00094	0.00112	-0.00006	0.00012	5.63E-09	2.25E-08
T_{air}	22 °C	0.2 °C	0.11	0.00105	0.00092	0.00005	-0.00008	8.26E-09	2.12E-08
$T_{arterial}$	37 °C	0.2 °C	0.19	0.00098	0.00100	-0.00002	0.00000	4.43E-10	0.00E+00
							Parameter Estimate Uncertainties	**ω_b**	**R_c**
								3.23E-04	**4.51E-04**

Interference Problems

During the spay tests (sensor A), an ultrasonic scalpel was used during the procedure. The scalpel is powered to cut at the desired time by applying pressure to a foot pedal. It was noticed during these tests that the output of the thermopile was strongly affected by the harmonic scalpel. In fact, when the scalpel was powered to cut, Test Point recorded a signal identical to an open circuit for the thermopile channel. The thermocouple channel remained unaffected.

It is not evident where the source of the problem lay, whether it be in the sensor, the leads, etc. However, it is strongly suggested that since the thermocouple channel was not affected, the problem should be traceable to exposed wires or the thermopile itself.

It is still possible to use data corrupted in this way. In cases where data were influenced by the use of the scalpel, the interference signal was removed from the data set and replaced with a linear curve fit.

Location of Air Temperature Thermocouple

In the previous version of the bioprobe, a hole exists in the air housing to allow for the insertion of a thermocouple to make measurements of air temperature. This method worked without incident until sensor B was used with the air housing. An electrical short developed between the thermopile in the new sensor and the thermocouple in the air housing, causing distortions to the measurements. Several methods of insulating the undesired circuit connection were tried, however the best result was achieved when the thermocouple was moved out of the air housing. A tiny hole was made in the air supply line, just before the air housing, and the thermocouple inserted to midstream and glued in place. No further problems with a short circuit were encountered.

5.2 Human Forearm Test Results

The results of the increased perfusion experiments are summarized in Table 5.2. Parameter estimates converged in every case. The numerical solutions correlate well to the experimental data sets with an average SSY value of 0.2. Plots of the recorded data with the estimated solution are shown for every case in Appendix B.1.

The average blood perfusion estimate for the resting data sets was 0.00045 ml/ml/s. Compare that to the average blood perfusion estimate of 0.00103 ml/ml/s for the exercise experiments and it appears that the bioprobe was able to detect a difference in blood flow after the subject exercised. However, a more rigorous treatment of the data was desired.

These data sets were further explored with a statistical analysis. A comparison of means was performed treating the three resting experiments as one group and the five exercise

experiments as the other group. A normal data distribution was assumed and various confidence intervals were calculated for the two data sets using the student's t in the formula:

$$\bar{x} \pm t(\alpha / 2; n-1)\frac{s}{\sqrt{n}} \qquad \text{Eq. 5.2}$$

where $\bar{x}$ is the sample mean, α determines the level of confidence, s is the sample variance, and n is the number of observances in the sample.

The data sets do not become fully separated until just under a 70% confidence interval is used. What this means is that we can say with no more than 70% certainty that measured mean perfusion values of the two sets of tests are different. This is actually quite a favorable result, considering the number of causes of variation in the measurements.

Table 5.2: Data Summary of Increased Perfusion Experiments – 07.11.2001

Data Set	Time (min)	$T_{arterial}$ (°C)	T_{air} (°C)	T_{skin} (°C)	Bp (ml/ml/s)	Rc (m^2K/W)	SSY
rest1	0	36.2	23.4	33.1	0.00048	0.00046	0.173
rest2	5	36.2	23.4	32.2	0.00068	0.00032	0.111
rest3	10	36.5	23.4	31.8	0.00019	0.00057	0.293
Average Values for Resting Measurements					0.00045	0.00045	0.192
work1	20	36.4	23.0	32.0	0.00161	0.00049	0.214
work2	25	36.2	23.1	32.9	0.00126	0.00032	0.160
work3	30	36.4	23.1	32.8	0.00043	0.00002	0.159
work4	35	36.5	23.0	33.0	0.00112	0.00028	0.332
work5	40	36.6	23.0	33.2	0.00074	0.00014	0.186
Average Values for Exercise Measurements					0.00103	0.00025	0.210

All data sets were taken on the same individual, on the same location. Experimental and estimated data sets are plotted in Appendix B.1

5.3 Dog Experiments

Spay Testing

The results of the spay test are summarized in Table 5.3. The three different sets of experiments are noted by *adog*, *bdog*, and *cdog*. Parameter estimates converged in every case, however, in several of the *bdog* data sets blood perfusion converged to a value of 0.0 ml/ml/s. The numerical solutions correlate well to the experimental data sets in the adog and cdog groups. Several of the data sets in the bdog group have unexpected shape characteristics in their recorded heat flux making accurate convergence of the parameter estimates difficult or impossible. Plots of the recorded data with the estimated solution are shown for every case in Appendix B.2.

An example of the unexpected shape found in most of the bdog data sets is shown in Figure 5.4. It is expected that the large dip coincides with movement of the probe during the

experiment. A large enough move could effectively change the contact resistance and change the response of the system. Also, these measurements were made with Sensor A, and the anomalies could be caused by the shorting problems described earlier. In spite of these difficulties, some of the parameter estimates produce a curve that closely correlates to the experimental data set for the final portion of the curve. In these cases, the estimates for blood perfusion are still considered reliable. Those data sets where the estimated curve does not correlate well with the end portion of the recorded data set are considered unreliable and are noted as such in Table 5.3.

Trends in the blood perfusion estimates for each group of tests (*adog, bdog, cdog*) are represented graphically in Figure 5.5. The first twenty minutes of *adog* data correspond well with the usable data from the *cdog* experiment. Very similar values for blood perfusion are predicted in both cases. The uncorrupted data sets from the *bdog* experiments also appear to be in agreement, however it is bit more difficult to determine without the rest of the data sets.

Table 5.3: Spay Test Experimental Results

Data Set	Time (min)	$T_{arterial}$ (°C)	T_{air} (°C)	T_{skin} (°C)	Bp (ml/ml/s)	Rc (m^2K/W)	SSY
adog data recorded: 7.19.2001							
adog1	0	35.70	20.35	32.95	0.00929	0.00352	0.241
adog2	10	35.60	20.45	32.56	0.01038	0.00371	0.269
adog3	20	35.60	19.65	32.36	0.00849	0.00390	0.379
adog4	30	35.40	19.65	32.21	0.00620	0.00328	0.558
adog5	40	35.40	19.45	32.28	0.01054	0.00339	1.501
adog6	50	35.20	19.35	32.39	0.01540	0.00313	0.199
adog7	63	35.20	19.05	32.84	0.01878	0.00301	0.273
bdog data recorded: 7.24.2001							
bdog1	0	36.00	22.60	34.39	0.00646	0.01070	0.847
bdog2	10	35.40	21.50	33.38	0.01270	0.00914	0.544
† bdog3	23	35.28	21.50	33.43	0.00000	0.00737	2.296
bdog4	33	35.22	21.40	32.84	0.00496	0.00856	0.180
† bdog5	43	35.06	20.60	32.82	0.00000	0.00479	65.650
† bdog6	53	35.00	20.30	32.62	0.00000	0.00122	270.491
bdog7	63	35.00	20.10	32.67	0.00034	0.00884	1.217
cdog data recorded: 7.26.2001							
cdog1	0	34.44	22.50	30.82	0.00768	0.00249	0.195
cdog2	10	34.28	21.90	30.43	0.00909	0.00345	0.353
cdog3	18	34.06	21.60	30.48	0.01167	0.00415	0.610

† These data sets have more variation than others in the same test. The cause of the added noise is unknown at this time, however it is important enough to call question to these data sets. Therefore, these data sets are regarded as being of questionable experimental accuracy. Plots of the data sets are available in Appendix B.2.

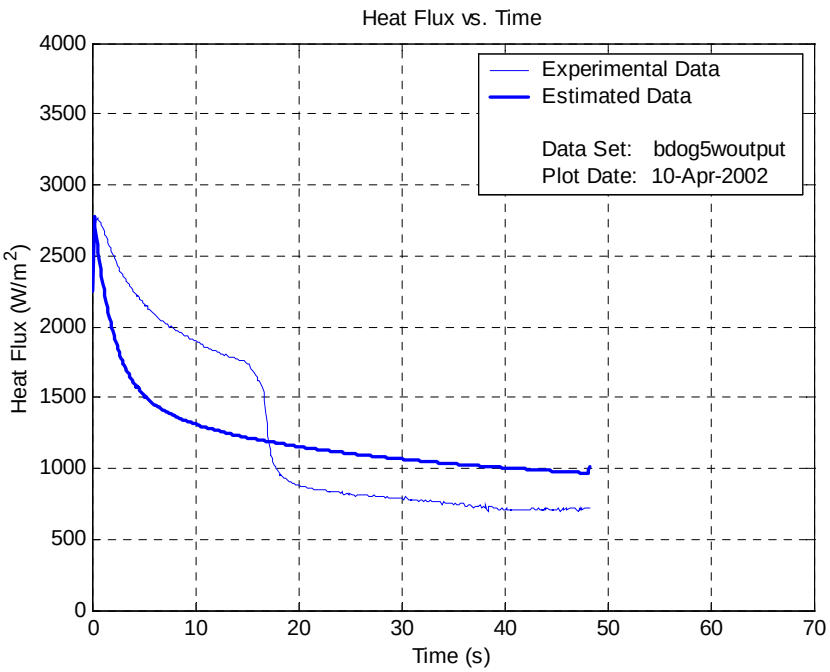

Figure 5.4: Example data set showing the unexpected shape of the recorded heat flux data set in some of the bdog tests. This shift is expected to come from movement of the probe during measurement.

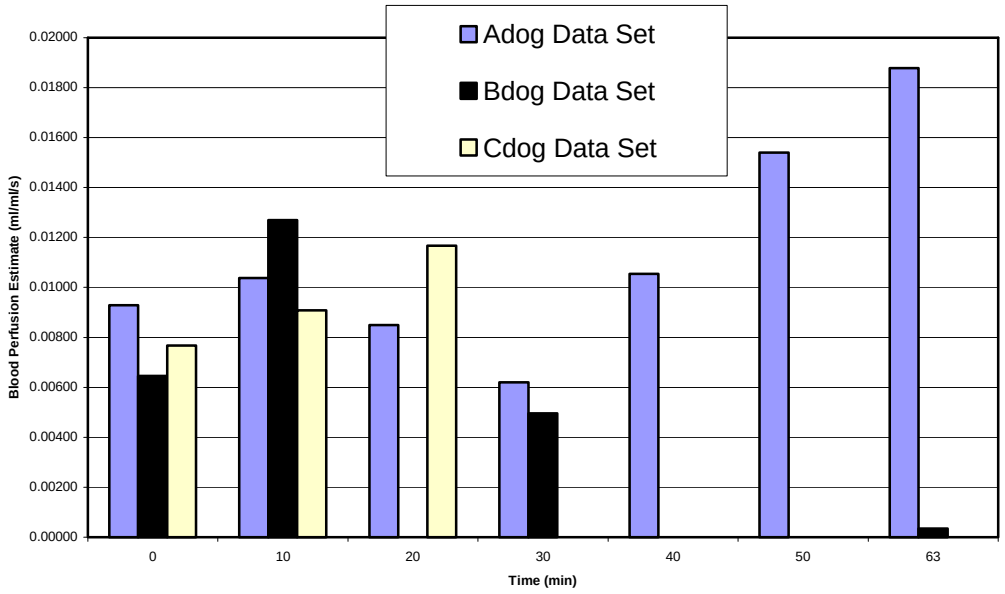

Figure 5.5: Plot of the blood perfusion estimates versus time for the three spay tests. No discernable pattern common to all three tests is evident.

Skin Flap Tests

The estimated parameters for the skin flap experiments are summarized in Tables 5.4-5. Every data set recorded in the first study converged successfully. In the second study, the first fourteen data sets converged, but there were problems with the remaining data sets (not including bflap17). Also in the second flap experiment, several of the recorded data sets contained a large amount of noise. Although it has not been confirmed, it is expected that this noise arose from movement of the probe. Severe enough movement would create a change in the thermal contact resistance, thereby changing the output of the sensor. As the current biomodel is not equipped to deal with varying contact resistance, these data sets, and their estimates, are considered unreliable. Plots of the blood perfusion estimates with time are shown in Figures 5.6-7 (the unreliable data sets are not included).

The data recorded during the first skin flap experiment correlate well with the expected physiological behavior of the skin flap site over the course of the procedure. The pre-surgery estimated values for blood flow to the surgical site are relatively uniform. This would be expected for undamaged tissue on a test subject under the effects of anesthesia. Once the surgical procedure to excise the flap is performed, and with the blood flow to the flap in tact, the bioprobe predicts a sharp drop in flap blood flow that lasts between 4 and 10 minutes. This is then followed by an increase in blood flow to the area in excess of that measured before surgery. It is theorized that the initial trauma creates a generalized vasoconstriction upstream from the flap diverting blood flow away from the injured skin area. The following increase in predicted blood flow is in accordance with the expected wound healing response [7]. Blood flow to the traumatized tissue is increased to promote recovery.

After the artery-vein pair is occluded there is a decrease in predicted flow to the skin flap. Although the magnitude of this change is not less than that predicted just after the excise of the flap, the decrease in flow is pronounced when compared to data recorded just before the blocking of the blood supply. The subsequent unblocking of the flow resulted in a marked increase in predicted blood perfusion as expected. Full reattachment of the skin flap to the surgical site resulted in another increase in estimated perfusion. It is possible that this further increase could be the result better contact between the excised flap and the body (more heat from the body is transferred into the flap from the body) or could be the result of improved circulation due to the flap being stretched to its preferred shape.

After completion of the first skin flap experiment, analysis of the data prompted changes to the experimental protocol. It was desired to see if patterns that were observed between the different flap orientations would continue, or become more pronounced, at longer times. Each subgroup of tests in the experiment (pre-surgery, flap excised no occlusion, flap excised occluded) were expanded to include more sets of data over a longer period of time. Data from

the second flap experimental set is listed in Table 5.5. Perfusion estimates versus time are shown graphically in Figure 5.7.

The change in protocol resulted in several difficulties that arose during the second flap experiment. The constant removal of nitrogen from the pressurized tank caused its temperature to continually decrease throughout the course of the experiment. While this did occur in the first skin flap experiment as well, the lower number of tests with the blood supply occluded prevented a problem from developing. In the second experiment, the flap was chilled to the point that it suffered a severe ischemic response. It did not recover during the remainder of the experiment. Also, large air temperature swings during several data sets resulted in data that would not converge, or not converge accurately.

However, several telling observations can still be made. Relatively stable blood perfusion is predicted before surgery was begun. Excise of the flap results in an increase in blood flow to the surgical site, similar to that witnessed in the first flap experiment. Also, as expected, occlusion of the blood supply to the flap results in a distinct drop in predicted perfusion.

Table 5.4: Data Summary of First Skin Flap Experiment – 12.06.2001

Data Set	Flap Condition	Time (min)	$T_{arterial}$ (°C)	T_{air} (°C)	T_{skin} (°C)	Bp (ml/ml/s)	Rc (m^2K/W)	SSY
Flap1w	Pre-Surgery	0	34.50	21.80	30.87	0.00380	0.00027	1.031
Flap2w		4	34.30	20.80	31.08	0.00420	0.00091	1.471
Flap3w		8	34.20	20.80	31.26	0.00453	0.00055	0.259
Flap4w	Flap Exised No Occlusion	42	33.20	20.90	29.03	0.00166	0.00285	1.459
Flap5w		46	33.20	20.60	28.90	0.00196	0.00306	3.427
Flap6w		53	33.10	20.20	28.56	0.00415	0.00215	0.150
Flap7w	Flap Exised Occluded	57	33.10	20.10	28.38	0.00293	0.00317	3.036
Flap8w		60	33.10	19.20	26.82	0.00287	0.00328	1.063
Flap9w		64	33.10	19.20	26.61	0.00243	0.00376	1.514
Flap10w	Flap Exised No Occlusion	66	33.10	18.70	26.36	0.00390	0.00328	5.376
Flap11w		70	33.10	18.80	27.33	0.00345	0.00394	11.796
		Lidocain administered						
Flap12w		73	33.10	18.60	27.48	0.00157	0.00432	16.225
Flap13w	Flap Reattached	91	32.90	20.20	30.16	0.00382	0.00172	0.317
Flap14w		93	32.60	19.40	28.11	0.00590	0.00187	1.283
Flap15w		96	32.60	19.10	28.15	0.00503	0.00192	2.565

Experimental and estimated data sets are plotted in Appendix B.3

Table 5.5: Data Summary of Second Skin Flap Experiment – 03.12.2002

Data Set	Flap Condition	Time (min)	$T_{arterial}$ (°C)	T_{air} (°C)	T_{skin} (°C)	Bp (ml/ml/s)	Rc (m^2K/W)	SSY
bFlap1	Pre-Surgery	0	36.90	21.00	32.03	0.00830	0.00047	0.168
bFlap2		5	36.90	19.50	31.21	0.00653	0.00024	0.206
bFlap3		10	36.80	18.60	30.66	0.00663	0.00027	0.118
bFlap4		15	36.80	18.30	30.79	0.00691	0.00041	0.071
bFlap5		20	36.80	17.90	30.69	0.00770	0.00049	0.297
† bFlap6	Flap Excised No Occlusion	52	36.60	20.70	31.02	0.01748	0.00578	256.398
bFlap7		57	36.60	19.40	30.66	0.01309	0.00119	1.644
† bFlap8		62	36.60	18.90	30.61	0.01186	0.00187	28.731
bFlap9		67	36.60	18.60	30.56	0.01051	0.00081	0.297
† bFlap10		72	36.60	18.40	30.70	0.00850	0.00052	24.396
bFlap11	Flap Excised Occluded	78	36.60	18.50	30.20	0.00501	0.00094	2.737
† bFlap12		83	36.60	17.40	27.90	0.00525	0.00270	59.960
bFlap13		88	36.60	17.10	27.44	0.00467	0.00147	0.128
bFlap14		93	36.50	17.10	26.51	0.00518	0.00137	0.646
† bFlap15		98	36.50	16.90	26.57	No Convergence		

† These data sets have more variation than others same test. The cause of the added noise is unknown at this time, however it is important enough to call question to these data sets. Therefore, these data sets are regarded as being of questionable experimental accuracy. Plots of the data sets are available in Appendix B.4.

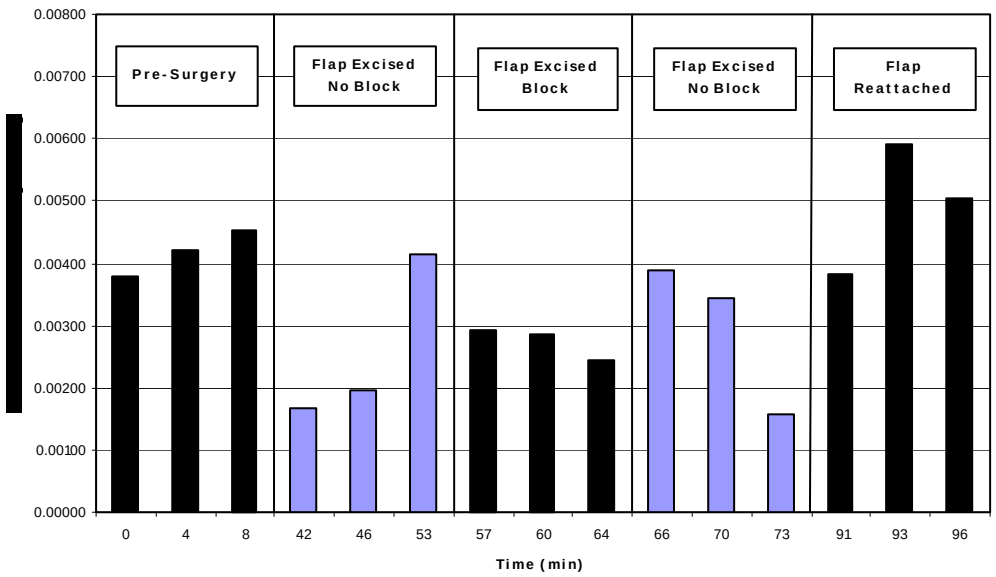

Figure 5.6: Plot of the blood perfusion estimates versus time for the first flap study. The alternating colors denote the different sub-groups of tests (i.e. flap excised-block, flap-excised-no block, etc).

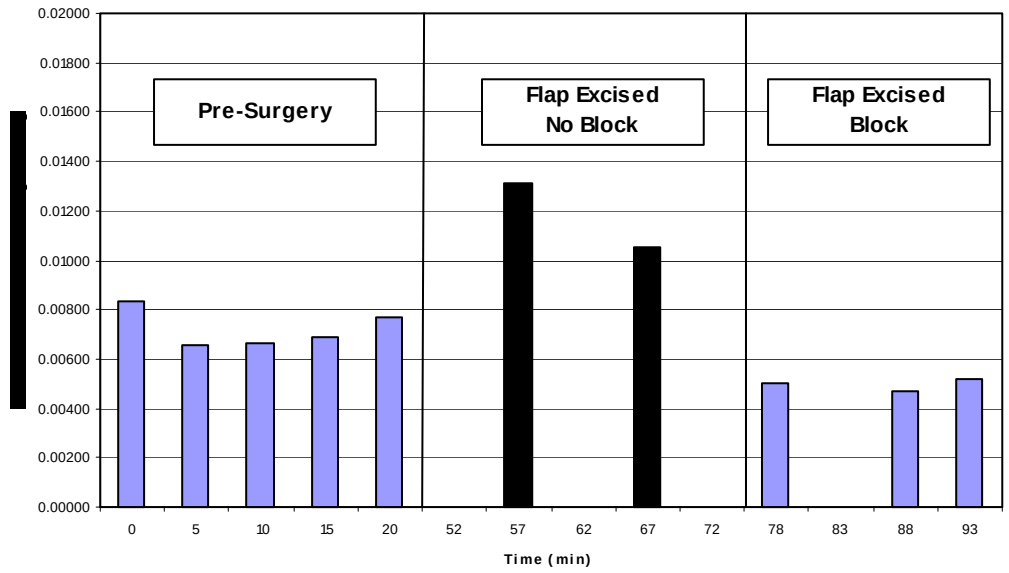

Figure 5.7: Plot of the blood perfusion estimates versus time for the second flap study. The alternating colors denote the different sub-groups of tests (i.e. flap excised-block, flap-excised-no block, etc). Unreliable data sets have been removed.

Open Artery Test

In the second flap study, a different experiment was improvised by altering the timing of one of the data sets. After the desired tests were taken with the blood supply to the flap closed off, data were recorded continually before and after the clamps were removed from the occluded vein and artery instead of waiting for the flap to reperfuse before recording data. Thirty seconds after data logging was begun, Dr. Lanz began by removing the clamp from the femoral vein. At forty seconds, the clamps were removed from the occluded artery and the vascular system supplying the flap was 'open'. At the 100 s mark, Dr. Lanz applied drops of saline to the test site. The resulting data set (bflap17) provides some very interesting results. The data are shown graphically in Figure 5.8.

This data set clearly shows the bioprobe responding to a change in blood perfusion under the tissue it is measuring. There is a distinct increase in heat flux coinciding with the opening of the artery supplying the excised skin flap. There were no other significant changes in experimental parameters at that time. The only conclusion is that the probe is responding to the change in blood perfusion in the flap. This data set also displays how quickly the bioprobe will

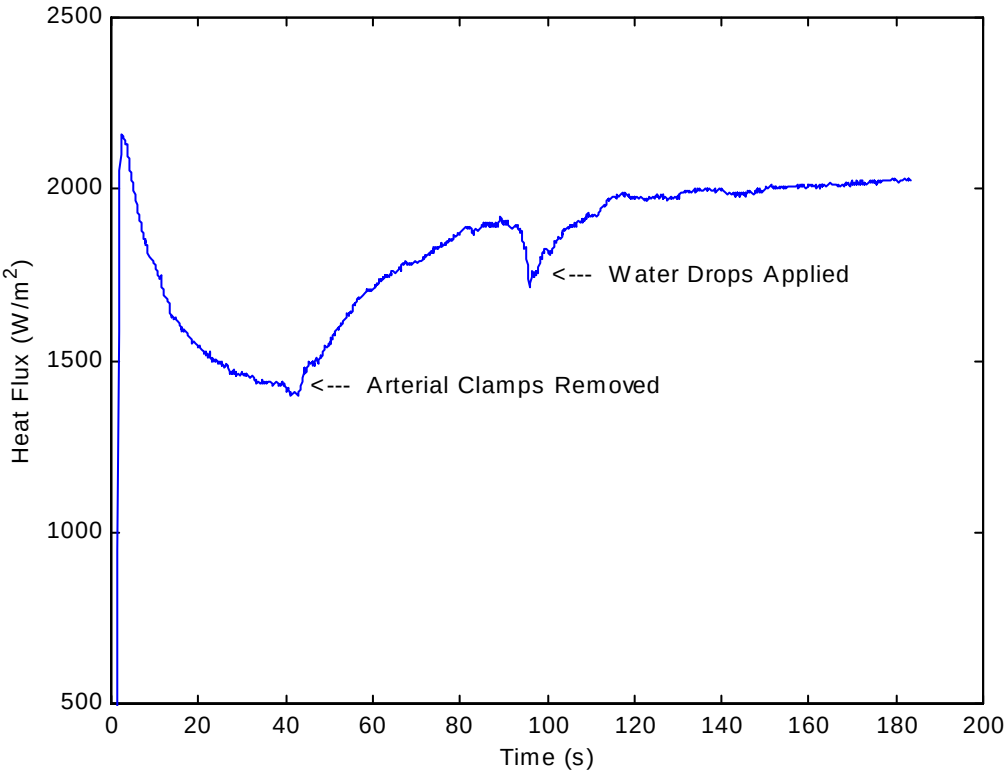

Figure 5.8: Data set recorded simultaneously with the unblocking of the skin flap. There is a rise in the recorded heat flux coinciding with the unclamping of the artery (40 s). A dip in heat flux occurs later in the curve (95 s) when a few drops of water are applied to the test site. No other experimental factors changed significantly during this test. The conclusion is that the sensor has responded directly (and positively) to a change in blood perfusion in the tissue being measured.

respond and recover to major disturbances in environment such as the saline application. This data set did, however, raise an important question: Would the current finite difference model predict this system behavior if subjected to the same disturbance?

To test this question, an adaptation was made to the biomodel code. The biomodel was changed so that a second blood perfusion value could be entered into the program that would replace the original estimate at a prescribed time (in this case, 40 s in the experiment). While this does now work with the parameter estimation routine, it allows a simulation using biomodel where the blood perfusion value is changed partway through the data set. The initial values for blood perfusion and contact resistance were determined by running the parameter estimation routine on only the first part of the curve before the artery was opened. This resulted in the estimate values of w_b=0.00519 ml/ml/s and R_c=0.00119 m^2K/W. Then a value of blood perfusion w_b=0.012 ml/ml/s, similar to those predicted by the biomodel for the unblocked tests, was selected for the changeover value, keeping the contact resistance constant. The new biomodel was accessed using these values to produce the curve shown in Figure 5.9. For comparison, the experimental data set is also plotted on the same set of axes.

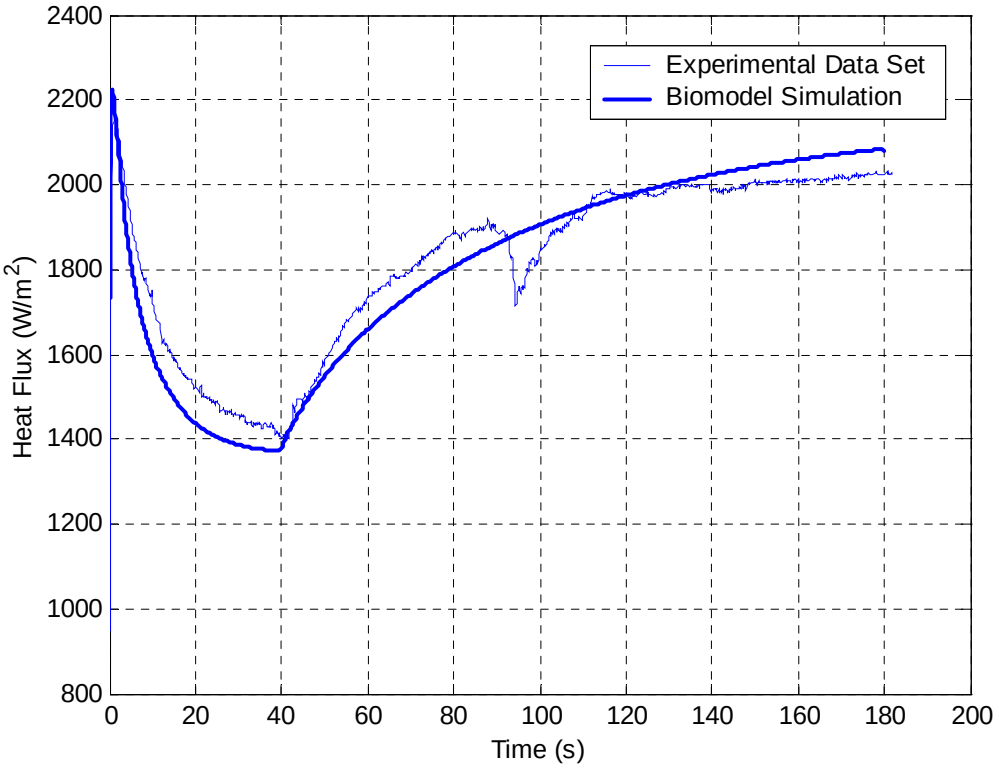

Figure 5.9: Plot of heat flux versus time showing the data set recorded when the blood supply to the flap was unblocked at 40 s with the approximated data set generated by the biomodel. The shape of the response curves are very similar, lending credibility to the accuracy of the biomodel design. ω_b=0.00519 ml/ml/s for the first 40 seconds of the numerically approximated curve and then switches to ω_b=0.012 ml/ml/s for the remainder.

It is quite clear from the graph that while the data sets do not exactly match, they do possess the same shape and response characteristics. The model predicts the same system behavior recorded experimentally when subjected to the same isolated disturbance. This is a very convincing argument in favor of the ability of the biomodel to approximate the tissue-bioprobe system. It should be possible, with modifications to the parameter estimation method, to determine ω_b as a function of time with the current biothermal model. Such development would bring the bioprobe closer to having the ability to make continuous measurements on systems with continually changing blood perfusion.

General Comments

It is interesting to note that in all of the experiments, with the exception of the second flap study, the blood perfusion estimated in the second data set is higher than that estimated in the first. Assuming these estimates are accurate, this effect is most likely explained as the result of the bioprobe interacting with the system it is measuring, i.e. the increased perfusion is probably the body's response to the artificial cooling of the measured tissue.

This effect can most easily be seen in the blood perfusion estimates in the first flap study and the *cdog* data sets. In both cases, the blood perfusion estimate increases steadily with time. This would make sense given blood perfusion's role in thermoregulatory control of the body. However, it should be noted that the effect is most noticeable in the dog experiments when nitrogen was used as the cooling air supply. It has already been noted that the air temperature was much colder than room temperature and would therefore invoke a larger sympathetic response than using a somewhat warmer air supply.

Also of importance is the performance of the canine skin flap model. Although strange behavior was observed in some instances (in the first skin flap experiement, lower perfusion is predicted when the flap is not blocked than when it is) the skin flap has been proven a very useful method of testing the bioprobe. It is recommended that future experiments would be helpful.

While further tests are required and no claims can be made at this time about the accuracy of the blood perfusion estimates, it is encouraging that the reliable data applear to be following expected trends.

Chapter 6 Conclusions and Recommendations

The work presented in this document represents a significant step in the ongoing bioprobe research at Virginia Tech. While the advancements attained during the course of this research are both promising and exciting, there remain many areas for improvement in the design and operation of the blood perfusion sensor. Several suggestions of where and how these improvements may be attained are included in this chapter.

6.1 Conclusions

It can be said with confidence that the main objective at the beginning of this research, validation of the bioprobe concept, has been reached. The data set bflap17 and the resulting model simulation clearly show that the bioprobe responds directly to changes in blood perfusion and that the biomodel accurately represents the living system being measured. This discovery lends credibility to the other experiments, and their interpretation, as reported in this work.

While more rigorous testing is needed, this work provides evidence of the bioprobe's usability in a clinical environment and the accuracy of measurements it can provide. While more research is needed to prove the reliability and repeatability of measurement, consistency in bioprobe output has been hinted at here.

The following conclusions represent the most important ideas that should be carried into the next steps of research on the bioprobe:

1. The biothermal model has been proved a sound approximation to the physical system being measured.
2. The Virginia Tech bioprobe has the ability to discern different levels of blood perfusion in perfuse tissue.
3. While flow control is limited, the canine skin flap model is an effective and versatile means of testing the bioprobe. The current procedure is effective but future experiments could be used to optimize the protocol.

4. The probe heat flux provides a more accurate representation of the system behavior than previous schemes. The restructuring of the biomodel to accept this change has resulted in a faster running estimation routine.
5. Variations in air temperature and movement of the probe during measurement cause disturbances that are not accounted for accurately in the biomodel, leading to inaccuracies in parameter estimation.

6.2 Recommendations

Computer System Improvements

A major inconvenience encountered during this research was moving the data acquisition setup to the Virginia-Maryland Regional College of Veterinary Medicine. The desktop pc, while reliable, is bulky, somewhat behind the times in terms of computing power, and contains older data acquisition equipment. There is room for many improvements.

The use of a laptop computer would greatly improve the portability of the data acquisition system. Now that it is possible to analyze a data set in under ten minutes, a quicker computer may be able to determine parameter estimates for a data set before the next data is recorded. This would allow a researched to evaluate the direction of a particular group of experiments as they are developing.

It is also believed that at this point, all of the input/output and estimation programs could be combined into a more efficient single program. This would drastically reduce the amount of user time associated with data reduction and output production.

Air Temperature Measurements

Due to the sizable influence air temperature has on the behavior of the bioprobe system, it is suggested that the data acquisition setup be renovated to include the measurement of air temperature as a function of time for the entire duration of an experiment. This can be accomplished through the addition of another channel to the existing Test Point program to accept measurements from the air temperature thermocouple.

Ideally, because of the added apparatus and the inconvenience associated with a required air supply, the use of air with the bioprobe would be removed. Another type of thermal event could replace the convective boundary condition at the surface of the sensor. A method employing a Thermo-Electric Cooler (TEC) instead of air cooling is currently under investigation.

Interference Problems

The interference of other equipment with the operation of the bioprobe should be explored. There should be some effort to determine the exact cause of the disturbances observed with the harmonic scalpel during the spay tests presented in this work. It is anticipated that normal

electromagnetic shielding commonly used with medical equipment would remove the problem, but this level of concern should be saved for much later in the design process of the bioprobe.

Improvements to Heat Flux Smoothing Routine

Near the end of this research, a possible improvement to the thru-probe heat flux smoothing routine was explored, however it was too late to include it in the research presented here. It was determined that an average of the convective and contact resistance heat flux produces a curve that even more closely correlates to a stable thru-probe heat flux. A time smoothing routine, similar to the one now used in the biomodel, using a convective/contact resistance average heat flux curve will more accurately approximate a stable thru-probe heat flux data set.

For example, the same set of smoothing functions outline in Chapter 3 (Eq. 3.4, five-point smoothing routine) would be used. However, here $q''_p(i)$ would be replaced with the average of convective heat flux and the heat flux across the contact resistance:

$$q''_{avg}(i) = \frac{q''(i)_c + q''_{Rc}(i)}{2} \qquad \text{Eq. 6.1}$$

Biomodel Initial Conditions

Currently, the biomodel uses the initial skin temperature as the initial temperature for the entire model. Knowing that small changes in skin temperature create large disturbances in model behavior, it could be theorized that this approximation could lead to inaccuracy in the prediction of system. Another way to represent the initial condition of the system would be to set all of the sensor nodes equal to the skin temperature but to create a gradient through the depth of the tissue blending from the skin temperature at the surface to the measured arterial temperature at the interior. This scheme should be explored to determine if any benefits of accuracy could be earned.

Accurate Skin Temperature Measurement

To ensure the accuracy of skin temperature measurement during testing, a routine could be included in Test Point that alerts the user when the system is at/near equilibrium. Test Point could monitor the temperature and heat flux signal and determine when the variation in output is below a certain percentage before data logging is begun. This would help a researcher gather data in a reliable and repeatable fashion.

Simultaneous Two-Probe Experiments

One possibility for exploring the accuracy and repeatability of the bioprobe would be to run experiments where two probes are used simultaneously on nearby patches of skin. The

estimates of the two probes could be compared to see if matching predictions of parameters would be calculated.

Homeostatic Testing

None of the measurements presented in this work could be used to rigorously explore the repeatability of the bioprobe. That is because none of the experiments were conducted under homeostatic conditions. Interactions with the subject, whether they be surgical or other, created changes in the environment being measured. It could be of some use to run experiments where care was taken to retain the subject in a homeostatic condition. This could be achieved by regulating the ambient air temperature, careful control of anesthesia, etc. A large number of tests where environmental characteristics were carefully controlled could in theory be used to explore the repeatability of the blood perfusion measurement.

Comparison With Another Measurement System

The goal of developing the bioprobe into a quantifiable and repeatable blood perfusion measurement system will not be attainable until the bioprobe is calibrated against known flow rates. In the absence of easily controllable blood flow (even in the experiments discussed here, the best control available was an 'on/off' situation), the blood perfusion sensor could be compared to other more accepted measurement systems (for example LDF, TDP, etc). Such a set up would have the added benefit of providing a secondary measurement to correlate to trends observed with the bioprobe.

Estimating Blood Perfusion as a Function of Time

The results of the bflap17 data set are encouraging and show that the biothermal model will respond accurately (as compared to system response) to changes in blood perfusion as a function of time. While the current estimation routine solves for constant parameters, there are estimation schemes that would facilitate the estimation of blood perfusion as a function of time. If this were achieved, continuous measurements could be recorded and analyzed with the bioprobe, instead of the current restriction to discrete (individual sets of data) measurements.

Bibliography

1. Robinson, P.S., 1998, “Development of Methodologies for the Noninvasive Estimation of Blood Perfusion”, Master of Science in Mechanical Engineering Thesis, Virginia Polytechnic Institute and State University, Blacksburg, VA.

2. Mitchner, M.D., 1991, “Measurements of Thermal Properties and Blood Perfusion Using the Heat Flux Microsensor”, Master of Science in Mechanical Engineering Thesis, Virginia Polytechnic Institute and State University, Blacksburg, VA.

3. Foquet, Y., Hager, J., Terrell, J., and Diller, T., 1993, “Blood Perfusion Estimation from Noninvasive Heat Flux Measurements”, in: *Advances in Bioheat and Mass Transfer – 1993: Microscale analysis of Thermal Injury Processes, Instrumentation, Modeling, and Clinical Applications*, ed. R. Roemer, ASME, N.Y., pp.53-60.

4. O’Reilly, T., Gonzales, T., and Diller, T., 1996, “Development of a Noninvasive Blood Perfusion Probe”, in: *Advances in Biological Heat and Mass Transfer*, eds. L. Hayes and S. Clegg, Vol. HTC 337/BED 34, ASME, pp. 67-73.

5. Scott, E., Robinson, P., and Diller, T., 1997, “Estimation of Blood Perfusion Using a Minimally Invasive Blood Perfusion Probe,” ASME Heat Transfer Div Publ Htd, **355**, pp. 205-212.

6. Scalise, L., de Mul, F., Steenbergen, WI, Petoukhova, A., 2000, “Recent Advances in Self-Mixing Laser-Doppler Velocimetry: Use as a In-Vivo Blood Flow Meter”, in: *Biomedical Diagnostic, Guidance, and Surgical-Assist Systems II*, eds. T. Vo-Dinh, W. Grundfest, and D. Benaron, Proceedings of SPIE Vol. 3911, pp. 95-104.

7. Lanz, O., 2002, Private discussion and correspondence

8. Forreser, K., Shymkiw, R., Tulip, J., Sutherland, C., Hart, D., Bray, R., 2000, “Spatially resolved diffuse reflectance with laser Doppler imaging for the simultaneous in-vivo measurement of tissue perfusion and metabolic state”, in: *Laser-Tissue Interaction XI: Photochemical, Photothermal, abnd Phtotmechanical*, eds. D. Duncan, J. Hollinger and S. Jacques, Proceedings of SPIE Vol. 3914, pp. 324-32.

9. Liebert, A,, Leahy, M., Maniewski, R., 1998, “Multichannel laser-Doppler probe for blood perfusion measurements with depth discrimination”, in: *Medical and Biological Engineering & Computing*, Vol. 36, pp. 740-747.

10. Valvano, J., Allen, J., and Bowman, H., 1984, “The Simultaneous Measurement of Thermal Conductivity, Thermal Diffusivity, and Perfusion in Small Volumes of Tissue,” *Journal of Biomechanical Engineering*, **106**, pp. 192-197.

11. Bowman, H., 1985, “Estimation of Tissue Blood Flow,” *Heat Transfer in Medicine and Biology*, **1**, Plenum Press, pp. 193-230.

12. Ott, C., and Vari, R., 1979, “Renal Autoregulation of Blood Flow and Filtratioin Rate in the Rabbit,” *American Journal of Physiology*, **237**, pp. F479-F482.

13. Yang, W.-J., 1989, *Biothermal Fluid Sciences*, Hemisphere Publishing Corp.

14. Lanz, O., Broadstone, R., Martin, R., Denger, D., 2001,” Effects of epidural anesthesia on microcirculatory blood flow in free medial saphenous fasciocutaneous flaps in dogs”, in: *Veterinary Surgery*, Jul-Aug, Vol. 30(4), pp.374-9.

15. Moffat, R. J., “Describing the Uncertainties in Experimental Results,” Experimental Thermal and Fluid Science, Vol. 1, 1988, pp. 3-17.

Appendix A Computer Programs

A.1 Parameter Estimation Code

This appendix contains the final form of the general parameter estimation code written in FORTRAN. This code can call the biomodel alone, run the parameter estimation scheme on a set of experimental data, or create a map of the SSY variable for a given range of parameter values. The final version of this code can be found in the file Parameter_Estimation.f.

```
      PROGRAM NEWEST
*******************************************************************************
     *****
*     PROGRAM NEWEST
*******************************************************************************
     *****
*
*    THIS PROGRAM IS DESIGNED FOR USE WITH THE BLOOD PERFUSION SENSOR DEVELOPED
*    AT VIRGINIA TECH.  THE PROGRAM SOLVES A BIOTHERMAL MODEL CONSISTING OF THE
*    BIOPROBE AND THE TISSUE IT IS RESTING ON.  THE PROGRAM ACCESSES A SPECIALLY
*    FORMATTED INPUT FILE PROVIDED BY THE USER WHICH CONTAINS THE NECESSARY INPUT
*    DATA.
*
*    THE PROGRAM CAN BE RUN IN TWO WAYS.
*         1)        THE MODEL CAN BE SOLVED FOR A GIVEN SET OF PARAMETERS AND
     DESIRED
*                   VALUES OF BLOOD PERFUSION AND CONTACT RESISTANCE
*         2)        BLOOD PERFUSION AND CONTACT RESISTANCE FOR A GIVEN SET OF
     EXPERIMENTAL
*                   DATA CAN BE DETERMINED USING THE PARAMETER ESTIMATION SUBROUTINE
*
*    THE MODEL IS SOLVED USING THE FINITE DIFFERENCE ADI METHOD.  THE PROGRAM
     ACCESSES
*    TWO EXTERNAL SUBROUTINES, BOTH OF WHICH HAVE SEVERAL INTERNAL SUBROUTINES.  THE
*    FULL PROGRAM TREE REQUIRED FOR SUCCESSFUL OPERATION IS:
*
*         PROGRAM NEWEST:
*                   1) EXTERNAL SUBROUTINE PARAMETER_ESTIMATION
*                              A) SUBROUTINE OUTPUT_FORMAT
*                              B) SUBROUTINE INITIALIZE_VARIABLES
*                              C) SUBROUTINE SENSITIVITY_COEFFICIENTS
*                   2) EXTERNAL SUBROUTINE MODEL
*                              A) SUBROUTINE OUTPUT_PAGE_FORMAT
*                              B) SUBROUTINE SET_CONSTANTS
*                              C) SUBROUTINE INITIALIZE_MATRICIES
*                              D) SUBROUTINE MATRIX_COEFFICIENTS
*                              E) SUBROUTINE FIRST_TIME_STEP
*                              F) SUBROUTINE SECOND_TIME_STEP
*                              G) SUBROUTINE FINAL_CALCULATIONS
*                              H) SUBROUTINE SMOOTH_PROBE_FLUX
*
*    THIS PROGRAM WAS DEVELOPED BY ADAPTING FORTRAN CODE WRITTEN BY PAUL ROBINSON
     AND
*    MICHAEL MICHENER.
*
*    THIS PROGRAM WAS WRITTEN BY ALEX CARDINALI ON: 6/11/01
*                          AND WAS LAST UPDATED ON: 6/11/01
*
*******************************************************************************
     *****
*
*                EXPLANATION OF VARIABLES
*                          ------------------------
*
*    REQUIRED INPUTS:
*     ----------------
*     N                    = number of data points in the experimental data
*    NP                    = number of parameters to be estimated
*     NI                   = number of independent variables
*    NEDGE                 = number of nodes in the r-direction in the probe
*     NNODES               = total number of nodes in the r-direction
*     LEDGE                = number of nodes in the z-direction in the probe
*    LNODES                = total number of nodes in the z-direction
*    B                     = new parameter estimate array (WB,RC)
*    THETAI                = initial theta value
*    airtemp               = air temperature recorded during experiment
*    Y                     = experimental heat flux data
*    VAR                   = variance of experimental data
*    T                     = experimental time data
*
*    OTHER:
*     ------
*    DECISION       = determines whether estimation or model is called
*    SMOOTHPQ       = heat flux data from MODEL
*    INFILE                 = formatted input data file
*    OUTFILE                = file containing all output data
*    I,J                    = counting integers
*
*******************************************************************************
     *****
      IMPLICIT NONE
     REAL*8 B,Y,VAR,T,THETAI,airtemp,SMOOTHPQ,WBLOW,WBHIGH,WBSTEP,RCLOW
     &,RCHIGH,RCSTEP,TEMP1,TEMP2,skintemp,artetemp
      INTEGER I,J,N,NP,NI,NEDGE,LEDGE,NNODES,LNODES,DECISION,CONT,MAXIT
      DIMENSION B(:),Y(:),VAR(:),T(:),SMOOTHPQ(:)
     ALLOCATABLE B,Y,VAR,T,SMOOTHPQ
      CHARACTER*40 INFILE,OUTFILE,OUTFILE2
C
C
C     ASK USER IF THEY WANT TO ACCESS THE MODEL ONLY OR RUN THE PARAMETER
C     ESTIMATION ROUTINE
C
     CONT=1
     DO 89 I = 1,1000
      IF (CONT.EQ.1) THEN
                    WRITE(*,*)'ENTER 1,2 OR 3 IF YOU WANT TO:'
          WRITE(*,*)'1)  ACCESS THE BIOMODEL'
          WRITE(*,*)'2)  RUN THE PARAMETER ESTIMATION ROUTINE'
          WRITE(*,*)'3)  MAP AN SSY FIELD'
          READ(*,*,ERR=89) DECISION
                    IF (DECISION.EQ.1.OR.DECISION.EQ.2.OR.DECISION.EQ.3) THEN
                      CONT=2
                    END IF
     END IF
  89 CONTINUE
C
C
C      PROMPT USER FOR INPUT AND OUTPUT FILE NAMES
C
      WRITE(*,*)'ENTER THE NAME OF THE INPUT DATA FILE'
      READ(*,'(A40)')INFILE
      OPEN(8,FILE=INFILE)
     WRITE(*,*)'ENTER THE NAME OF THE OUTPUT FILE'
      READ(*,'(A40)')OUTFILE
     OPEN(7,FILE=OUTFILE)
     WRITE(*,*)'ENTER THE NAME OF ANOTHER OUTPUT FILE'
      READ(*,'(A40)')OUTFILE2
     OPEN(10,FILE=OUTFILE2)
     OPEN(9,FILE='DEBUG')
C
C
C      READ DATA FROM INPUT FILE
C
C      READ IN MODEL AND DATA GENERAL INFORMATION AND ALLOCATE VARIABLES
C
      READ(8,*)N,NP,NI
     ALLOCATE(B(NP),Y(N),VAR(N),T(N),SMOOTHPQ(N))
C     READ IN TISSUE/PROBE ARRAY INFORMATION DIMENSIONS
     READ(8,*) NEDGE,LEDGE,NNODES,LNODES
C      READ IN INITIAL PARAMETER ESTIMATES
      READ(8,*)(B(I),I=1,NP)
C      READ IN INITITAL CONDITIONS
      READ(8,*)airtemp,artetemp,skintemp
     THETAI=(artetemp-skintemp)/(artetemp-airtemp)
C
C      DIVERT THE PROGRAM ACCORDING TO [DECISION] AND READ IN EXPERIMENTAL DATA
C     IF NECESSARY
C
     CALL OUTPUT_FORMAT(airtemp,artetemp,skintemp,THETAI,INFILE,B,
     &NEDGE,LEDGE,NNODES,LNODES,NP,DECISION)
C
C
C
     IF (DECISION.EQ.2.OR.DECISION.EQ.3) THEN
```

```
      DO 10 I = 1,N
        READ(8,*)J,Y(I),VAR(I),T(I)
  10   CONTINUE

     WRITE(*,*) J,Y(1),VAR(1),T(1)

       IF (DECISION.EQ.2) THEN
        MAXIT=30
        CALL PARAMETER_ESTIMATION(N,NP,NEDGE,LEDGE,NNODES,LNODES,B,
     &THETAI,airtemp,Y,VAR,DECISION,MAXIT,artetemp)
       ELSE IF (DECISION.EQ.3) THEN
         MAXIT=1

          WRITE(*,*)'ENTER WB DATA RANGE: LOW,HIGH,STEP SIZE'
          READ(*,*)WBLOW,WBHIGH,WBSTEP
          WRITE(*,*)'ENTER RC DATA RANGE: LOW,HIGH,STEP SIZE'
          READ(*,*)RCLOW,RCHIGH,RCSTEP
          WRITE(*,*)WBLOW,WBHIGH,WBSTEP,RCLOW,RCHIGH,RCSTEP

          WRITE(7,'(A2)')'% '
          WRITE(7,887)'% INPUT DATA:  WB = ',B(1),'    RC = ',B(2)
  887              FORMAT(A20,F9.5,A9,F9.5)
          WRITE(7,'(A2)')'% '

          DO 888 TEMP1=WBLOW,WBHIGH,WBSTEP
           DO 889 TEMP2=RCLOW,RCHIGH,RCSTEP
             B(1)=TEMP1
             B(2)=TEMP2
             CALL PARAMETER_ESTIMATION(N,NP,NEDGE,LEDGE,NNODES,LNODES,B
     &,THETAI,airtemp,Y,VAR,DECISION,MAXIT,artetemp)
  889                CONTINUE
  888              CONTINUE

       END IF
C
     ELSE IF (DECISION.EQ.1) THEN
      CALL MODEL(B(1),B(2),THETAI,airtemp,N,NNODES,NEDGE,LNODES,LEDGE,
     &SMOOTHPQ,DECISION,artetemp)
C
     END IF
C
C
C
     END PROGRAM NEWEST
*******************************************************************************
     *****
*     SUBROUTINE OUTPUT_FORMAT
*******************************************************************************
     *****
*
*     THIS SUBROUTINE FORMATS THE OUTPUT FILE WITH LABELS AND NECESSARY INFORMATION
*    FOR THE PROGRAM NEWEST.
*
*******************************************************************************
     *****
*
*                EXPLANATION OF VARIABLES
*                        ----------------------
*    THETAI                  = initial theta value
*    airtemp                 = air temperature recorded during experiment
*    VALUES                  = array containing date and time information
*
*******************************************************************************
     *****
      SUBROUTINE OUTPUT_FORMAT(airtemp,artetemp,skintemp,THETAI,INFILE,B
     &,NEDGE,LEDGE,NNODES,LNODES,NP,DECISION)
     REAL*8 airtemp,artetemp,skintemp,THETAI,B
     INTEGER VALUES,NP,DECISION,NEDGE,LEDGE,NNODES,LNODES
     CHARACTER*10 DATE,CTIME,ZONE,INFILE
     DIMENSION VALUES(8),B(NP)
C
C
     CALL DATE_AND_TIME(DATE,CTIME,ZONE,VALUES)
C
     WRITE(7,'(2A16)')'%  INPUT FILE:  ',INFILE

     IF(DECISION.EQ.1)THEN
       WRITE(7,'(A24)')'%  METHOD:  Model Access'
     ELSE IF(DECISION.EQ.2)THEN
       WRITE(7,'(A32)')'%  METHOD:  Parameter Estimation'
     END IF

      WRITE(7,'(A3)')'%  '
     WRITE(7,115) '%  DATE: ',VALUES(2),'.',VALUES(3),'.',VALUES(1)
      WRITE(7,116) '%  TIME: ',VALUES(5),':',VALUES(6),':',VALUES(7)
      WRITE(7,'(A3)')'%  '
     WRITE(7,118)'%  ARTETEMP = ',artetemp,'      SKINTEMP      = ',ski
     &ntemp
     WRITE(7,118)'%  AIRTEMP  = ',airtemp,'      THETA INITIAL = ',THET
     &AI
      WRITE(7,'(A3)')'%  '
     WRITE(7,117)'%  NEDGE  = ',NEDGE,'           LEDGE  = ',LEDGE
     WRITE(7,117)'%  NNODES = ',NNODES,'           LNODES = ',LNODES
      WRITE(7,'(A3)')'%  '
     WRITE(7,120)'%  WB = ',B(1),'RC = ',B(2)
      WRITE(7,'(A3)')'%  '

     IF(DECISION.EQ.1)THEN
       WRITE(7,99)'%  ','TIME   ','CONVECTIVE','PROBE  ','SMOOTH PROBE'
     &,'RC    '
       WRITE(7,99)'%  ','----   ','----------','-----  ','------------'
     &,'--    '
     ELSE IF(DECISION.EQ.2)THEN
       WRITE(7,119) '%  ','ITERATION','   BLOOD PERFUSION','   CONTACT
     & RESISTANCE','       SUM OF SQUARES'
       WRITE(7,119) '%  ','---------','   ---------------','   --------
     &----------','       --------------'
     END IF
C
    99 FORMAT(A3,A7,A12,A14,A15,A13)
   115     FORMAT(A9,I2,A1,I2,A1,I4)
   116     FORMAT(A9,I2,A1,I2,A1,I2)
   117 FORMAT(A12,I5,A20,I5)
   118 FORMAT(A14,F8.4,A22,F8.4)
   119 FORMAT(A3,A9,A18,A21,A21)
   120 FORMAT(A7,F8.4,A7,F8.4)
C
      RETURN
      END SUBROUTINE OUTPUT_FORMAT
*******************************************************************************
     *****
*     SUBROUTINE PARAMETER_ESTIMATION
*******************************************************************************
     *****
*
*     THIS SUBROUTINE USES THE SUPPLIED DATA AND GAUSS ESTIMATION TO APPROXIMATE
     BLOOD
*    PERFUSION AND CONTACT RESISTANCE.  THIS SUBROUTINE ACCESSES SUBROUTINE MODEL AT
*    SEVERAL POINTS TO RETRIEVE NECESSARY DATA.
*
*******************************************************************************
     *****
*
*                EXPLANATION OF VARIABLES
*                        ----------------------
*     N                      = number of data points in the experimental data
*    NP                      = number of parameters to be estimated
*    NEDGE                   = number of nodes in the r-direction in the probe
*     NNODES                 = total number of nodes in the r-direction
*     LEDGE                  = number of nodes in the z-direction in the probe
*    LNODES                  = total number of nodes in the z-direction
*    B                       = new parameter estimate array (WB,RC)
*    BS                      = parameter estimates from previous iteration
*    THETAI                  = initial theta value
```

```
*    airtemp                 = air temperature recorded during experiment
*    Y                       = experimental heat flux data
*    VAR                     = variance of experimental data
*    DECISION       = determines whether estimation or model is called
*    SMOOTHPQ       = heat flux data from MODEL
*    CRITER                  = represents the desired accuracy in the parameter
     estimates
*    RESID                   = difference between experimental data and calculated
     heat flux
*    SSY                     = sum of the squares of RESID
*    RATIO                   = percent change in estimate
*    MAXIT                   = maximum number of iterations in the estimation
*    CONTROL                 = iterative variable that governs estimation loop
*    CUTOFF                  = designates the useful data range for estimation
*    CHANGE                  = counts how many of the parameters have converged
*    CONVTEST       = allows program to stop when both parameters have converged
*    SC,CO                   = sensitivity coefficients
*    DELTAB,D,P,    = matricies used in the gaussian estimation scheme
*    PINV,C,CI
*    DET                     = matrix determinant
*    I,J,K,K1       = counting integers
*
********************************************************************************
     *****
      SUBROUTINE PARAMETER_ESTIMATION(N,NP,NEDGE,LEDGE,NNODES,
     &LNODES,B,THETAI,airtemp,Y,VAR,DECISION,MAXIT,artetemp)
      IMPLICIT NONE
      REAL*8 B,Y,VAR,THETAI,airtemp,BS,DELTAB,D,P,PINV,C,CRITER,RESID,
     &CI,SSY,SC,DET,RATIO,SMOOTHPQ,artetemp
       INTEGER I,J,N,NP,NEDGE,LEDGE,NNODES,LNODES,MAXIT,CONTROL,CUTOFF
     &,K,K1,CHANGE,CONVTEST,DECISION
      PARAMETER (CUTOFF=1,CRITER=0.0001)
       DIMENSION B(NP),Y(N),VAR(N),SC(2,N),RESID(N),C(NP,NP),
     &D(NP),PINV(NP,NP),P(2,2),DELTAB(NP),BS(NP),CI(NP),SMOOTHPQ(N)
C
C
C
      IF (NP.EQ.1) THEN
        BS(2)=B(2)
      END IF
C
C
C
      CONVTEST=0
      DO 1000 CONTROL=1,MAXIT,1

      WRITE(9,*) 'CONVTEST DECISION = ',CONVTEST

      IF (CONVTEST.EQ.0) THEN
C
C
C
      CALL INITIALIZE_VARIABLES(B,NP,BS,DELTAB,D,P,PINV,C)
C
C
C        MAIN LOOP OF GAUSS METHOD, RETURN POINT FOR ALL ITERATIONS
C
       SSY = 0.D0
C

      WRITE(9,*) 'INTO MODEL',B(1),B(2)

       CALL MODEL(B(1),B(2),THETAI,airtemp,N,NNODES,NEDGE,LNODES,LEDGE,
     &SMOOTHPQ,DECISION,artetemp)

      WRITE(9,*) 'OUT OF MODEL, INTO SENSE'

       CALL SENSITIVITY_COEFFICIENTS(B(1),B(2),SMOOTHPQ,airtemp,N,THETAI,
     &NNODES,NEDGE,LNODES,LEDGE,SC,DECISION,artetemp)

      WRITE(9,*) 'OUT OF SENSE'
C
      DO 120 I = CUTOFF,N
C
C
C     CALCULATE THE SUM OF THE SQUARES
C
      RESID(I) = Y(I) - SMOOTHPQ(I)
      SSY = SSY + RESID(I)*RESID(I)/VAR(I)
C
C
C       CALCULATE THE C MATRIX
C
        DO 47 K = 1,NP
          DO 46 K1 = 1,NP
              C(K,K1) = C(K,K1)+SC(K,I)*SC(K1,I)/VAR(I)
  46      CONTINUE
  47    CONTINUE
C
C
C       CALCULATE "D"
C
     WRITE(9,444) CONTROL,I,RESID(I),Y(I),SMOOTHPQ(I),SSY
  444 FORMAT(2I6,4F14.4)


        DO 60 K = 1,NP
          D(K) = D(K)+SC(K,I)*RESID(I)/VAR(I)
  60    CONTINUE
C
 120  CONTINUE


     WRITE(9,*) 'OUT OF DO 120'
C
C
C     CALCULATE P MATRIX FROM C COEFFICIENTS
C
      DO 122 K = 1,NP
        DO 121 J = 1,NP
          PINV(K,J) = C(K,J)
 121    CONTINUE
 122  CONTINUE
C
      IF(NP.EQ.1) THEN
        P(1,1) = 1.D0/PINV(1,1)
      ELSE
C
C
C       Invert DELTA matrix by formula
C
        DET = (PINV(1,1)*PINV(2,2)-PINV(1,2)*PINV(2,1))
        P(1,1) = PINV(2,2)/DET
        P(2,2) = PINV(1,1)/DET
        P(1,2) = -1.D0*PINV(1,2)/DET
        P(2,1) = -1.D0*PINV(2,1)/DET
      ENDIF
C
      DO 124 K = 1,NP
        DO 123 J = 1,NP
          DELTAB(K) = DELTAB(K) + P(K,J)*D(J)
 123    CONTINUE
 124  CONTINUE
C
      DO 125 K = 1,NP
        B(K) = BS(K) + DELTAB(K)/2.0
 125  CONTINUE
C
     DO 155 K=1,NP
       IF (B(K).LT.0) THEN
         WRITE(9,*) 'NEGATIVE VALUE:  ',B(1),B(2)
         B(K)=0.000001
       END IF
```

```
  155 CONTINUE
C
      DO 126 K = 1,NP
        CI(K) = SQRT(ABS(P(K,K)))*1.96D0
 126  CONTINUE

     WRITE(9,*) 'DONE WITH CALCS',DELTAB(1),DELTAB(2),D(1),D(2)

C
C       END OF SEQUENTIAL GAUSS ESTIMATION PROCEDURE
*******************************************************************************
     *****
*******************************************************************************
     *****
C
C       Check each parameter estimate against the critera for a
C       converged solution.  Increment "CHANGE" accordingly.
C
      CHANGE = 0
      DO 170 J = 1,NP
        RATIO = (B(J)-BS(J))/(BS(J))
        RATIO = ABS(RATIO)
        IF (RATIO.LE.CRITER) THEN
          CHANGE = CHANGE+1
        ENDIF
 170  CONTINUE

     WRITE(9,*) CHANGE
C
C       Check to see if all parameters have converged, and if not, if
C       the maximum number of iterations have been used.  If no
C       convergence and the program is not at the maximum number of
C       iterations, then the process begins again with the sequential
C       Gauss loop using the latest parameter estimates as the initial
C       guesses.
C
      IF (CHANGE.EQ.NP.AND.DECISION.EQ.2) THEN
          WRITE(7,'(A70)') '------------------------- FINAL ESTIMATION
     & ---------------------------'
          CONVTEST=1

     DO 1001 I=1,N
        WRITE(10,777)I,Y(I),SMOOTHPQ(I),I/9.5
 1001     CONTINUE
  777 FORMAT(I4,F12.4,F12.4,F10.4)

      ENDIF
C
     WRITE(7,222) CONTROL,BS(1),BS(2),SSY
C
     IF (CONTROL.GE.MAXIT.AND.DECISION.EQ.2) THEN
       WRITE(7,*)'MAXIMUM NUMBER OF ITERATIONS REACHED'
     ENDIF
  222     FORMAT(I8,F18.5,F19.5,F26.5)
C
C
C

     ENDIF
 1000 CONTINUE
C
C
     CONTAINS
*******************************************************************************
     *****
*     SUBROUTINE INITIALIZE_VARIABLES
*******************************************************************************
     *****
*
*     THIS SUBROUTINE READS IN THE NECESSARY OUTSIDE VARIABLE FOR THE
*     PROGRAM NEWMOD.
*
*******************************************************************************
     *****
*
*                EXPLANATION OF VARIABLES
*                        ------------------------
*    B                   = new parameter estimate array (WB,RC)
*    BS                  = parameter estimates from previous iteration
*    DELTAB,D,P,    = matricies used in the gaussian estimation scheme
*    PINV,C
*    NP                  = number of parameters to be estimated
*
*******************************************************************************
     *****
      SUBROUTINE INITIALIZE_VARIABLES(B,NP,BS,DELTAB,D,P,PINV,C)
     REAL*8 B,BS,DELTAB,D,P,PINV,C
     INTEGER NP
     DIMENSION BS(NP),B(NP),DELTAB(NP),D(NP),P(NP,NP),PINV(NP,NP),
     &C(NP,NP)
C
C
      DO 20 I = 1,NP
        BS(I)=B(I)
        DELTAB(I) = 0.D0
        D(I) = 0.D0
        DO 15 K = 1,NP
          P(I,K)=0.D0
          PINV(I,K) = 0.D0
          C(I,K) = 0.D0
  15    CONTINUE
  20  CONTINUE
C
C
     RETURN
      END SUBROUTINE INITIALIZE_VARIABLES
*******************************************************************************
     *****
*******************************************************************************
     *****
*    SUBROUTINE SENSITIVITY_COEFFICIENTS
*******************************************************************************
     *****
*
*    THIS SUBROUTINE CALCUALTES THE SENSITIVITY COEFFICIENTS REQUIRED BY THE
*    PARAMETER ESTIMATION SCHEME USED IN PROGRAM NEWEST.
*
*******************************************************************************
     *****
*
*                EXPLANATION OF VARIABLES
*                        ------------------------
*    BETA1               = blood perfusion
*    BETA1P              = blood perfusion with slight change
*    BETA2               = contact resistance
*    BETA2P              = contact resistance with slight change
*    ETA                 = heat flux data calculated using BETA1,BETA2
*    HI1                 = heat flux data calculated using BETA1P,BETA2
*    HI2                 = heat flux data calculated using BETA1,BETA2P
*     N                  = number of data points in the experimental data
*    NP                  = number of parameters to be estimated
*    NEDGE               = number of nodes in the r-direction in the probe
*     NNODES             = total number of nodes in the r-direction
*     LEDGE              = number of nodes in the z-direction in the probe
*    LNODES              = total number of nodes in the z-direction
*    THETAI              = initial theta value
*    airtemp             = air temperature recorded during experiment
*    DECISION       = determines whether estimation or model is called
*    CO                  = sensitivity coefficients
*
*******************************************************************************
     *****
      SUBROUTINE SENSITIVITY_COEFFICIENTS(BETA1,BETA2,ETA,airtemp,N,
     &THETAI,NNODES,NEDGE,LNODES,LEDGE,CO,DECISION,artetemp)
```

```
      REAL*8 BETA1,BETA2,BETA1P,BETA2P,ETA,airtemp,THETAI,CO,HI1,HI2,
     &FACTOR,artetemp
     INTEGER I,N,NNODES,NEDGE,LNODES,LEDGE,DECISION
     PARAMETER (FACTOR=1.01)
      DIMENSION CO(2,N),ETA(N),HI1(N),HI2(N)
C
C
      BETA1P = BETA1*FACTOR
      BETA2P = BETA2*FACTOR
C
      CALL MODEL(BETA1P,BETA2,THETAI,airtemp,N,NNODES,NEDGE,LNODES,LEDGE
     &,HI1,DECISION,artetemp)
      CALL MODEL(BETA1,BETA2P,THETAI,airtemp,N,NNODES,NEDGE,LNODES,LEDGE
     &,HI2,DECISION,artetemp)
C
     DO 900 I=1,N
        CO(1,I) = (HI1(I)-ETA(I))/(BETA1P-BETA1)
        CO(2,I) = (HI2(I)-ETA(I))/(BETA2P-BETA2)
  900      CONTINUE
C
C
     RETURN
      END SUBROUTINE SENSITIVITY_COEFFICIENTS
*******************************************************************************
     *****
C
C
C     END OF THE PARAMETER ESTIMATION SUBROUTINE, RETURN VALS AND END SUBROUTINE
C
      END SUBROUTINE PARAMETER_ESTIMATION
*******************************************************************************
     *****
*     NEWMOD(WB,RC,airtemp,THETAI,NTSTP,SMOOTHPQ,TGS)
*******************************************************************************
     *****
*
*     THIS PROGRAM WAS WRITTEN TO REPLACE PESTT.F
*
*     CREATED BY ALEX CARDINALI:  05/13.01
*
*******************************************************************************
     *****
*
*                 EXPLANATION OF VARIABLES
*                             ------------------------
*
*         RHOB                = blood density
*         RHOP                = probe density
*         SHB                           = blood specific heat
*         SHP                           = probe specific heat
*         KT                            = tissue thermal conductivity
*         KP                            = probe thermal conductivity
*         ALPHT               = tissue diffusivity
*         ALPHP               = probe diffusivity
*         FF                            = ratio of probe diffusivity to tissue
     diffusivity
*         R                             = effective probe radius
*         M                             = blood perfusion term
*         artetemp  = arterial temperature
*         Thickness = probe thickness
*         CONV                = convection coefficient at probe surface
*         TSTP                = time step correlating to the data sampling rate
*         N                             = number of tissue nodes in the r-direction
*         NEDGE               = number of probe nodes in the r-direction
*         L                             = number of total nodes (tissue + probe) in
     the z-direction
*         LEDGE               = number of probe nodes in the z-direction
*         DH                            = radial length of each element (non-
     dimensionalized)
*         DZ                            = thickness of each element (non-
     dimensionalized)
*         CRFP                =
*         CRFT                =
*         TSTP                =
*         NTSTP               =
*         THETAINF  =
*
*         WB                            = blood perfusion guess
*         RC                            = contact resistance guess
*         airtemp             = supply air temperature
*
*******************************************************************************
     *****
     SUBROUTINE MODEL(WB,RC,THETAI,airtemp,NTSTP,N,NEDGE,L,LEDGE,
     &SMOOTHPQ,DECISION,artetemp)
      IMPLICIT NONE
     REAL*8 WB,RC,airtemp,ALPHT,ALPHP,RHOB,RHOP,SHB,SHP,KT,KP,R,M
     &,artetemp,Thickness,FF,CONV,TSTP,DH,DZ,DT,THETAINF,CRFP,CRFT,THETA
     &,A,B,C,D,E,F,G,H,ETA,BETA,GAMMA,TEMP,PROBFLUX,PROBQ,TIME,CONVFLUX,
     &RCFLUX,CONVQ,RCQ,SMOOTHPQ,THETAI,GTEMP,GAGETEMP
      INTEGER I,COUNTER,NEDGE,LEDGE,N,L,NTSTP,DECISION
     DIMENSION A(N,L),B(N,L),C(N,L),D(N,L),E(N,L),F(N,L),G(N,L),H(N,L),
     &BETA(N,L),GAMMA(N,L),THETA(N,L),TEMP(N,L),ETA(N),TIME(NTSTP)
     &,PROBQ(NTSTP),CONVQ(NTSTP),RCQ(NTSTP),SMOOTHPQ(NTSTP),
     &GAGETEMP(NTSTP)
C
C
C     DEFINE VARIABLES THAT ARE CONSTANT WITH TIME AND SPACE
C
     CALL SET_CONSTANTS(ALPHT,ALPHP,RHOB,RHOP,SHB,SHP,KT,KP,R,M,
     &Thickness,FF,CONV,TSTP,DH,DZ,DT,THETAINF,CRFP,CRFT,NEDGE,LEDGE,RC,
     &WB)
C
C
C      INITIALIZE PROBE MATRICES
C
     CALL INITIALIZE_MATRICIES(NEDGE,LEDGE,N,L,THETA,A,B,C,D,E,F,G,H,
     &ETA,BETA,GAMMA,TEMP,THETAI)
C
C
C    DETERMINE THE MATRIX COEFFICIENTS FOR BOTH TIME STEP CALCULATIONS
C
     CALL MATRIX_COEFFICIENTS(FF,DT,DH,LEDGE,NEDGE,L,N,M,DZ,CONV,KP,
     &CRFP,CRFT,A,B,C,E,F,G,ETA,R)
C
C
C    ALL SPATIAL CONSTANTS HAVE BEEN DETERMINED, BEGIN TIME CALCULATIONS
C
      DO 23 COUNTER=1,NTSTP,1
C
C
C     PERFORM FIRST TIME STEP CALCULATIONS
C
     CALL FIRST_TIME_STEP(LEDGE,NEDGE,L,N,CONV,THETAINF,KP,DZ,R,FF,DT,
     &THETA,CRFP,CRFT,A,B,C,D,BETA,GAMMA)
C
C
C     PERFORM SECOND TIME STEP CALCULATIONS
C
     CALL SECOND_TIME_STEP(LEDGE,NEDGE,L,N,CONV,THETAINF,KP,DZ,R,FF,DT,
     &THETA,ETA,F,E,G,H,BETA,GAMMA,TEMP,DH,artetemp,airtemp)
C
C
C     CALCULATED FINAL DESIRED VALUES FOR THIS TIME STEP
C
     CALL FINAL_CALCULATIONS(KP,DZ,R,CONV,THETA,airtemp,artetemp,LEDGE,
     &NEDGE,KT,RC,TEMP,THETAINF,CRFP,N,L,PROBFLUX,CONVFLUX,RCFLUX,GTEMP,
     &ETA)
C
     CONVQ(COUNTER)=CONVFLUX
     PROBQ(COUNTER)=PROBFLUX
     RCQ(COUNTER)=RCFLUX
     TIME(COUNTER)=COUNTER*TSTP
     GAGETEMP(COUNTER)=GTEMP
```

```
C
C
C     NOW RETURN TO THE BEGINNING OF THE MODEL SOLUTION LOOP AND PROCEED TO THE
C     NEXT TIME STEP
C
  23  CONTINUE
C
C
C     REMOVE OSCILLATIONS FROM THE PROBE HEAT FLUX USING A SMOOTHING ALGORITHM
C
      CALL SMOOTH_PROBE_FLUX(PROBQ,NTSTP,SMOOTHPQ)
C
C
C     OUTPUT DESIRED DATA TO THE DESIGNATED OUTPUT FILE IF ACCESSING THE
C     MODEL ONLY
C
      IF (DECISION.EQ.1) THEN
       DO 606 I=1,NTSTP,1
           WRITE(7,100) TIME(I),CONVQ(I),PROBQ(I),SMOOTHPQ(I),RCQ(I)
  606      CONTINUE
  100      FORMAT(F8.4,F14.4,F14.4,F14.4,F13.4)
      END IF
C
C
C     LISTING OF INTERNAL SUBROUTINES
C
      CONTAINS
*******************************************************************************
      *****
*******************************************************************************
      *****
*     SUBROUTINE SET_CONSTANTS
*******************************************************************************
      *****
*
*     THIS SUBROUTINE DEFINES ALL VARIABLES THAT ARE CONSTANT WITH TIME
*     THAT ARE USED IN THE PROGRAM NEWMOD.
*
*******************************************************************************
      *****
       SUBROUTINE SET_CONSTANTS(ALPHT,ALPHP,RHOB,RHOP,SHB,SHP,KT,KP,R,M,
      &Thickness,FF,CONV,TSTP,DH,DZ,DT,THETAINF,CRFP,CRFT,NEDGE,
      &LEDGE,RC,WB)
       REAL*8 ALPHT,ALPHP,RHOB,RHOP,SHB,SHP,KT,KP,R,M,Thickness,
      &FF,CONV,TSTP,DH,DZ,DT,THETAINF,CRFP,CRFT,RC,WB
       INTEGER NEDGE,LEDGE
C
C
C      DEFINE TISSUE AND BLOOD PROPERTIES
C
       ALPHT = 0.150D-06
       RHOB = 1000.D0
       SHB = 4000.D0
       KT = 0.50D0
       R = 0.00953D0
       M = ((RHOB*SHB*WB)/(KT))*R**2.D0
C
C
C     DEFINE PROBE PROPERTIES
C
       Thickness = 0.0006D0
       RHOP = 2022.0D0
       SHP = 875.0D0
       KP = 177.0D0
       ALPHP = KP/RHOP/SHP
       FF = ALPHP/ALPHT
      CONV = 480.0D0
C
C
C      DEFINE GEOMETRIC PROPERTIES
C
       TSTP = 1.D0/9.5D0
       DH=1.0D0/Dble(NEDGE)
       DZ=Thickness/(Dble(LEDGE)*R)
       DT=ALPHT*TSTP/(2.D0*R**2.D0)
       THETAINF=1.0D0
C
       CRFP=(DZ*R)/(KP*(RC+((DZ*R)/(2.D0*KT))+((DZ*R)/(2.D0*KP))))
       CRFT=(DZ*R)/(KT*(RC+((DZ*R)/(2.D0*KT))+((DZ*R)/(2.D0*KP))))
C
       RETURN
       END SUBROUTINE SET_CONSTANTS
*******************************************************************************
      *****
*******************************************************************************
      *****
*     SUBROUTINE INITIALIZE_MATRICIES
*******************************************************************************
      *****
*
*     THIS SUBROUTINE INITIALIZES ALL OF THE MATRICIES USED IN THE PROGRAM NEWMOD.
*
*******************************************************************************
      *****
       SUBROUTINE INITIALIZE_MATRICIES(NEDGE,LEDGE,N,L,THETA,A,B,C,D,E,F,
      &G,H,ETA,BETA,GAMMA,TEMP,THETAI)
       REAL*8 THETA,A,B,C,D,E,F,G,H,ETA,BETA,GAMMA,TEMP,THETAI
      INTEGER NEDGE,LEDGE,N,L,I,J
      DIMENSION A(N,L),B(N,L),C(N,L),D(N,L),E(N,L),F(N,L),G(N,L),H(N,L),
      &BETA(N,L),GAMMA(N,L),THETA(N,L),TEMP(N,L),ETA(N)
C
       DO 1 I=1,NEDGE,1
       DO 2 J=1,LEDGE,1
       THETA(I,J)=THETAI
       A(I,J)=0.D0
       B(I,J)=0.D0
       C(I,J)=0.D0
       D(I,J)=0.D0
       E(I,J)=0.D0
       F(I,J)=0.D0
       G(I,J)=0.D0
       H(I,J)=0.D0
       ETA(I)=0.D0
       BETA(I,J)=0.D0
       GAMMA(I,J)=0.D0
       TEMP(I,J)=0.D0
  2    CONTINUE
  1    CONTINUE
C
C
C      INITIALIZE TISSUE THETA MATRIX
C
       DO 3 I=1,N,1
       DO 4 J=LEDGE+1,L,1
       THETA(I,J)=THETAI
       A(I,J)=0.D0
       B(I,J)=0.D0
       C(I,J)=0.D0
       D(I,J)=0.D0
       E(I,J)=0.D0
       F(I,J)=0.D0
       G(I,J)=0.D0
       H(I,J)=0.D0
       ETA(I)=0.D0
       BETA(I,J)=0.D0
       GAMMA(I,J)=0.D0
       TEMP(I,J)=0.D0
  4    CONTINUE
  3    CONTINUE
C
       RETURN
       END SUBROUTINE INITIALIZE_MATRICIES
*******************************************************************************
      *****
```

```
*******************************************************************************
     *****
*     SUBROUTINE MATRIX_COEFFICIENTS
*******************************************************************************
     *****
*
*     THIS SUBROUTINE DETERMINES THE SPATIAL MATRIX COEFFICIENTS THAT DO NOT CHANGE
*     WITH TIME FOR PROGRAM NEWMOD.  COEFFICIENTS FOR BOTH TIME STEPS ARE
     CALCULATED.
*
*******************************************************************************
     *****
      SUBROUTINE MATRIX_COEFFICIENTS(FF,DT,DH,LEDGE,NEDGE,L,N,M,DZ,CONV,
     &KP,CRFP,CRFT,A,B,C,E,F,G,ETA,R)
     REAL*8 FF,DT,DH,M,DZ,CONV,KP,CRFP,CRFT,A,B,C,E,F,G,ETA,R
     INTEGER NEDGE,LEDGE,N,L,I,J
     DIMENSION A(N,L),B(N,L),C(N,L),E(N,L),F(N,L),G(N,L),ETA(N)
C
C
C     COMPUTE ETA(I) VALUES
C
      DO 5 I=1,N,1
      ETA(I)=((2.D0*Dble(I)-1.D0)/2.D0)*DH
  5   CONTINUE
C
C
C     DEFINE COEFFICIENTS OF 1ST TIME STEP MATRICES
C     A(I,J),B(I,J),C(I,J)
C     1ST COLUMN PROBE
C
      I=1
      DO 6 J= 1,LEDGE,1
      A(1,J)=0.D0
      B(1,J)=1.D0/(FF*DT)+1.D0/(((DH)**2.D0))+1.D0/(2.D0*ETA(I)*DH)
      C(1,J)=-1.D0/((DH**2.D0))-1.D0/(2.D0*ETA(I)*DH)
  6   CONTINUE
C
C
C     MIDDLE COLUMNS, PROBE
C
      DO 7 I= 2,NEDGE-1,1
      DO 8 J= 1,LEDGE,1
      A(I,J)=-1.D0/((DH)**2.D0)+1.D0/(2.D0*ETA(I)*DH)
      B(I,J)=1.D0/(FF*DT)+2.D0/((DH)**2.D0)
      C(I,J)=-1.D0/((DH)**2.D0)-1.D0/(2.D0*ETA(I)*DH)
  8   CONTINUE
  7   CONTINUE
C
C
C     FINAL COLUMN, PROBE
C
      I=NEDGE
      DO 9 J=1,LEDGE,1
      A(I,J)=1.D0/(2.D0*ETA(I)*DH)-1.D0/((DH)**2.D0)
      B(I,J)=1.D0/(FF*DT)+1.D0/((DH)**2.D0)-1.D0/(2.D0*ETA(I)*DH)
      C(I,J)=0.D0
  9   CONTINUE
C
C
C     1ST COLUMN TISSUE
C
      I=1
      DO 10 J=LEDGE+1,L,1
      A(1,J)=0.D0
      B(1,J)=1.D0/(ETA(I)*(2.D0*DH))+1.D0/((DH)**2.D0)+1.D0/DT+M
      C(1,J)=-1.D0/((DH)**2.D0)-1.D0/(ETA(I)*(2.D0*DH))
  10  CONTINUE
C
C
C     MIDDLE COLUMNS
C
      DO 11 I=2,N-1,1
      DO 12 J=LEDGE+1,L,1
      A(I,J)= 1.D0/(ETA(I)*(2.D0*DH))-1.D0/(DH)**2.D0
      B(I,J)=1.D0/DT+2.D0/(DH)**2.D0+M
      C(I,J)=-1.D0/(DH)**2.D0-1.D0/(ETA(I)*(2.D0*DH))
  12  CONTINUE
  11  CONTINUE
C
C
C     FINAL COLUMN
C
      I=N
      DO 13 J=LEDGE+1,L,1
      A(N,J)= 1.D0/(ETA(I)*(2.D0*DH))-1.D0/(DH**2.D0)
      B(N,J)= 1.D0/DT+1.D0/(DH)**2.D0-1.D0/(ETA(I)*(2.D0*DH))+M
      C(N,J)=0.D0
  13  CONTINUE
C
C
C     DEFINE E(I,J),F(I,J),G(I,J)
C     COEFFICIENTS OF 2ND TIME STEP MATRIX
C     FIRST ROW,PROBE
C
      J=1
      DO 14 I=1,NEDGE,1
      E(I,1)=0.D0
      F(I,1)=((-CONV/2.D0+KP/(DZ*R))/(KP/(DZ*R)+CONV/2.D0))*(-1.D0/((DZ)
     $**2.D0))+2.D0/((DZ)**2.D0)+1.D0/(FF*DT)
      G(I,1)=-1.D0/((DZ)**2.D0)
  14  CONTINUE
C
C
C     MIDDLE ROWS
C
      DO 15 J=2,LEDGE-1,1
      DO 16 I=1,NEDGE,1
      E(I,J)=-1.D0/((DZ)**2.D0)
      F(I,J)=2.D0/((DZ)**2.D0)+1.D0/(FF*DT)
      G(I,J)=-1.D0/((DZ)**2.D0)
  16  CONTINUE
  15  CONTINUE
C
C
C     BOTTOM ROW, PROBE
C
      J=LEDGE
      DO 17 I = 1,NEDGE,1
      E(I,J)=-1.D0/((DZ)**2.D0)
      F(I,J)=2.D0/((DZ)**2.D0)+1.D0/(FF*DT)+(-CRFP+1.D0)*(-1.D0/(DZ
     $**2.D0))
      G(I,J)=CRFP*(-1.D0/((DZ)**2.D0))
  17  CONTINUE
C
C
C     TOP ROW OF TISSUE UNDER PROBE SURFACE
C
      J=LEDGE+1
      DO 18 I=1,NEDGE,1
      E(I,J)=(CRFT)*(-1.D0/((DZ)**2.D0))
      F(I,J)=(-CRFT+1.D0)*(-1.D0/((DZ)**2.D0))+1.D0/DT
     $+2.D0/((DZ)**2.D0)+M
      G(I,J)=-1.D0/((DZ)**2.D0)
  18  CONTINUE
C
C
C     DEFINE TOP TISSUE ROW, OUTSIDE OF PROBE
C
      J=LEDGE+1
      DO 19 I=NEDGE+1,N,1
      E(I,J)=0.D0
      F(I,J)=1.D0/DT+1.D0/(DZ**2.D0)+M
      G(I,J)=-1.D0/(DZ**2.D0)
  19  CONTINUE
```

```
C
C
C     DEFINE MIDDLE ROWS
C
      DO 20 J=LEDGE+2,L-1,1
      DO 21 I=1,N,1
      E(I,J)=-1.D0/(DZ**2.D0)
      F(I,J)=1.D0/DT+2.D0/(DZ**2.D0)+M
      G(I,J)=-1.D0/(DZ**2.D0)
  21  CONTINUE
  20  CONTINUE
C
C
C     BOTTOM ROW
C
      J=L
      DO 22 I=1,N,1
      E(I,L)=-1.D0/(DZ**2.D0)
      F(I,L)=1.D0/DT+1.D0/(DZ**2.D0)+M
      G(I,L)=0.D0
  22  CONTINUE
C
      RETURN
      END SUBROUTINE MATRIX_COEFFICIENTS
*******************************************************************************
     *****
*******************************************************************************
     *****
*     SUBROUTINE FIRST_TIME_STEP
*******************************************************************************
     *****
*
*     THIS SUBROUTINE CALCULATES THE SOLUTION FOR THE FIRST HALF OF A TIME STEP
     USING
*     THE ADI METHOD.
*
*******************************************************************************
     *****
      SUBROUTINE FIRST_TIME_STEP(LEDGE,NEDGE,L,N,CONV,THETAINF,KP,DZ,R,
     &FF,DT,THETA,CRFP,CRFT,A,B,C,D,BETA,GAMMA)
     REAL*8 CONV,THETAINF,KP,DZ,R,FF,DT,THETA,CRFP,CRFT,A,B,C,D,BETA,
     &GAMMA
     INTEGER NEDGE,LEDGE,N,L,I,J,K,IFP1,LAST,IF
     DIMENSION A(N,L),B(N,L),C(N,L),D(N,L),BETA(N,L),GAMMA(N,L),
     &THETA(N,L)
C
C
C     FIRST TIME STEP CALCULATIONS
C     DEFINE RHS COLUMN D(I,J)
C     PROBE ELEMENTS
C
C     TOP ROW PROBE
C
      J=1
      DO 24 I=1,NEDGE,1
      D(I,1)=((CONV*THETAINF)/(KP/(DZ*R)+CONV/2.D0))*(1.D0/((DZ)**2.D0))
     $+THETA(I,1)*(-2.D0/((DZ)**2.D0)+1.D0/(FF*DT)+((-CONV/2.D0+KP/(DZ
     $*R))/(KP/(DZ*R)+CONV/2.D0))*(1.D0/((DZ)**2.D0)))+THETA(I,2)*(1.D0
     $/((DZ)**2.D0))
  24  CONTINUE
C
C
C     MIDDLE ROWS, PROBE
C


      DO 25 J=2,LEDGE-1,1
      DO 26 I=1,NEDGE,1
      D(I,J)=THETA(I,J-1)*(1.D0/((DZ)**2.D0))+THETA(I,J)*(-2.D0/
     $((DZ)**2.D0)+1.D0/(FF*DT))+THETA(I,J+1)*(1.D0/((DZ)**2.D0))
  26  CONTINUE
  25  CONTINUE
C
C
C     BOTTOM ROW, PROBE
C
      J=LEDGE
      DO 27 I=1,NEDGE,1
      D(I,J)=THETA(I,J-1)*(1.D0/((DZ)**2.D0))+THETA(I,J)*((-2.D0/
     $((DZ)**2.D0))+1.D0/(FF*DT)+(-CRFP+1.D0)*(1.D0/((DZ)**2.D0)))
     $+THETA(I,J+1)*((CRFP)*(1.D0/((DZ)**2.D0)))
  27  CONTINUE
C
C
C     TISSUE ELEMENTS
C     TOP ROW UNDER PROBE
C
      J=LEDGE+1
      DO 28 I=1,NEDGE,1
      D(I,LEDGE+1)=THETA(I,LEDGE)*((CRFT)*(1.D0/((DZ)
     $**2.D0)))+THETA(I,LEDGE+1)*((-CRFT+1.D0)*(1.D0/((DZ)
     $**2.D0))+1.D0/DT-2.D0/(DZ**2.D0))+THETA(I,LEDGE+2)*(1.D0/(DZ**2.D0
     $))
  28  CONTINUE
C
      DO 29 I=NEDGE+1,N,1
      D(I,LEDGE+1)=THETA(I,LEDGE+1)*(1.D0/DT-1.D0/(DZ**2.D0))+
     $THETA(I,LEDGE+2)*(1.D0/(DZ**2.D0))
  29  CONTINUE
C
      DO 30 J=LEDGE+2,L-1,1
      DO 31 I=1,N,1
      D(I,J)=THETA(I,J-1)*(1.D0/(DZ**2.D0))+THETA(I,J)*(1.D0/DT-
     $2.D0/(DZ**2.D0))+THETA(I,J+1)*(1.D0/(DZ**2.D0))
  31  CONTINUE
  30  CONTINUE
C
      DO 32 I=1,N,1
      J=L
      D(I,L)=THETA(I,L-1)*(1.D0/(DZ**2.D0))+THETA(I,L)*(1.D0/DT-1.D0/
     $(DZ**2.D0))
  32  CONTINUE
C
C
C     USE TRIDIAGONAL MATRIX SOLVER TO GET
C     THETA VALUES AT THE FIRST TIME STEP
C
      IF=1
      DO 33 J=1,LEDGE,1
      BETA(IF,J)=B(1,J)
      GAMMA(IF,J)=D(1,J)/BETA(IF,J)
      IFP1=IF+1
C
      DO 34 I=IFP1,NEDGE
      BETA(I,J)=B(I,J)-A(I,J)*C(I-1,J)/BETA(I-1,J)
      GAMMA(I,J)=(D(I,J)-A(I,J)*GAMMA(I-1,J))/BETA(I,J)
  34  CONTINUE
C
      THETA(NEDGE,J)=GAMMA(NEDGE,J)
      LAST=NEDGE-IF
C
      DO 35 K=1,LAST
      I=NEDGE-K
      THETA(I,J)=GAMMA(I,J)-C(I,J)*THETA(I+1,J)/BETA(I,J)
  35  CONTINUE
  33  CONTINUE
C
C
C     MATRIX SOLVER FOR TISSUE ELEMENTS
C
      IF=1
      DO 36 J=LEDGE+1,L,1
      BETA(IF,J)=B(1,J)
      GAMMA(IF,J)=D(1,J)/BETA(IF,J)
```

```
      IFP1=IF+1
C
      DO 37 I=IFP1,N,1
      BETA(I,J)=B(I,J)-A(I,J)*C(I-1,J)/BETA(I-1,J)
      GAMMA(I,J)=(D(I,J)-A(I,J)*GAMMA(I-1,J))/BETA(I,J)
  37  CONTINUE
C
      THETA(N,J)=GAMMA(N,J)
      LAST=N-IF
C
      DO 38 K=1,LAST
      I=N-K
      THETA(I,J)=GAMMA(I,J)-C(I,J)*THETA(I+1,J)/BETA(I,J)
  38  CONTINUE
  36  CONTINUE
C
      RETURN
      END SUBROUTINE FIRST_TIME_STEP
*******************************************************************************
     *****
*******************************************************************************
     *****
*     SUBROUTINE SECOND_TIME_STEP
*******************************************************************************
     *****
*
*     THIS SUBROUTINE CALCULATES THE SOLUTION FOR THE SECOND HALF OF A TIME STEP
     USING
*     THE ADI METHOD.
*
*******************************************************************************
     *****
      SUBROUTINE SECOND_TIME_STEP(LEDGE,NEDGE,L,N,CONV,THETAINF,KP,DZ,R,
     &FF,DT,THETA,ETA,F,E,G,H,BETA,GAMMA,TEMP,DH,artetemp,airtemp)
     REAL*8 CONV,THETAINF,KP,DZ,R,FF,DT,THETA,ETA,E,F,G,H,BETA,GAMMA,
     &TEMP,DH,artetemp,airtemp
     INTEGER NEDGE,LEDGE,N,L,I,J,K,IFP1,LAST,IF
     DIMENSION E(N,L),F(N,L),G(N,L),H(N,L),BETA(N,L),GAMMA(N,L),
     &THETA(N,L),TEMP(N,L),ETA(N)
C
C
C     SECOND TIME STEP CALCULATIONS
C     DEFINE H(I,J) VALUES
C     1ST ROW PROBE
C
      H(1,1)=((-CONV*THETAINF)/(KP/(DZ*R)+CONV/2.D0))*(-1.D0/((DZ)**2.D
     $0))+THETA(1,1)*(1.D0/(FF*DT)-1.D0/((DH)**2.D0)-1.D0/(2.D0*ETA(1
     $)*DH))+THETA(2,1)*(1.D0/((DH**2.D0))+1.D0/(2.D0*ETA(1)*DH))
C
      J=1
      DO 39 I=2,NEDGE-1,1
      H(I,1)=((-CONV*THETAINF)/(KP/(DZ*R)+CONV/2.D0))*(-1.D0/((DZ**
     $2.D0)))+THETA(I-1,1)*(1.D0/((DH**2.D0))-1.D0/(2.D0*ETA(I)*
     $DH))+THETA(I,1)*(1.D0/(FF*DT)-2.D0/((DH**2.D0)))+THETA(I+1,1)*
     $(1.D0/((DH**2.D0))+1.D0/(2.D0*ETA(I)*DH))
  39  CONTINUE
C
      H(NEDGE,1)=((-CONV*THETAINF)/(KP/(DZ*R)+CONV/2.D0))*(-1.D0/((DZ**
     $2.D0)))+THETA(NEDGE-1,1)*(1.D0/((DH**2.D0))-1.D0/(2.D0*
     $ETA(I)*DH))+THETA(NEDGE,1)*(1.D0/(FF*DT)-1.D0/((DH**2.D0))+1.D0/
     $(2.D0*ETA(I)*DH))
C
C
C     LEFT PROBE COLUMN
C
      I=1
      DO 40 J=2,LEDGE,1
      H(1,J)=THETA(1,J)*(1.D0/(FF*DT)-1.D0/((DH**2.D0))-1.D0/(2.D0*
     $ETA(I)*DH))+THETA(2,J)*(1.D0/((DH**2.D0))+1.D0/(2.D0*
     $ETA(I)*DH))
  40  CONTINUE
C
C
C     RIGHT PROBE COLUMN
C
      I=NEDGE
      DO 41 J=2,LEDGE,1
      H(NEDGE,J)=THETA(NEDGE-1,J)*(1.D0/((DH**2.D0))-1.D0/(2.D0*
     $ETA(I)*DH))+THETA(NEDGE,J)*(1.D0/(FF*DT)-1.D0/((DH**2.D0))+1.D0/
     $(2.D0*ETA(I)*DH))
  41  CONTINUE
C
C
C     MIDDLE AND BOTTOM MIDDLE ROW PROBE ELEMENTS
C
      DO 42 I=2,NEDGE-1,1
      DO 43 J=2,LEDGE,1
      H(I,J)=THETA(I-1,J)*(1.D0/((DH**2.D0))-1.D0/(2.D0*ETA(I)
     $*DH))+THETA(I,J)*(1.D0/(FF*DT)-2.D0/((DH**2.D0)))+THETA(I+1,J)*
     $(1.D0/((DH**2.D0))+1.D0/(2.D0*ETA(I)*DH))
  43  CONTINUE
  42  CONTINUE
C
C
C     DEFINE TISSUE ELEMENTS
C     TOP LEFT CORNER NODE
C
      I=1
      J=LEDGE+1
      H(I,J)=THETA(1,LEDGE+1)*(1.D0/DT-1.D0/(DH**2.D0)-1.D0/
     $(ETA(I)*(2.D0*DH)))+THETA(2,LEDGE+1)*(1.D0/(DH**2.D0)+1.D0/(ETA(I)
     $*(2.D0*DH)))
C
      DO 44 J=LEDGE+2,L,1
      H(1,J)=THETA(1,J)*(1.D0/DT-1.D0/(DH**2.D0)-1.D0/(ETA(I)*(2.D0*DH
     $)))+THETA(2,J)*(1.D0/(DH**2.D0)+1.D0/(ETA(I)*(2.D0*DH)))
  44  CONTINUE
C
C
C     REST OF TOP ROW UNDER PROBE
C
      J=LEDGE+1
      DO 45 I=2,NEDGE,1
      H(I,LEDGE+1)=THETA(I-1,LEDGE+1)*(1.D0/(DH**2.D0)-1.D0/(
     $ETA(I)*(2.D0*DH)))+THETA(I,LEDGE+1)*(1.D0/DT-2.D0/(DH**2.D0))+
     $THETA(I+1,LEDGE+1)*(1.D0/(DH**2.D0)+1.D0/(ETA(I)*(2.D0*DH)))
  45  CONTINUE
C
      DO 46 I=NEDGE+1,N-1,1
      H(I,LEDGE+1)=THETA(I-1,LEDGE+1)*(1.D0/(DH**2.D0)-1.D0/(
     $ETA(I)*(2.D0*DH)))+THETA(I,LEDGE+1)*(1.D0/DT-2.D0/(DH**2.D0))
     $+THETA(I+1,LEDGE+1)*(1.D0/(DH**2.D0)+1.D0/(ETA(I)*(2.D0*DH)))
  46  CONTINUE
C
      DO 47 J=LEDGE+2,L,1
      DO 48 I=2,N-1,1
      H(I,J)=THETA(I-1,J)*(1.D0/(DH**2.D0)-1.D0/(ETA(I)*(2.D0*DH)))
     $+THETA(I,J)*(1.D0/DT-2.D0/(DH**2.D0))+THETA(I+1,J)*(1.D0/(DH**
     $2.D0)+1.D0/(ETA(I)*(2.D0*DH)))
  48  CONTINUE
  47  CONTINUE
C
      DO 49 J=LEDGE+1,L,1
      I=N
      H(N,J)=THETA(N-1,J)*(1.D0/(DH**2.D0)-1.D0/(ETA(I)*(2.D0*DH)))
     $+THETA(N,J)*(1.D0/DT-1.D0/(DH**2.D0)+1.D0/(ETA(I)*(2.D0*DH)))
  49  CONTINUE
C
C
C     USE TRIDIAGONAL MATRIX SOLVER TO GET
C     THETA VALUES AT SECOND TIME STEP
C
      IF=1
      DO 50 I=1,NEDGE,1
```

```
      BETA(I,IF)=F(I,1)
      GAMMA(I,IF)=H(I,1)/BETA(I,IF)
      IFP1=IF+1
C
      DO 51 J=IFP1,L,1
      BETA(I,J)=F(I,J)-E(I,J)*G(I,J-1)/BETA(I,J-1)
      GAMMA(I,J)=(H(I,J)-E(I,J)*GAMMA(I,J-1))/BETA(I,J)
  51  CONTINUE
C
      THETA(I,L)=GAMMA(I,L)
      LAST=L-IF
C
      DO 52 K=1,LAST,1
      J=L-K
      THETA(I,J)=GAMMA(I,J)-G(I,J)*THETA(I,J+1)/BETA(I,J)
  52  CONTINUE
  50  CONTINUE
C
C
C     MATRIX SOLVER FOR ADDITIONAL ELEMENTS
C
      IF=LEDGE+1
      DO 53 I=NEDGE+1,N,1
      BETA(I,IF)=F(I,IF)
      GAMMA(I,IF)=H(I,IF)/BETA(I,IF)
      IFP1=IF+1
C
      DO 54 J=IFP1,L,1
      BETA(I,J)=F(I,J)-E(I,J)*G(I,J-1)/BETA(I,J-1)
      GAMMA(I,J)=(H(I,J)-E(I,J)*GAMMA(I,J-1))/BETA(I,J)
  54  CONTINUE
C
      THETA(I,L)=GAMMA(I,L)
      LAST=L-IF
C
      DO 55 K=1,LAST,1
      J=L-K
      THETA(I,J)=GAMMA(I,J)-G(I,J)*THETA(I,J+1)/BETA(I,J)
C
  55  CONTINUE
  53  CONTINUE
C
      DO 56 I=1,N,1
      DO 57 J=1,L,1
      TEMP(I,J)=THETA(I,J)*(airtemp-artetemp)+artetemp
  57  CONTINUE
  56  CONTINUE
C
      RETURN
      END SUBROUTINE SECOND_TIME_STEP
*******************************************************************************
     *****
*******************************************************************************
     *****
*     SUBROUTINE FINAL_CALCULATIONS
*******************************************************************************
     *****
*
*     THIS SUBROUTINE PERFORMS THE FINAL NECESSARY CALCULATIONS FOR THE MODEL
     SOLUTION
*     IN THE PROGRAM NEWMOD.
*
*******************************************************************************
     *****
      SUBROUTINE FINAL_CALCULATIONS(KP,DZ,R,CONV,THETA,airtemp,artetemp,
     &LEDGE,NEDGE,KT,RC,TEMP,THETAINF,CRFP,N,L,PROBFLUX,CONVFLUX,RCFLUX,
     &GTEMP,ETA)
     REAL*8 KP,DZ,R,CONV,THETA,airtemp,artetemp,KT,RC,TEMP,
     &THETAINF,CRFP,THETAJM1,THETATOP,QH,QAN,QIN,TPIM,TGS,PROBFLUX,
     &TOPTEMP,QSUM,QSUM2,QSUM3,QSUM4,CONVFLUX,RCFLUX,GTEMP,ETA,ETASUM
     INTEGER NEDGE,LEDGE,N,L,I
     DIMENSION THETA(N,L),TEMP(N,L),THETAJM1(NEDGE),THETATOP(NEDGE),
     &QH(NEDGE),QAN(NEDGE),QIN(NEDGE),TPIM(NEDGE),TGS(NEDGE),
     &TOPTEMP(NEDGE),ETA(N)
C
C
      DO 58 I=1,NEDGE,1
C
C
C     COMPUTE HEAT FLUX AT PROBE TOP
C
      THETAJM1(I) = (((KP/(DZ*R))-(CONV/2.D0))*THETA(I,1)+(CONV*
     $THETAINF))/((KP/(DZ*R))+CONV/2.D0)
      THETATOP(I) = (THETA(I,1)+THETAJM1(I))/2.D0
      QH(I)=CONV*((THETATOP(I)-THETAINF)*(airtemp-artetemp))
      TOPTEMP(I) = THETATOP(I)*(airtemp-artetemp)+artetemp
C
C
C     COMPUTE HEAT FLUX AT INTERFACE OF TISSUE AND PROBE
C
      QAN(I)=((airtemp-artetemp)*((THETA(I,LEDGE+1)-THETA(I,LEDGE))
     $/(RC+((DZ*R)/(2.D0*KT))+((DZ*R)/(2.D0*KP)))))
C
C
C     COMPUTE HEAT FLUX USING NODES WITHIN PROBE
C
      QIN(I)=KP*(TEMP(I,LEDGE)-TEMP(I,1))/((LEDGE-1)*DZ*R)
C
C
C     COMPUTE GAGE SURFACE TEMPERATURE
C
      TPIM(I)=CRFP*(TEMP(I,LEDGE+1)-TEMP(I,LEDGE))+TEMP(I,LEDGE)
      TGS(I)=(TEMP(I,LEDGE)+TPIM(I))/2.D0
C
  58  CONTINUE
C
      QSUM = 0.D0
      QSUM2 = 0.D0
     ETASUM=0.D0
     QSUM3 = 0.D0
     QSUM4 = 0.D0
C
      DO 59 I=1,NEDGE,1
        QSUM  = QSUM + QH(I)
        QSUM2 = QSUM2 + QIN(I)
       QSUM3 = QSUM3 + QAN(I)
       QSUM4 = QSUM4 + TGS(I)
  59  CONTINUE

C    DO 818 I=1,NEDGE,1
C      QSUM2= QSUM2 + ETA(I)*QIN(I)
C      ETASUM= ETASUM +ETA(I)
C  818 CONTINUE

C
C
C     ADD DESIRED VALUES TO MODEL OUTPUT DATA ARRAYS
C
     CONVFLUX=QSUM/(DBLE(NEDGE))
     PROBFLUX=QSUM2/(DBLE(NEDGE))
C    PROBFLUX=QSUM2/ETASUM
     RCFLUX=QSUM3/(DBLE(NEDGE))
     GTEMP=QSUM4/(DBLE(NEDGE))
C
      RETURN
      END SUBROUTINE FINAL_CALCULATIONS
*******************************************************************************
     *****
*******************************************************************************
     *****
*     SUBROUTINE SMOOTH_PROBE_FLUX
*******************************************************************************
     *****
*
```

```
*      THIS SUBROUTINE SMOOTHS OUT THE OSCILLATING PROBE HEAT FLUX FOR THE
*      PROGRAM NEWMOD.
*
********************************************************************************
      *****
       SUBROUTINE SMOOTH_PROBE_FLUX(PROBQ,NTSTP,SMOOTHQ)
      REAL*8 PROBQ,A,B,C,D,E,SMOOTHQ
      INTEGER NTSTP,I
      DIMENSION PROBQ(NTSTP),SMOOTHQ(NTSTP)
C
C
C      SET CONSTANTS FOR SMOOTHING SCHEME
C
      A=0.1D0
      B=0.25D0
      C=0.3D0
      D=B
      E=A
C
C
C      PERFORM SMOOTHING
C
C
       SMOOTHQ(1)=(C*PROBQ(1)+D*PROBQ(2)+E*PROBQ(3))/(A+B+C+D+E)
      SMOOTHQ(2)=(B*PROBQ(1)+C*PROBQ(2)+D*PROBQ(3)+E*PROBQ(4))/(A+B+C+D+
      &E)
      DO 500 I=3,NTSTP-2,1
        SMOOTHQ(I)=A*PROBQ(I-2)+B*PROBQ(I-1)+C*PROBQ(I)+D*PROBQ(I+1)+
      &E*PROBQ(I+2)
  500 CONTINUE
      SMOOTHQ(NTSTP-1)=(A*PROBQ(NTSTP-3)+B*PROBQ(NTSTP-2)+
      &C*PROBQ(NTSTP-1)+D*PROBQ(NTSTP))/(A+B+C+D)
      SMOOTHQ(NTSTP)=(A*PROBQ(NTSTP-2)+B*PROBQ(NTSTP-1)+C*PROBQ(NTSTP))/
      &(A+B+C)
C
       RETURN
       END SUBROUTINE SMOOTH_PROBE_FLUX
********************************************************************************
      *****
C
C
C      END OF SUBROUTINE MODEL, RETURN VALS AND END SUBROUTINE
C
       END SUBROUTINE MODEL
********************************************************************************
      *****
********************************************************************************
      *****
```

A.2 Input File Generation

This appendix contains the Matlab file used to sort the ASCII file output by Test Point and create an input file for the parameter estimation program. The program asks the user to enter a series of experimental parameters and other data. An electronic version of this code is available in datasort.m.

```
%  This Matlab program reads in an ASCII file as output by the Test Point
%  data acquisition file 'biosens.t'  The user is prompted to input the
%  raw data file name, an output file name, the parameters of the experiment,
%  values for the biomodel mesh size, and a bias for the heat flux measurement.
%
%  The code then sorts the data, removes unnecessary data from the beginning
%  of the data set, and creates a file that is ready to be read by the
%  parameter estimation routine.
%
%  Created By:   Alex Cardinali
%  Last Update:  04.05.02

clear all, close all

%Add the appropriate path to Matlab's search string and create a variable to record it
fprintf(1,'%s\n','Remember to enter the correct file path to the folder holding the input files')
fprintf(1,'%s\n','by editing datasort.m.  The folder that is entered must contain the input')
fprintf(1,'%s\n','files and will contain the output files generated by this m-file.')

addpath c:\Alex_Backup\Matlab_Files\Access\%MUST CHANGE HERE AND ON LINE 34

morefiles=1;
while morefiles>0.5

  %Clear variables from last iteratoin, prompt and open new raw data file, read in data set
  clear all
  filename=input('Enter the name of the Raw data file:  ','s');
  fid=fopen(filename);
  datainput=fscanf(fid,'%g %g %g %g',[4 inf]);
  datainput=datainput';
  fclose(fid);

  %Create output file
  outputfile=input('Enter the name of the output file:  ','s');
  filepath='c:\Alex_Backup\Matlab_Files\Access\';
  fulloutputname=strcat(filepath,outputfile);

  %Read in experimental variables, parameter guesses, and heat flux bias
  arterial_temperature=input('Enter the body temperature:  ');
  air_temperature=input('Enter the air temperature:  ');
  initial_guesses(1)=input('Enter the blood perfusion guess:  ');
  initial_guesses(2)=input('Enter the contact resistance guess:  ');
  heat_flux_bias=input('Enter heat flux bias:  ');

  %Allow the user the option to weight the input data
  answer=input('Do you want to weight the end data (yes=1,no=2)');
  if answer == 1
    weight_start=input('Starting at what time in seconds:   ')*9.5;
    weight_start=round(weight_start);
    weight_factor=input('By what factor:    ');
  end

  %This loop set sorts the data and creates the arrays needed for the output file
  checkpoint=1;
  for i=2:length(datainput(:,1))
    if checkpoint == 1
      if datainput(i,2) < 0
```

```
        for b=1:100
          if datainput(i+b,2) > 0
            if checkpoint == 1
              skin_temperature=datainput(i+b,3);
              for n=1:length(datainput(:,1))-(i+b)
                heatflux(n)=datainput(n+i+b-1,2)-heat_flux_bias;
                counter(n)=n;
                time(n)=n/9.5;
                checkpoint=2;
              end
            end
          end
        end
      end
    end
  end

  %Constants input;  must occur this late b/c of variables(1)
  variables(1)=length(counter);
  variables(2)=2;
  variables(3)=1;

  %Set mesh parameters
  mesh(1)=10;
  mesh(2)=10;
  mesh(3)=20;
  mesh(4)=150;

  temperatures(1)=air_temperature;
  temperatures(2)=arterial_temperature;
  temperatures(3)=skin_temperature;

  variance=(std(heatflux))^2;

  dataout(:,1)=counter';
  dataout(:,2)=heatflux';
  dataout(:,3)=variance;
  dataout(:,4)=time';

  %Weight the data if desired
  if answer==1
    for n=1:145
      dataout(n,3)=variance*weight_factor;
    end
  end

  temp=dataout';

  %Formatted output and file creation
  fid=fopen(fulloutputname,'w');
  fprintf(fid,'%-3.0f %1.0f %1.0f \n',variables);
  fprintf(fid,'%-2.0f %2.0f %2.0f %3.0f \n',mesh);
  fprintf(fid,'%-5.3f %5.3f \n',initial_guesses);
  fprintf(fid,'%-5.2f %5.2f %5.2f \n',temperatures);
  fprintf(fid,'%-6.0f %11.4f %15.4f %9.4f \n',temp);
  fclose(fid);

  fid2=fopen('expdata','w');
  fprintf(fid2,'%-6.0f %11.4f %15.4f %9.4f \n',temp);
  fclose(fid2);

  %Create graph to visually check that the new data set is appropriate
  plot(datainput(:,4),datainput(:,2),'r')
  hold
  plot(dataout(:,4),dataout(:,2),'g')
  legend('Raw Data','Sorted Data',filename)

  morefiles=input('Do you want to sort another file (1=yes, 0=no)?  ');

end
```

A.3 Comparison of Estimated Data Set to Experimental Data

This appendix contains the Matlab file used to plot a comparison of the estimated data set to the experimental data set by reading in the file output by the parameter estimation code. An electronic version of this code is available in estcomp.m.

```
clear all, close all

addpath d:\data\access
filename=input('Enter the name of the input data file:  ','s');
graphtext=['Data Set:   ',filename];
datetext=['Plot Date:  ',date];

fid=fopen(filename);
data=fscanf(fid,'%g %g %g %g',[4 inf]);
data=data';
fclose(fid);

plot(data(:,4),data(:,2))
hold
plot(data(:,4),data(:,3),'LineWidth',2)
%title('Heat Flux vs. Time')
xlabel('Time (s)')
ylabel('Heat Flux (W/m^2)')
%grid
orient tall
orient landscape
axis([0 70 0 3500])
legend('Experimental Data','Estimated Data',' ',graphtext,datetext)
```

A.4 Smoothing Function Test Program

This appendix contains the Matlab file used to test different heat flux smoothing schemes. An electronic version of this code is available in smoothitcomp.m.

```
clear all,close all

addpath c:\Alex_Backup\Matlab_Files\Access\
filename1=input('Enter the name of the low time step input data file:  ','s');
filename2=input('Enter the name of the regular time step input data file:  ','s');
graphtext=['Data Sets:   ',filename1,',',filename2];
datetext=['Plot Date:  ',date];

fid1=fopen(filename1);
data1=fscanf(fid1,'%g %g %g %g %g',[5 inf]);
data1=data1';
fclose(fid1);

fid2=fopen(filename2);
data2=fscanf(fid2,'%g %g %g %g %g',[5 inf]);
data2=data2';
fclose(fid2);

q=data2(:,3);
t=data2(:,1);

for m=1:length(data2(:,1))
  avgflux(m)=(data2(m,2)+data2(m,5))/2;
end

q=avgflux;

A=0.1;
B=0.25;
C=0.3;
D=B;
E=A;

qnew(1)=(C.*q(1)+D.*q(2)+E.*q(3))./(A+B+C);%+D+E);
qnew(2)=(B.*q(1)+C.*q(2)+D.*q(3)+E.*q(4))./(A+B+C+D);%+E);
for n=3:1:length(q)-2
  qnew(n)=A.*q(n-2)+B.*q(n-1)+C.*q(n)+D.*q(n+1)+E.*q(n+2);
end
qnew(length(q)-1)=(A.*q(length(q)-3)+B.*q(length(q)-2)+C.*q(length(q)-1)+D.*q(length(q))./(A+B+C+D);
qnew(length(q))=(A.*q(length(q)-2)+B.*q(length(q)-1)+C.*q(length(q)))./(A+B+C);

for m=1:length(data2(:,1))
  number=42+(m-1)*43;
  correlator(m,2)=data1(number,3);
  residual(m)=data2(m,3)-data1(number,3);
  avgflux(m)=(data2(m,2)+data2(m,5))/2;
end

ssy=0.0;numerator=0.0;denominator1=0.0;denominator2=0.0;
correlator(:,1)=qnew';
for l=1:length(data2(:,1))
  ssy=ssy+(correlator(l,1)-correlator(l,2))^2/(std(qnew))^2;
  numerator=numerator+(correlator(l,1)-mean(correlator(:,1))).*(correlator(l,2)-mean(correlator(:,2)));
  denominator1=denominator1+(correlator(l,1)-mean(correlator(:,1)))^2;
  denominator2=denominator2+(correlator(l,2)-mean(correlator(:,2)))^2;
end

correlation=numerator/(sqrt(denominator1).*sqrt(denominator2))
ssy

%plot(data2(:,1),residual)
```

```
figure
plot(data2(:,1),qnew,'r')
hold
plot(data2(:,1),qnew,'ro')
plot(data1(:,1),data1(:,3))
%title('Smoothed vs. Non-Smoothed Data')
xlabel('Time (s)'),ylabel('Heat Flux (W/m^2)')
axis([0 8 1800 2900])
legend('Unstable Data Set - Smoothed','Unstable Data Set Points - Smoothed','Stable Data Set')

figure
plot(data1(:,1),data1(:,3))
hold
plot(data2(:,1),avgflux)
%figure
%plot(t,q,'r')
%hold
%plot(t,qnew)
%orient tall,orient landscape
%title('Smoothed vs. Non-Smoothed Data')
%xlabel('time'),ylabel('Heat Flux')
%gtext({'qnew(n)=A.*q(n-2)+B.*q(n-1)+C.*q(n)+D.*q(n+1)+E.*q(n+2)','A=0.1','B=0.25','C=0.3','D=0.25','E=0.1'})

%figure
%plot(t,q,'r')
%hold
%plot(t,qnew)
%axis([0 7 2750 3150])
%orient tall,orient landscape
%title('Smoothed vs. Non-Smoothed Data: Close Up')
%xlabel('time'),ylabel('Heat Flux')
```

A.5 Model Output Comparison

This appendix contains the Matlab file used to compare the different heat flux data sets (convective heat flux, unstable thru-probe heat flux, smoothed thru-probe heat flux, heat flux across the contact resistance)output by accessing the biomodel. An electronic version of this code is available in oscillationcomp.m.

```
clear all,close all

addpath c:\Alex_Backup\Matlab_Files\Access\
filename=input('Enter the name of the input data file:  ','s');
graphtext=['Data Set:   ',filename];
datetext=['Plot Date:  ',date];

fid=fopen(filename);
data=fscanf(fid,'%g %g %g %g %g',[5 inf]);
data=data';
fclose(fid);

plot(data(:,1),data(:,2),'r')
hold
plot(data(:,1),data(:,5),'r')
plot(data(:,1),data(:,3),'b')
plot(data(:,1),data(:,4),'b','LineWidth',2)
orient tall,orient landscape
title('Smoothed vs. Non-Smoothed Data')
xlabel('time'),ylabel('Heat Flux')
%gtext({'qnew(n)=A.*q(n-2)+B.*q(n-1)+C.*q(n)+D.*q(n+1)+E.*q(n+2)','A=0.1','B=0.25','C=0.3','D=0.25','E=0.1'})

figure
plot(data(:,1),data(:,2),'r:')
hold
plot(data(:,1),data(:,5),'r:')
plot(data(:,1),data(:,3),'b')
plot(data(:,1),data(:,4),'b','LineWidth',2)
axis([0 10 1000 3500])
orient tall,orient landscape
%title('Smoothed vs. Non-Smoothed Data: Close Up')
xlabel('Time (s)'),ylabel('Heat Flux (W/m^2)')
gtext({'<--- Convective Heat Flux'})
gtext({'<--- Heat Flux Across the Contact Resistance'})

for i=1:length(data(:,1))
   averageddata(i)=(data(i,2)+data(i,5))/2;
end

figure
plot(data(:,1),averageddata,'r')
hold
plot(data(:,1),data(:,4),'b')
axis([0 5 2200 2400])
```

Appendix B Graphical Representation of Recorded Data

B.1 Human Forearm Tests

This Appendix contains plots of the human forearm exercise tests outlined in Table 5.1. Each figure contains the experimentally recorded data plotted with the converged numerical solution for comparison. The data sets appear in the order they are listed below. The data file used to create the plot is noted in the legend of each graph. These figures were made using the estcomp.m Matlab program.

Data Sets

Data Set	Time (min)	$T_{arterial}$ (°C)	T_{air} (°C)	T_{skin} (°C)	Bp (ml/ml/s)	Rc (m^2K/W)	SSY
rest1	0	36.2	23.4	33.1	0.00048	0.00046	0.173
rest2	5	36.2	23.4	32.2	0.00068	0.00032	0.111
rest3	10	36.5	23.4	31.8	0.00019	0.00057	0.293
Average Values for Resting Measurements					0.00045	0.00045	0.192
work1	20	36.4	23.0	32.0	0.00161	0.00049	0.214
work2	25	36.2	23.1	32.9	0.00126	0.00032	0.160
work3	30	36.4	23.1	32.8	0.00043	0.00002	0.159
work4	35	36.5	23.0	33.0	0.00112	0.00028	0.332
work5	40	36.6	23.0	33.2	0.00074	0.00014	0.186
Average Values for Exercise Measurements					0.00103	0.00025	0.210

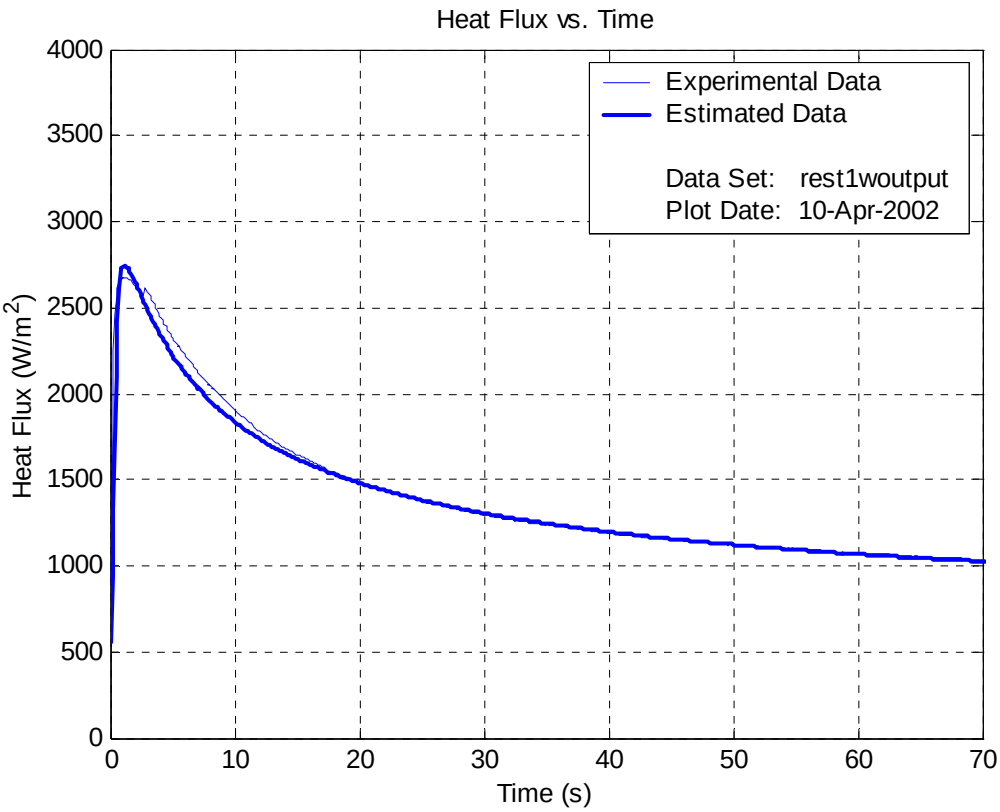
Heat Flux vs. Time
Experimental Data
Estimated Data
Data Set: rest1woutput
Plot Date: 10-Apr-2002
Heat Flux (W/m2)
Time (s)
0
500
1000
1500
2000
2500
3000
3500
4000
0
10
20
30
40
50
60
70

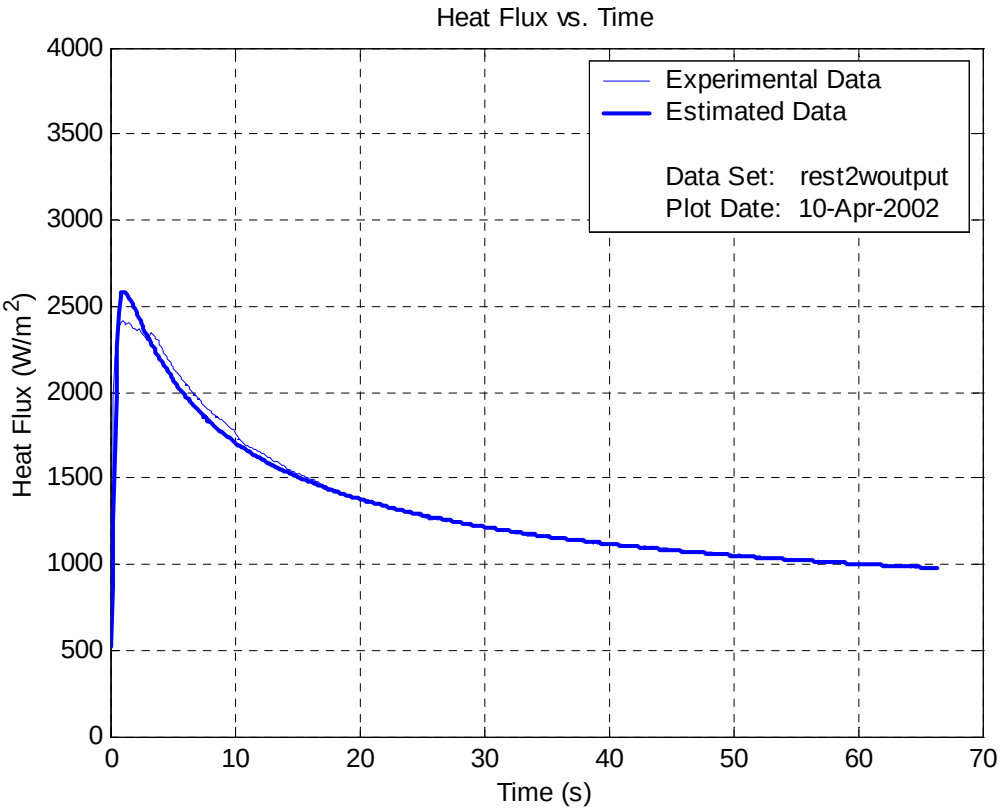
Heat Flux vs. Time
Experimental Data
Estimated Data
Data Set: rest2woutput
Plot Date: 10-Apr-2002
Heat Flux (W/m2)
Time (s)
0
500
1000
1500
2000
2500
3000
3500
4000
0
10
20
30
40
50
60
70

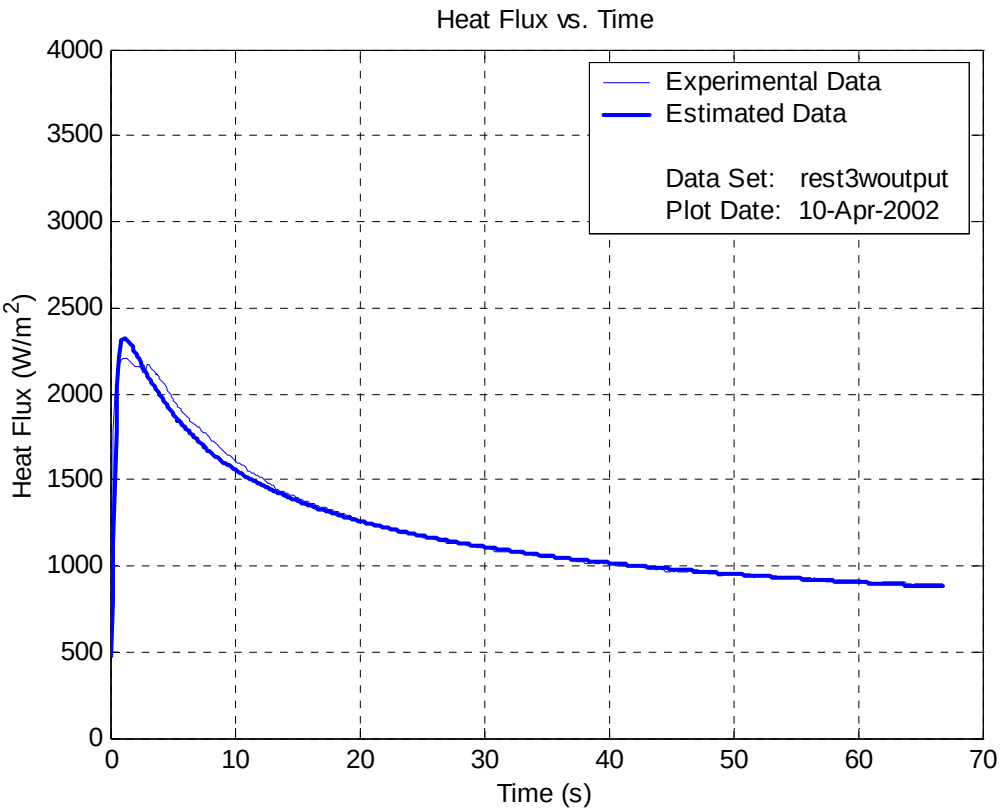
Heat Flux vs. Time
Experimental Data
Estimated Data
Data Set: rest3woutput
Plot Date: 10-Apr-2002
Heat Flux (W/m2)
Time (s)
0
500
1000
1500
2000
2500
3000
3500
4000
0
10
20
30
40
50
60
70

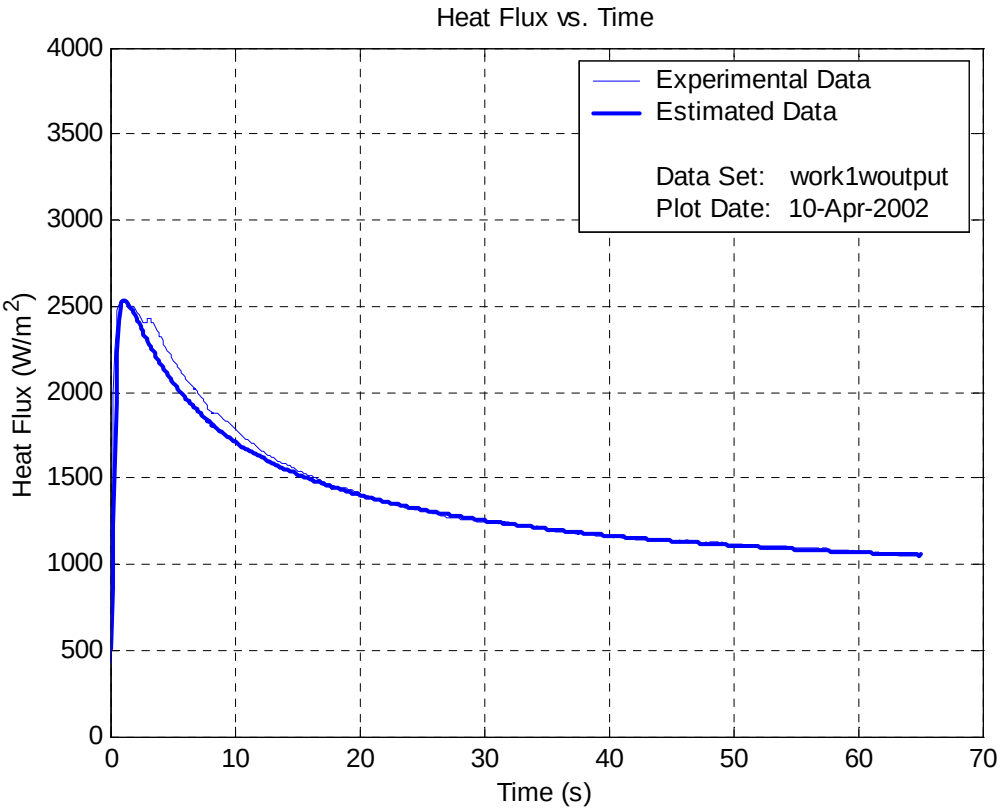
Heat Flux vs. Time
Experimental Data
Estimated Data
Data Set: work1woutput
Plot Date: 10-Apr-2002
Heat Flux (W/m2)
Time (s)
0
500
1000
1500
2000
2500
3000
3500
4000
0
10
20
30
40
50
60
70

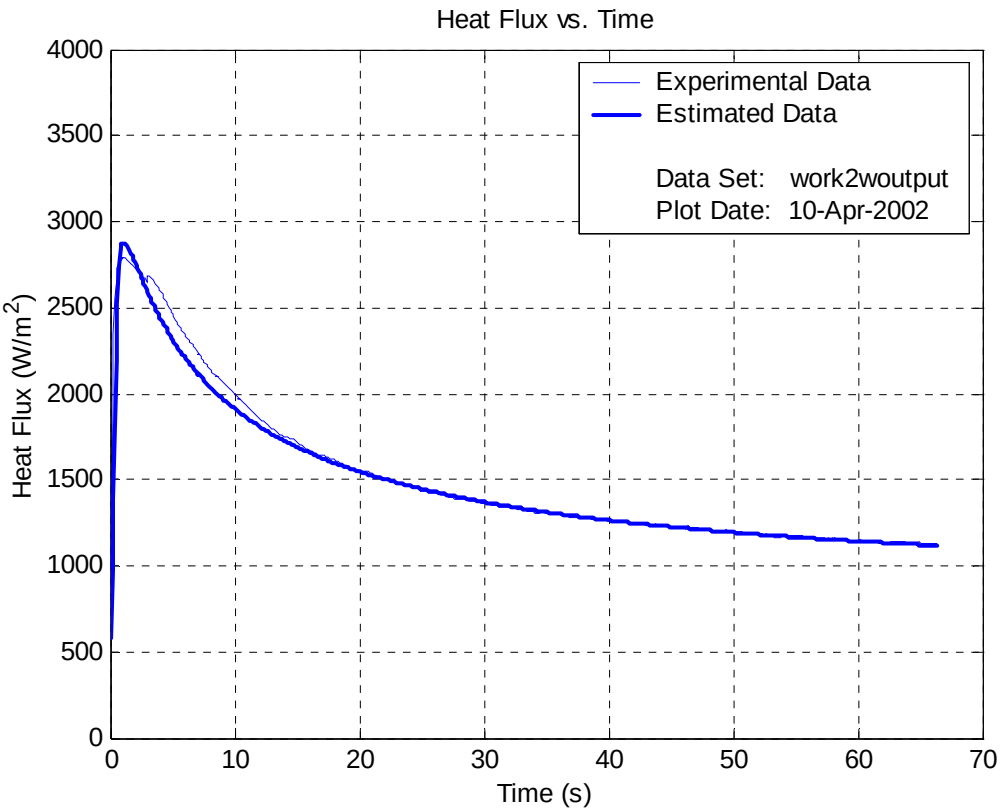
Heat Flux vs. Time
Experimental Data
Estimated Data
Data Set: work2woutput
Plot Date: 10-Apr-2002
Heat Flux (W/m^2)
Time (s)
0
500
1000
1500
2000
2500
3000
3500
4000
0
10
20
30
40
50
60
70

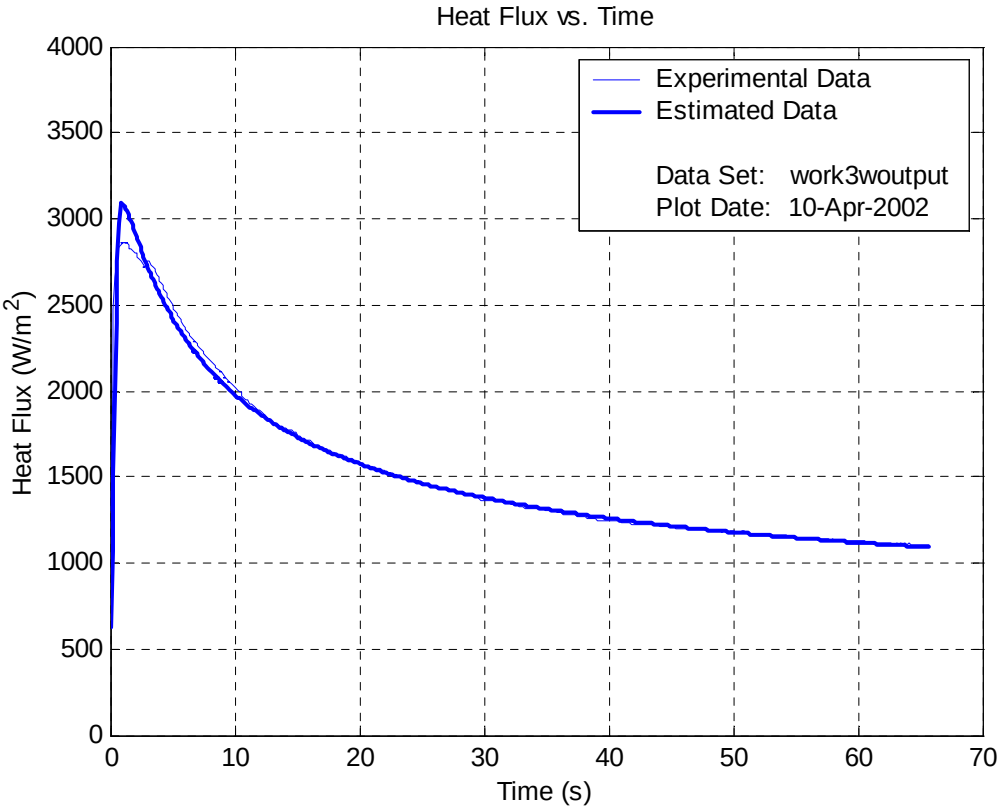
Heat Flux vs. Time
Experimental Data
Estimated Data
Data Set: work3woutput
Plot Date: 10-Apr-2002
Heat Flux (W/m^2)
Time (s)
0
500
1000
1500
2000
2500
3000
3500
4000
0
10
20
30
40
50
60
70

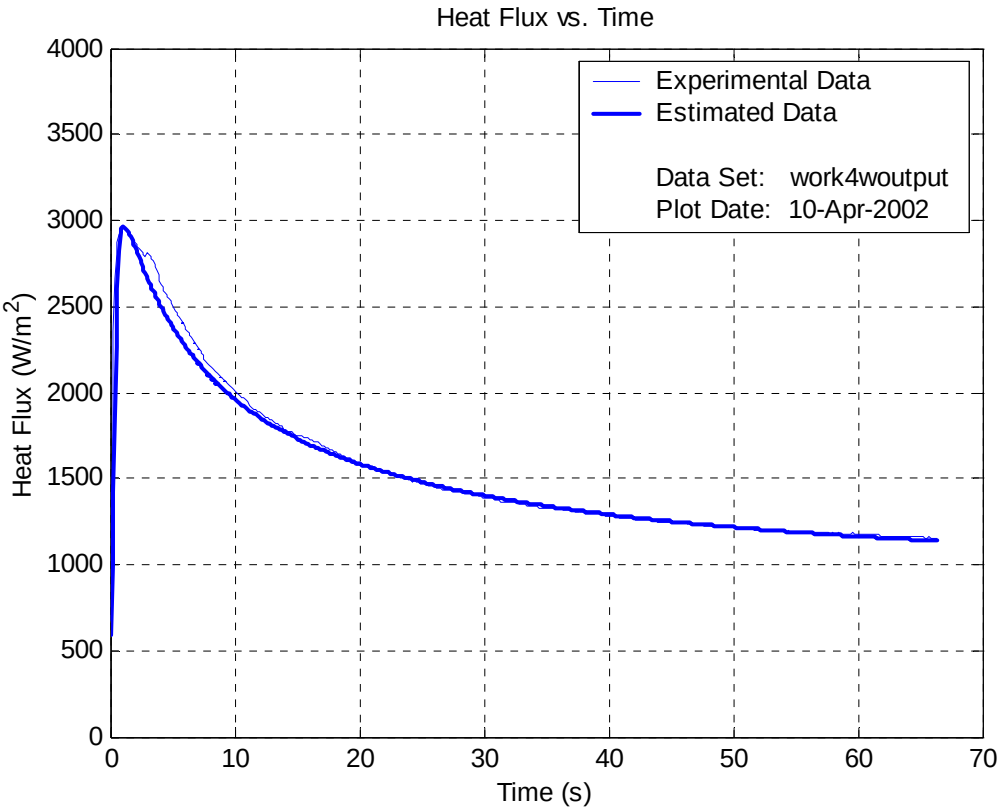
Heat Flux vs. Time
Experimental Data
Estimated Data
Data Set: work4woutput
Plot Date: 10-Apr-2002
Heat Flux (W/m2)
Time (s)
0
500
1000
1500
2000
2500
3000
3500
4000
0
10
20
30
40
50
60
70

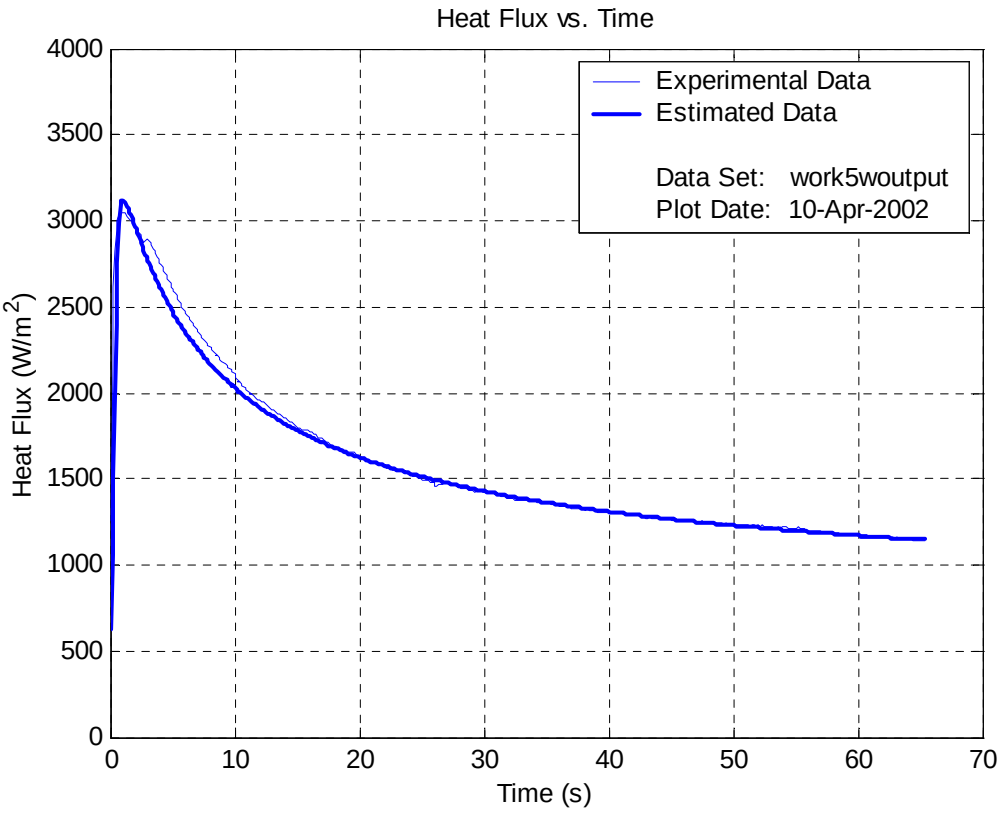
Heat Flux vs. Time
Experimental Data
Estimated Data
Data Set: work5woutput
Plot Date: 10-Apr-2002
Heat Flux (W/m2)
Time (s)
0
500
1000
1500
2000
2500
3000
3500
4000
0
10
20
30
40
50
60
70

B.2 Spay Test Experimental Results

This Appendix contains plots of the canine spay tests outlined in Table 5.2. Each figure contains the experimentally recorded data plotted with the converged numerical solution for comparison. The data sets appear in the order they are listed below. The data file used to create the plot is noted in the legend of each graph. These figures were made using the estcomp.m Matlab program.

Data Sets

Data Set	Time (min)	$T_{arterial}$ (°C)	T_{air} (°C)	T_{skin} (°C)	Bp (ml/ml/s)	Rc (m^2K/W)	SSY
adog data recorded: 7.19.2001							
adog1	0	35.70	20.35	32.95	0.00929	0.00352	0.241
adog2	10	35.60	20.45	32.56	0.01038	0.00371	0.269
adog3	20	35.60	19.65	32.36	0.00849	0.00390	0.379
adog4	30	35.40	19.65	32.21	0.00620	0.00328	0.558
adog5	40	35.40	19.45	32.28	0.01054	0.00339	1.501
adog6	50	35.20	19.35	32.39	0.01540	0.00313	0.199
adog7	63	35.20	19.05	32.84	0.01878	0.00301	0.273
bdog data recorded: 7.24.2001							
bdog1	0	36.00	22.60	34.39	0.00646	0.01070	0.847
bdog2	10	35.40	21.50	33.38	0.01270	0.00914	0.544
† bdog3	23	35.28	21.50	33.43	0.00000	0.00737	2.296
bdog4	33	35.22	21.40	32.84	0.00496	0.00856	0.180
† bdog5	43	35.06	20.60	32.82	0.00000	0.00479	65.650
† bdog6	53	35.00	20.30	32.62	0.00000	0.00122	270.491
bdog7	63	35.00	20.10	32.67	0.00034	0.00884	1.217
cdog data recorded: 7.26.2001							
cdog1	0	34.44	22.50	30.82	0.00768	0.00249	0.195
cdog2	10	34.28	21.90	30.43	0.00909	0.00345	0.353
cdog3	18	34.06	21.60	30.48	0.01167	0.00415	0.610

† These data sets have more variation than others in the same test. The cause of the added noise is unknown at this time, however it is important enough to call question to these data sets. Therefore, these data sets are regarded as being of questionable experimental accuracy.

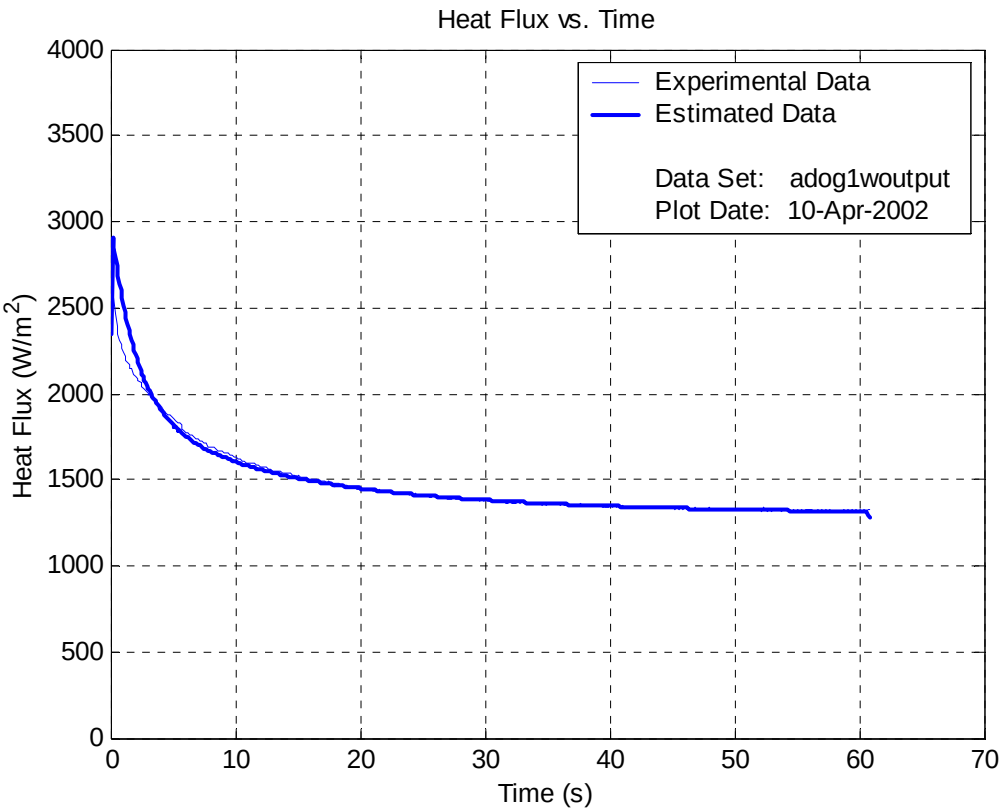
Heat Flux vs. Time
Experimental Data
Estimated Data
Data Set: adog1woutput
Plot Date: 10-Apr-2002
Heat Flux (W/m2)
Time (s)
0
500
1000
1500
2000
2500
3000
3500
4000
0
10
20
30
40
50
60
70

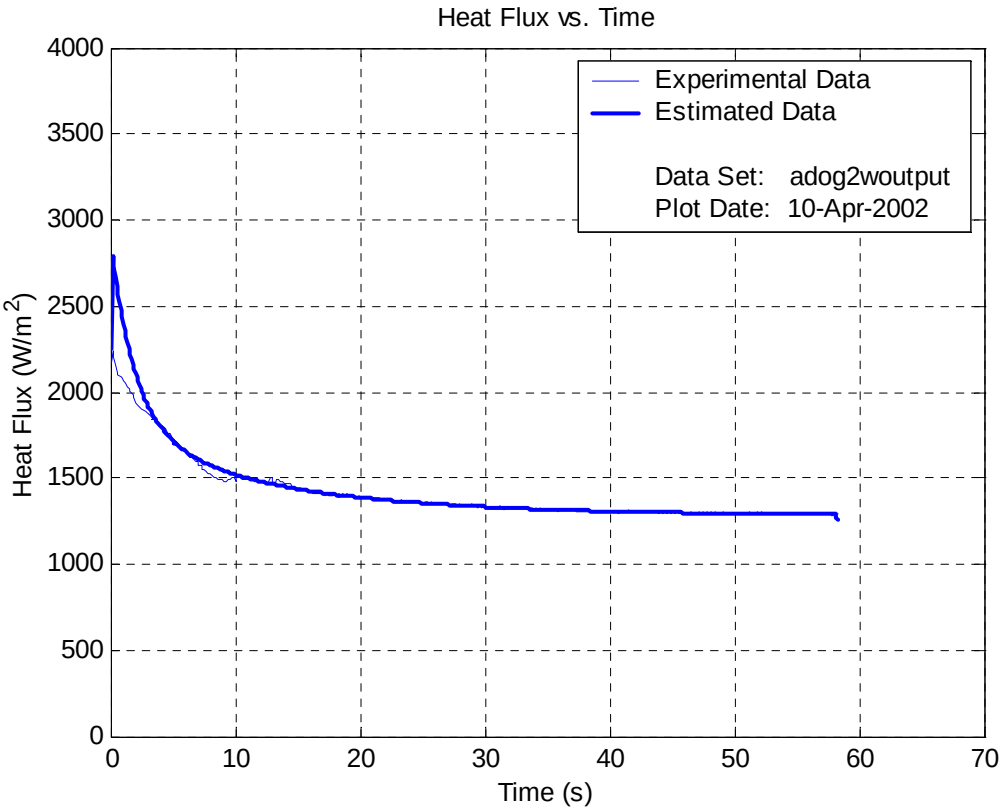
Heat Flux vs. Time
Experimental Data
Estimated Data
Data Set: adog2woutput
Plot Date: 10-Apr-2002
Heat Flux (W/m2)
Time (s)
0
500
1000
1500
2000
2500
3000
3500
4000
0
10
20
30
40
50
60
70

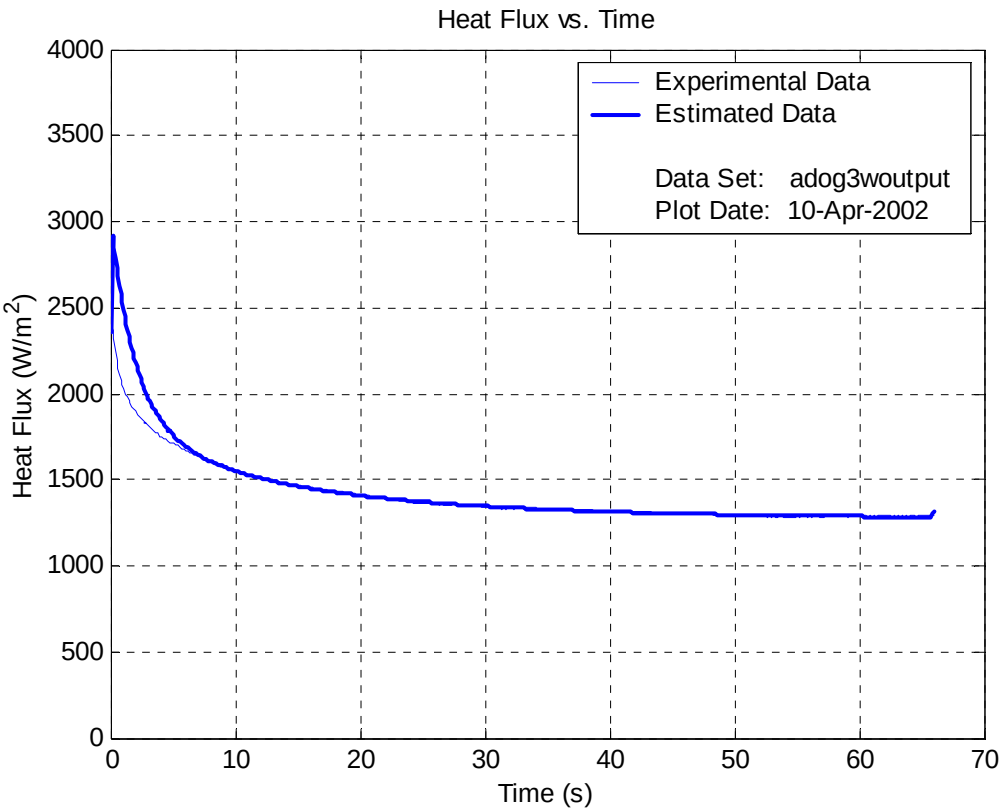
Heat Flux vs. Time
Experimental Data
Estimated Data
Data Set: adog3woutput
Plot Date: 10-Apr-2002
Heat Flux (W/m2)
Time (s)
0
500
1000
1500
2000
2500
3000
3500
4000
0
10
20
30
40
50
60
70

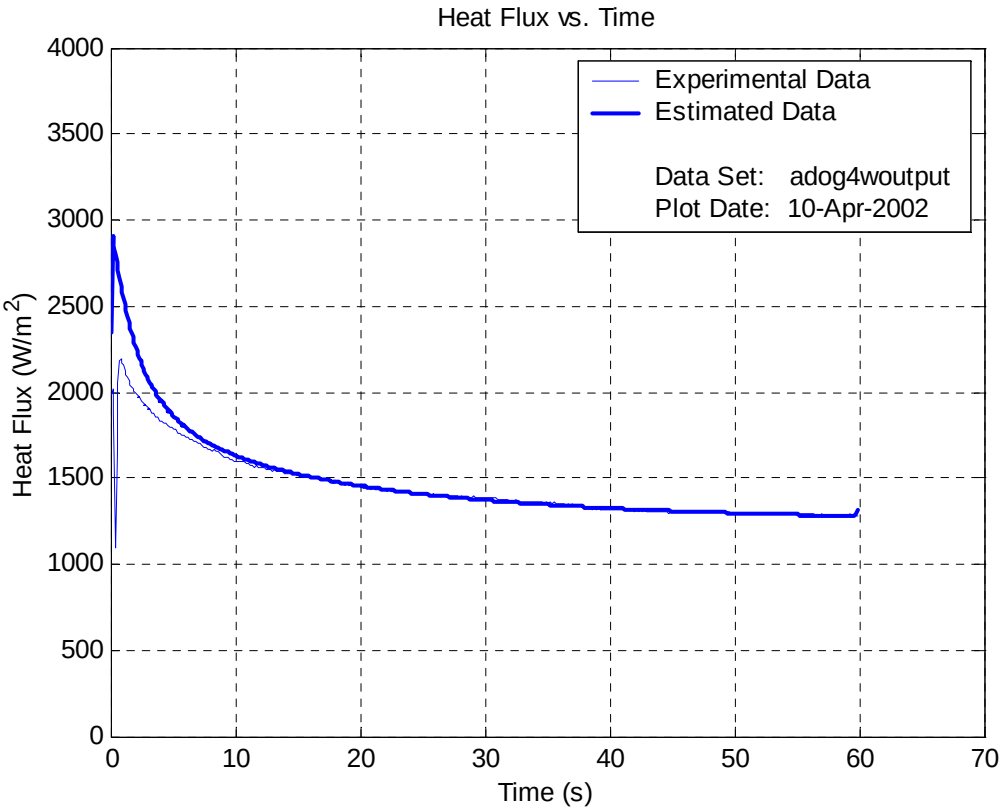
Heat Flux vs. Time
Experimental Data
Estimated Data
Data Set: adog4woutput
Plot Date: 10-Apr-2002
Heat Flux (W/m2)
Time (s)
0
500
1000
1500
2000
2500
3000
3500
4000
0
10
20
30
40
50
60
70

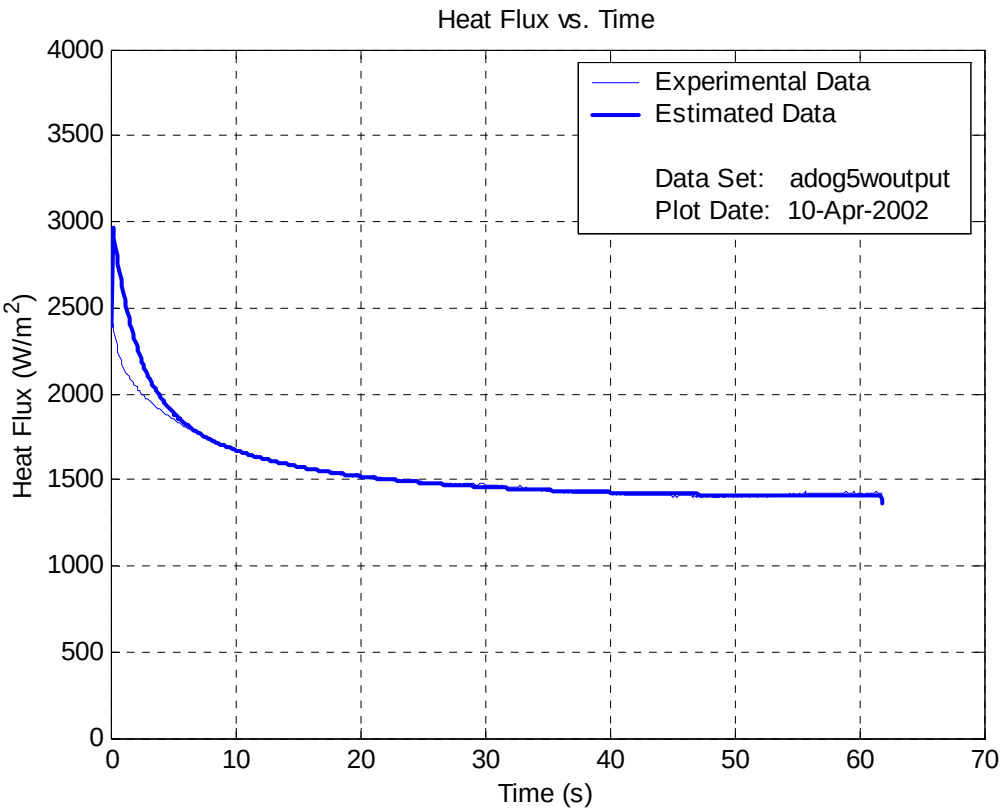
Heat Flux vs. Time
Experimental Data
Estimated Data
Data Set: adog5woutput
Plot Date: 10-Apr-2002
Heat Flux (W/m2)
Time (s)
0
500
1000
1500
2000
2500
3000
3500
4000
0
10
20
30
40
50
60
70

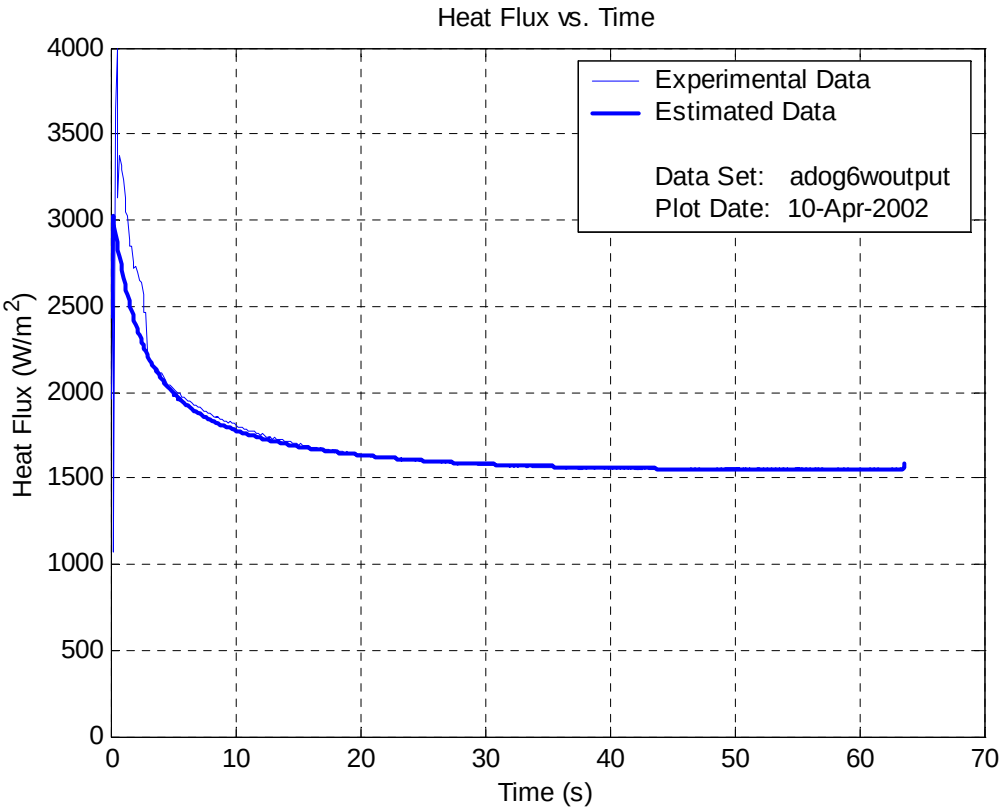
Heat Flux vs. Time
Experimental Data
Estimated Data
Data Set: adog6woutput
Plot Date: 10-Apr-2002
Heat Flux (W/m2)
Time (s)
0
500
1000
1500
2000
2500
3000
3500
4000
0
10
20
30
40
50
60
70

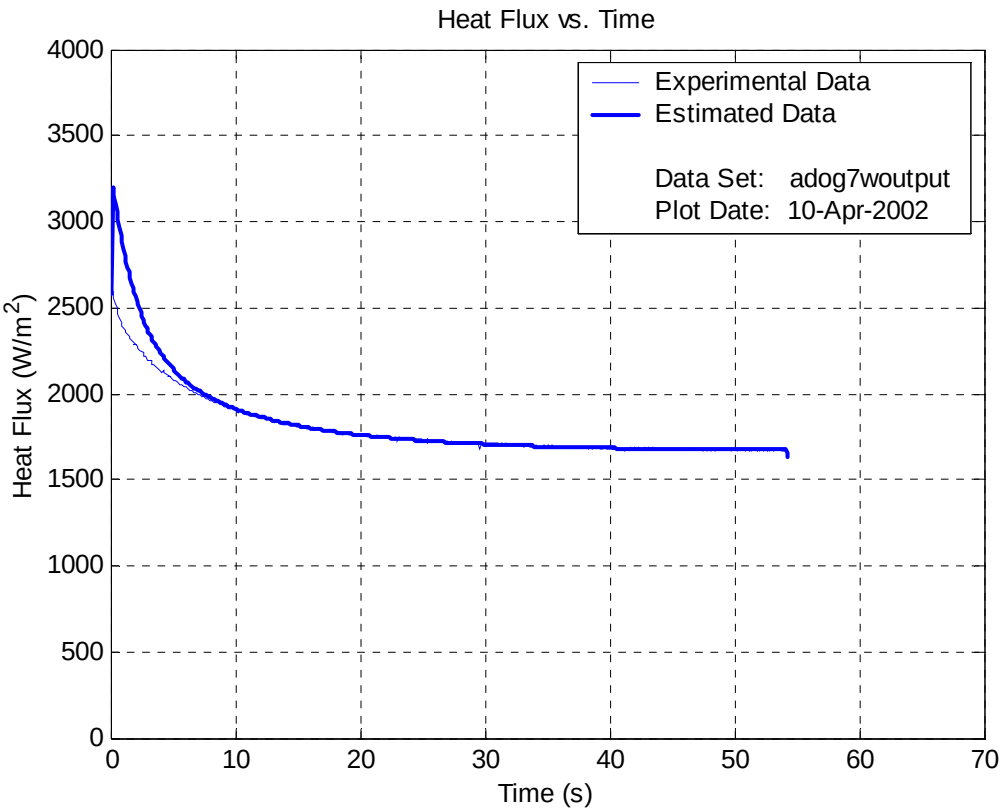
Heat Flux vs. Time
Experimental Data
Estimated Data
Data Set: adog7woutput
Plot Date: 10-Apr-2002
Heat Flux (W/m2)
Time (s)
0
500
1000
1500
2000
2500
3000
3500
4000
0
10
20
30
40
50
60
70

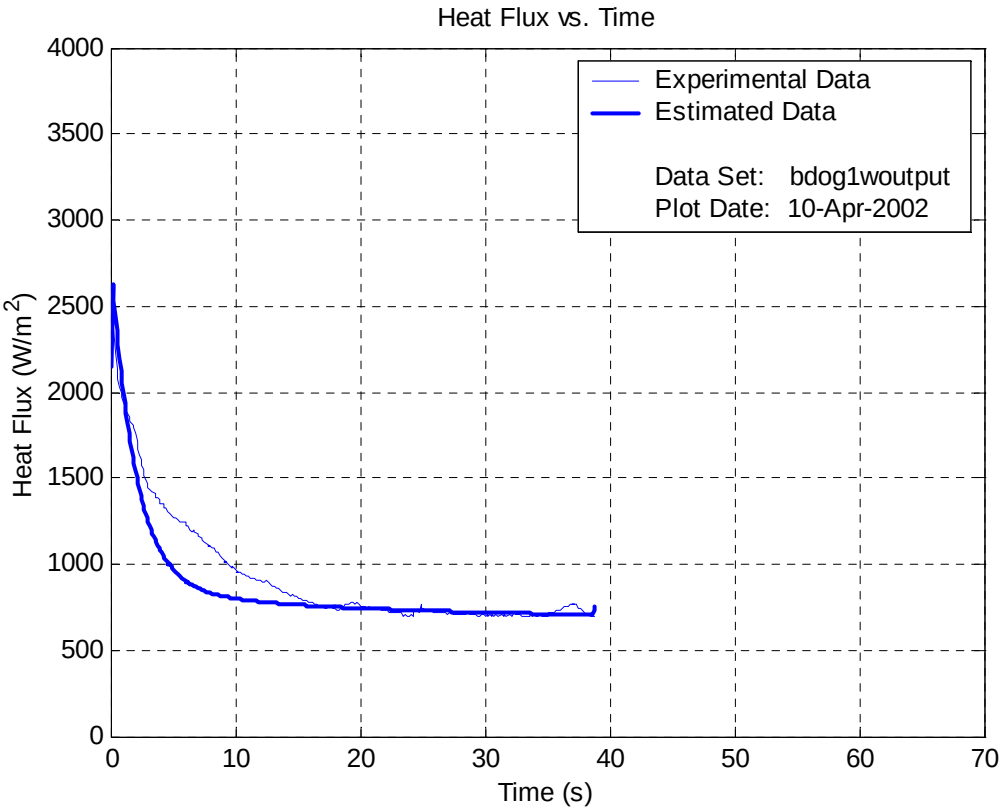
Heat Flux vs. Time
Experimental Data
Estimated Data
Data Set: bdog1woutput
Plot Date: 10-Apr-2002
Heat Flux (W/m2)
Time (s)
0
500
1000
1500
2000
2500
3000
3500
4000
0
10
20
30
40
50
60
70

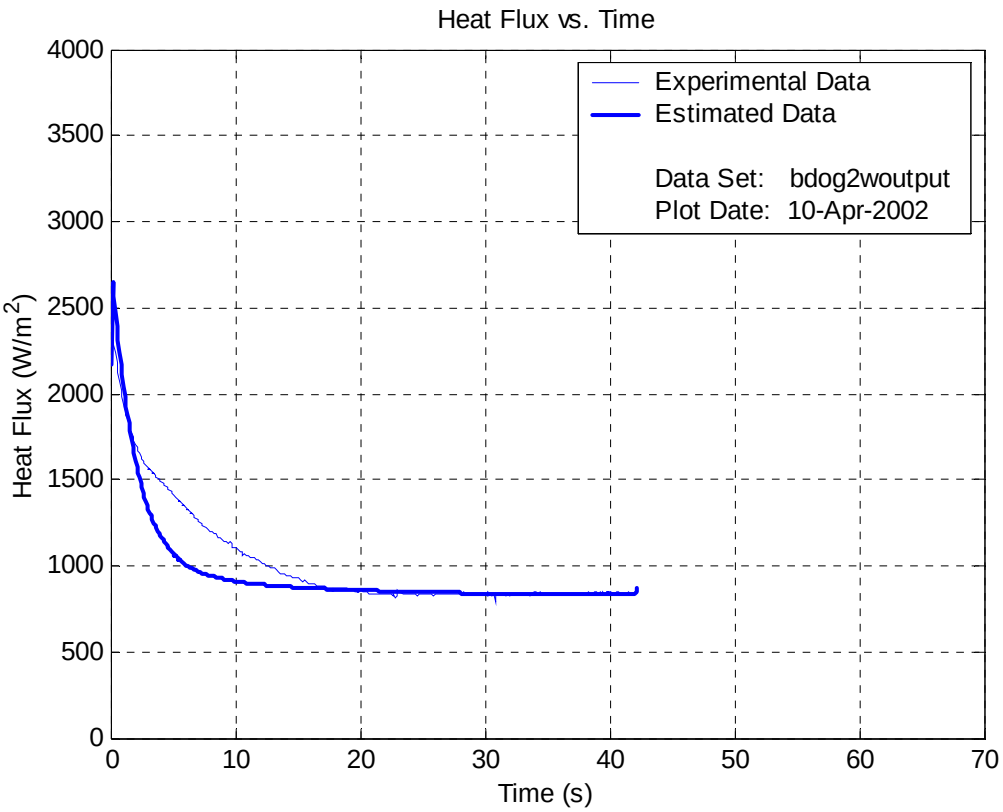
Heat Flux vs. Time
Experimental Data
Estimated Data
Data Set: bdog2woutput
Plot Date: 10-Apr-2002
Heat Flux (W/m2)
Time (s)
0
500
1000
1500
2000
2500
3000
3500
4000
0
10
20
30
40
50
60
70

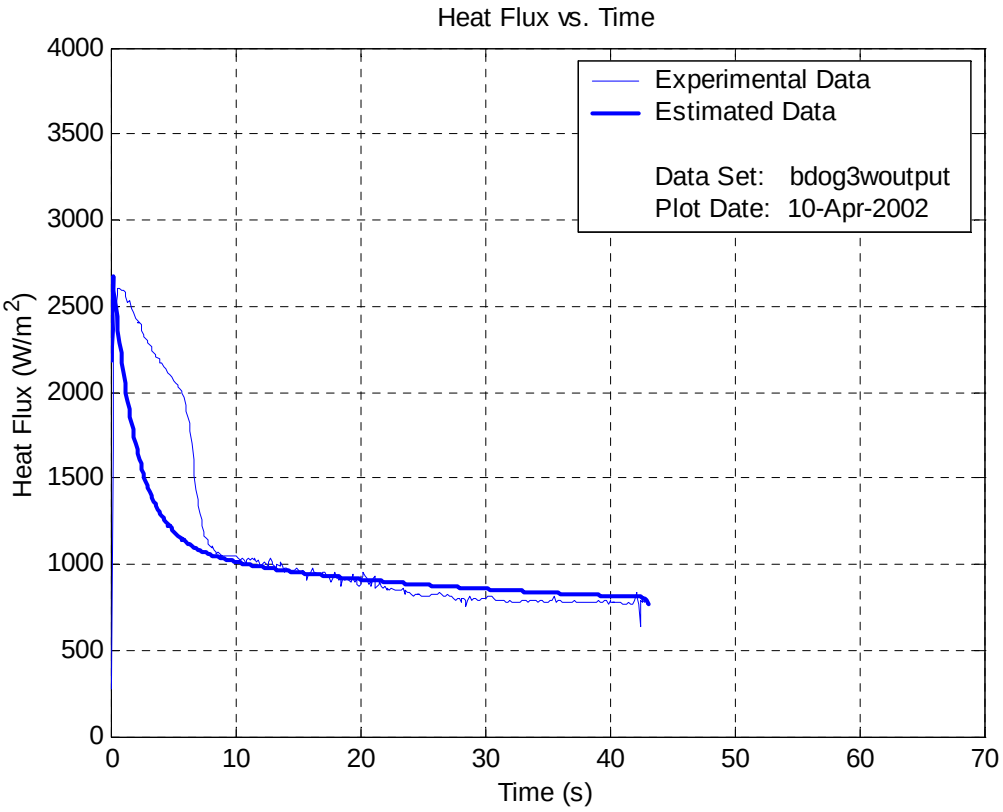
Heat Flux vs. Time
Experimental Data
Estimated Data
Data Set: bdog3woutput
Plot Date: 10-Apr-2002
Heat Flux (W/m2)
Time (s)
0
500
1000
1500
2000
2500
3000
3500
4000
0
10
20
30
40
50
60
70

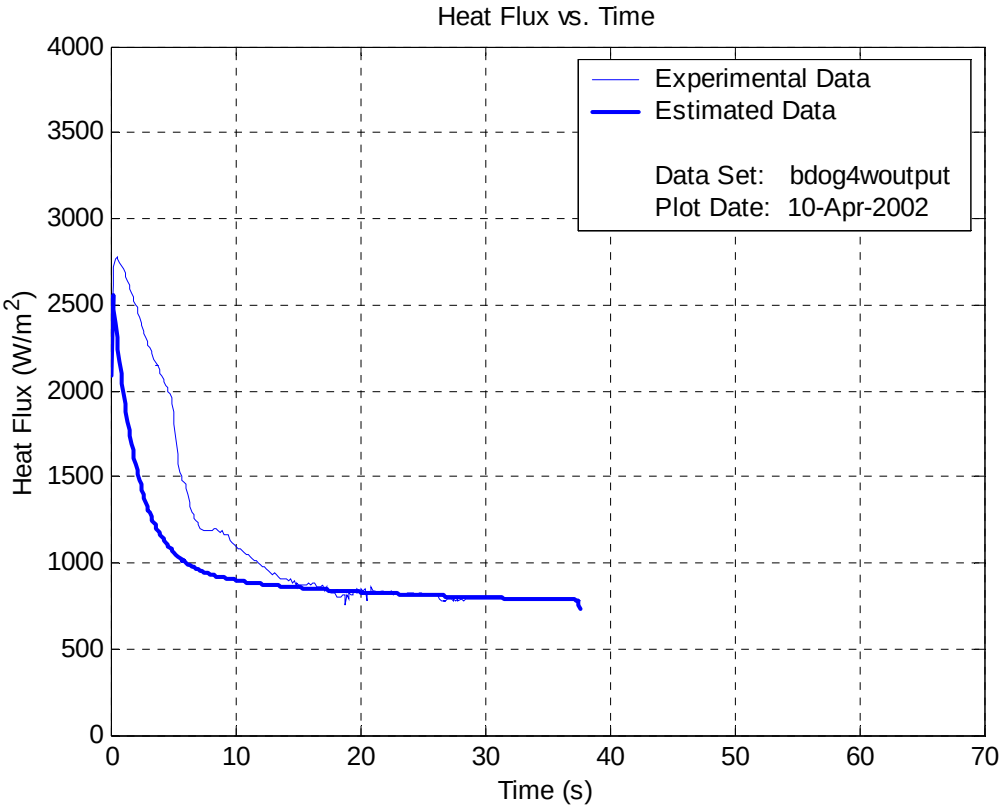
Heat Flux vs. Time
Experimental Data
Estimated Data
Data Set: bdog4woutput
Plot Date: 10-Apr-2002
Heat Flux (W/m2)
Time (s)
0
500
1000
1500
2000
2500
3000
3500
4000
0
10
20
30
40
50
60
70

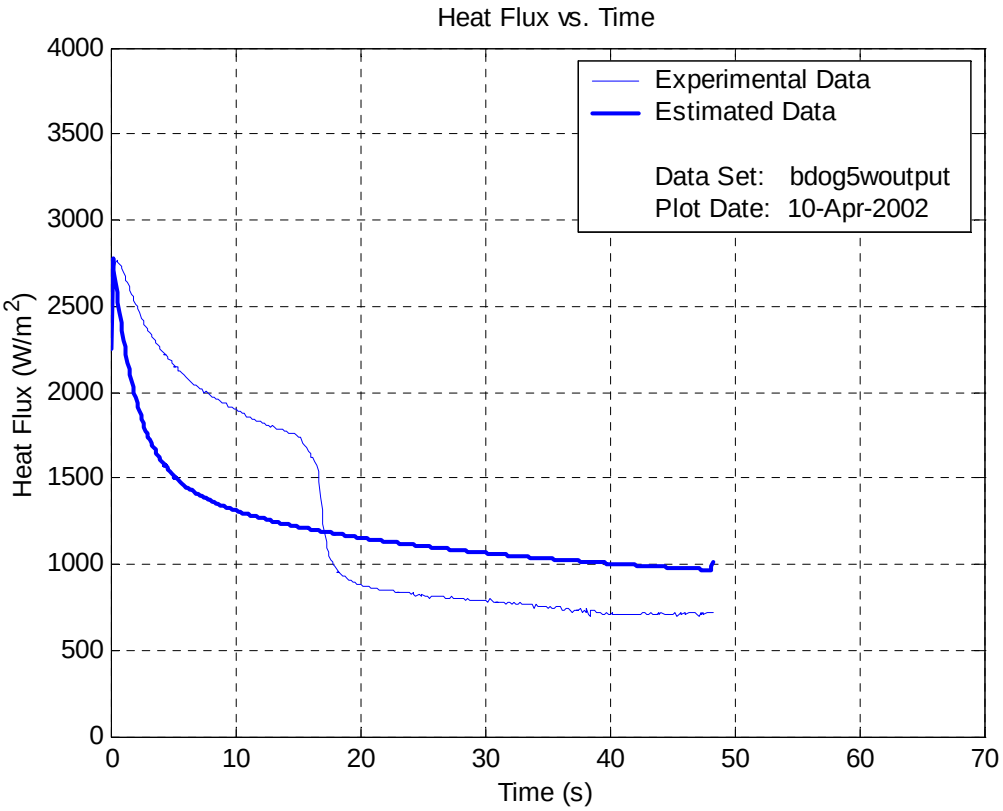
Heat Flux vs. Time
Experimental Data
Estimated Data
Data Set: bdog5woutput
Plot Date: 10-Apr-2002
Heat Flux (W/m2)
Time (s)
0
500
1000
1500
2000
2500
3000
3500
4000
0
10
20
30
40
50
60
70

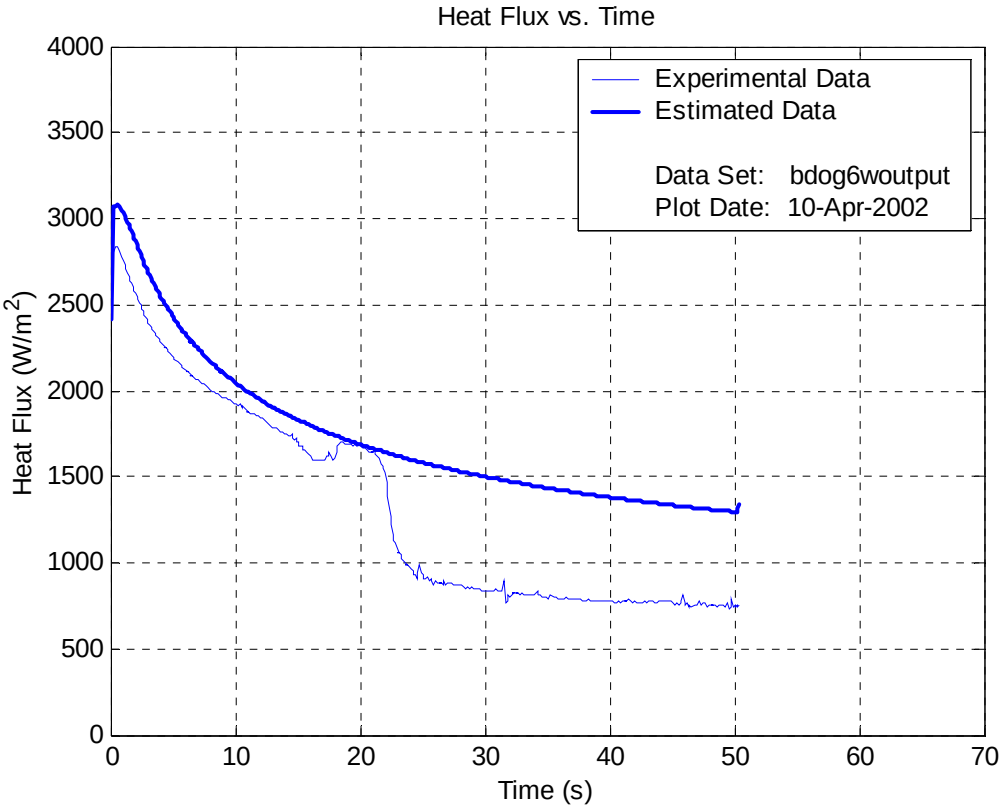
Heat Flux vs. Time
Experimental Data
Estimated Data
Data Set: bdog6woutput
Plot Date: 10-Apr-2002
Heat Flux (W/m2)
Time (s)
0
500
1000
1500
2000
2500
3000
3500
4000
0
10
20
30
40
50
60
70

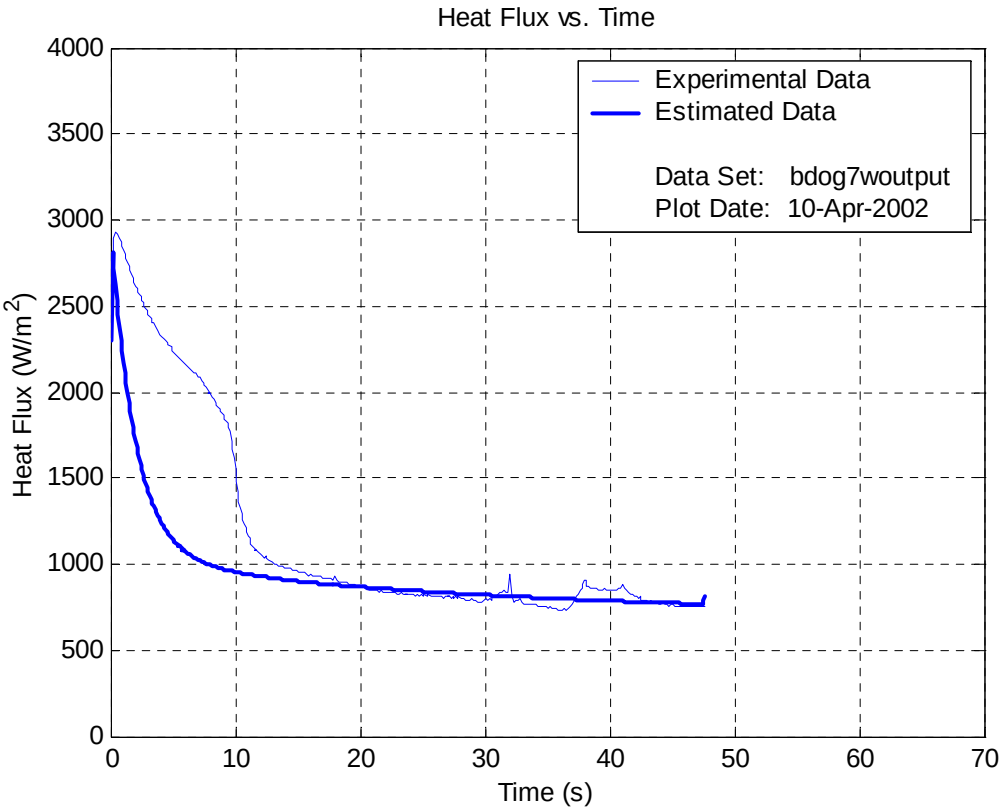
Heat Flux vs. Time
Experimental Data
Estimated Data
Data Set: bdog7woutput
Plot Date: 10-Apr-2002
Heat Flux (W/m2)
Time (s)
0
500
1000
1500
2000
2500
3000
3500
4000
0
10
20
30
40
50
60
70

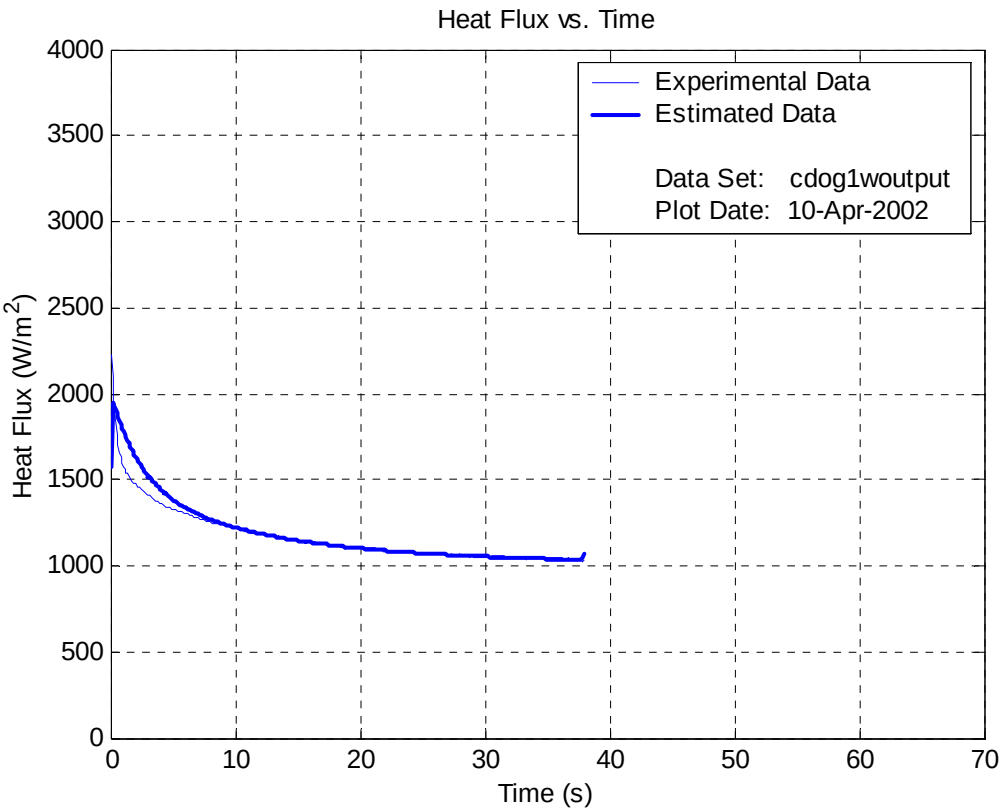
Heat Flux vs. Time
Experimental Data
Estimated Data
Data Set: cdog1woutput
Plot Date: 10-Apr-2002
Heat Flux (W/m2)
Time (s)
0
500
1000
1500
2000
2500
3000
3500
4000
0
10
20
30
40
50
60
70

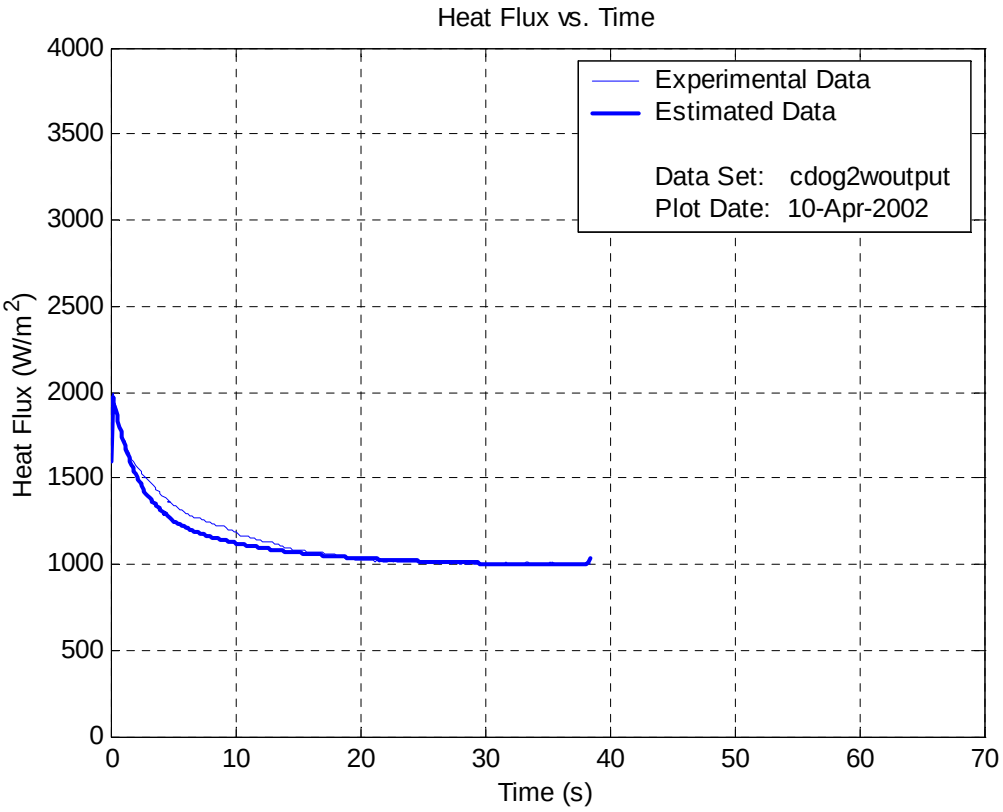
Heat Flux vs. Time
Experimental Data
Estimated Data
Data Set: cdog2woutput
Plot Date: 10-Apr-2002
Heat Flux (W/m2)
Time (s)
0
500
1000
1500
2000
2500
3000
3500
4000
0
10
20
30
40
50
60
70

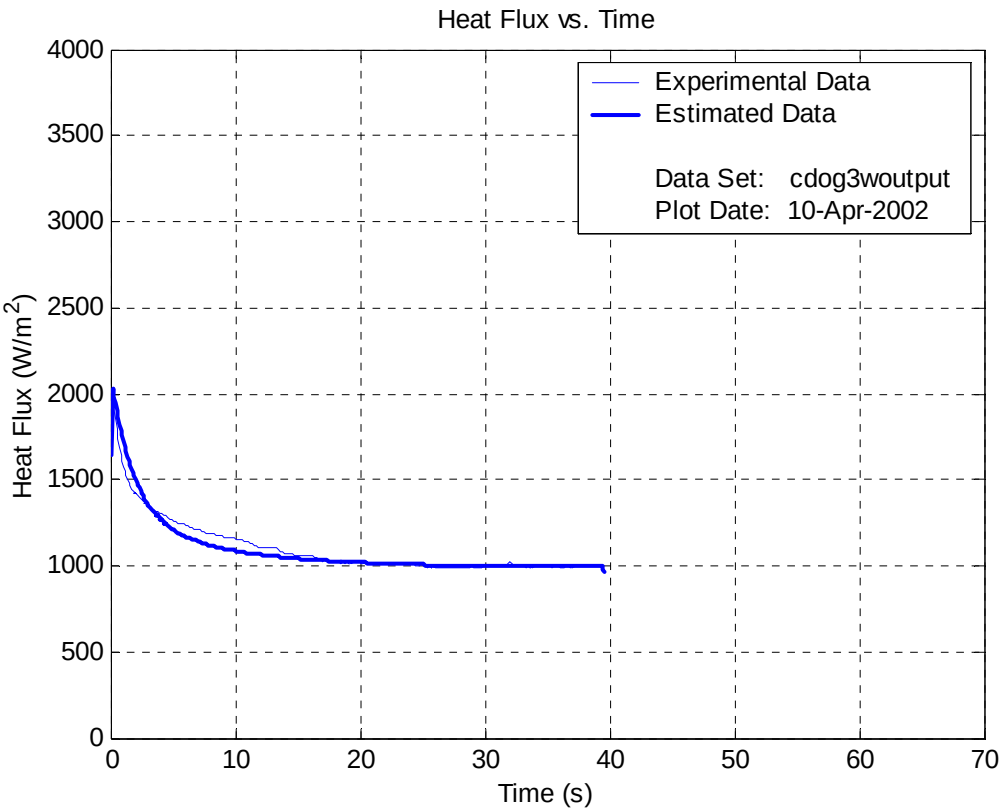
Heat Flux vs. Time
Experimental Data
Estimated Data
Data Set: cdog3woutput
Plot Date: 10-Apr-2002
Heat Flux (W/m^2)
Time (s)
4000
3500
3000
2500
2000
1500
1000
500
0
0
10
20
30
40
50
60
70

B.3 First Tissue Flap Study Results

This Appendix contains plots of the canine skin flap experiments outlined in Table 5.3. Each figure contains the experimentally recorded data plotted with the converged numerical solution for comparison. The data sets appear in the order they are listed below. The data file used to create the plot is noted in the legend of each graph. These figures were made using the estcomp.m Matlab program.

Data Sets

Data Set	Flap Condition	Time (min)	$T_{arterial}$ (°C)	T_{air} (°C)	T_{skin} (°C)	Bp (ml/ml/s)	Rc (m^2K/W)	SSY
Flap1w	Pre-Surgery	0	34.50	21.80	30.87	0.00380	0.00027	1.031
Flap2w		4	34.30	20.80	31.08	0.00420	0.00091	1.471
Flap3w		8	34.20	20.80	31.26	0.00453	0.00055	0.259
Flap4w	Flap Exised No Occlusion	42	33.20	20.90	29.03	0.00166	0.00285	1.459
Flap5w		46	33.20	20.60	28.90	0.00196	0.00306	3.427
Flap6w		53	33.10	20.20	28.56	0.00415	0.00215	0.150
Flap7w	Flap Exised Occluded	57	33.10	20.10	28.38	0.00293	0.00317	3.036
Flap8w		60	33.10	19.20	26.82	0.00287	0.00328	1.063
Flap9w		64	33.10	19.20	26.61	0.00243	0.00376	1.514
Flap10w	Flap Exised No Occlusion	66	33.10	18.70	26.36	0.00390	0.00328	5.376
Flap11w		70	33.10	18.80	27.33	0.00345	0.00394	11.796
		Lidocain administered						
Flap12w		73	33.10	18.60	27.48	0.00157	0.00432	16.225
Flap13w	Flap Reattached	91	32.90	20.20	30.16	0.00382	0.00172	0.317
Flap14w		93	32.60	19.40	28.11	0.00590	0.00187	1.283
Flap15w		96	32.60	19.10	28.15	0.00503	0.00192	2.565

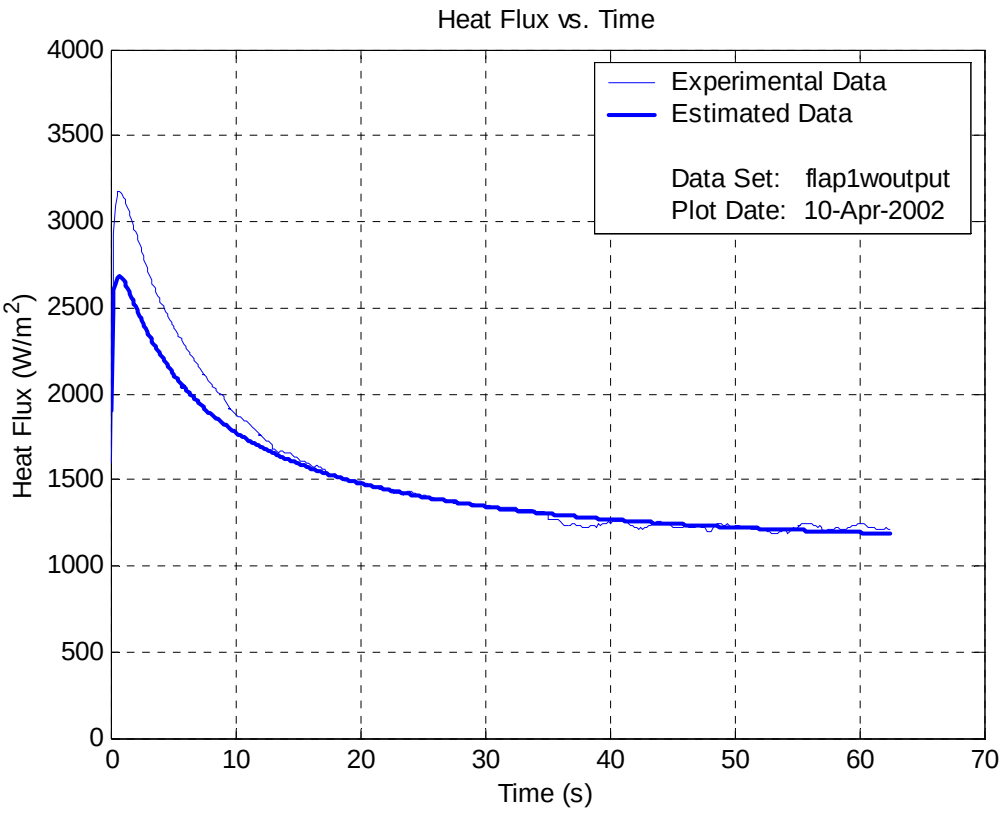
Heat Flux vs. Time
Experimental Data
Estimated Data
Data Set: flap1woutput
Plot Date: 10-Apr-2002
Heat Flux (W/m2)
Time (s)
0
500
1000
1500
2000
2500
3000
3500
4000
0
10
20
30
40
50
60
70

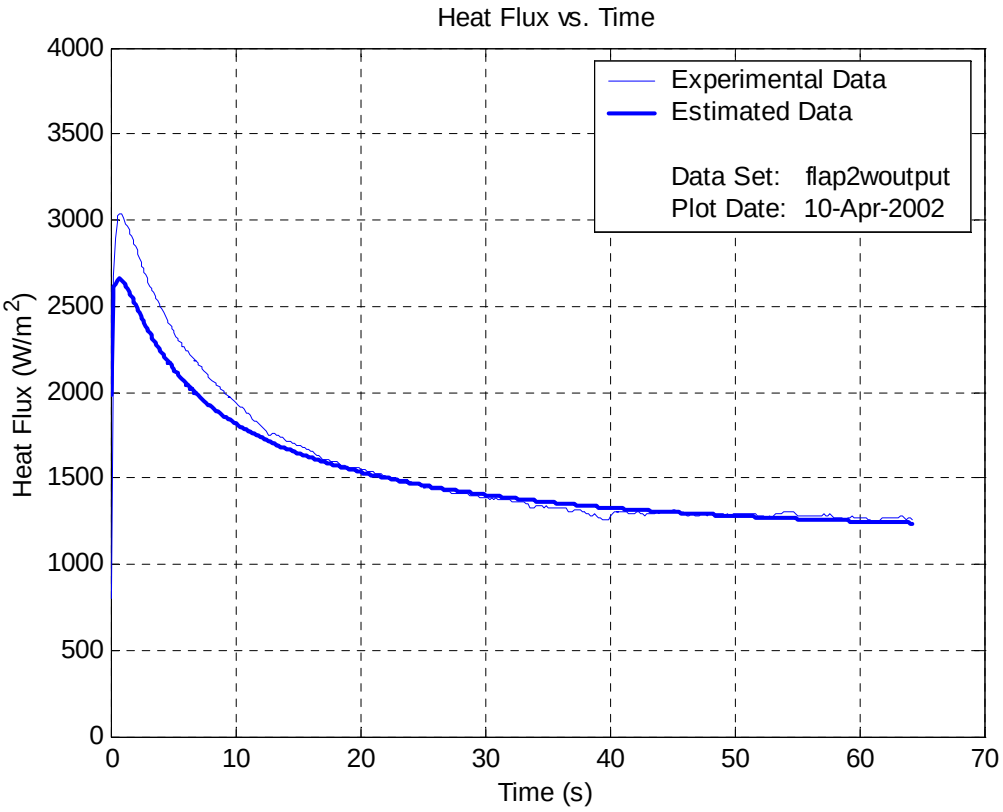
Heat Flux vs. Time
Experimental Data
Estimated Data
Data Set: flap2woutput
Plot Date: 10-Apr-2002
Heat Flux (W/m2)
Time (s)
0
500
1000
1500
2000
2500
3000
3500
4000
0
10
20
30
40
50
60
70

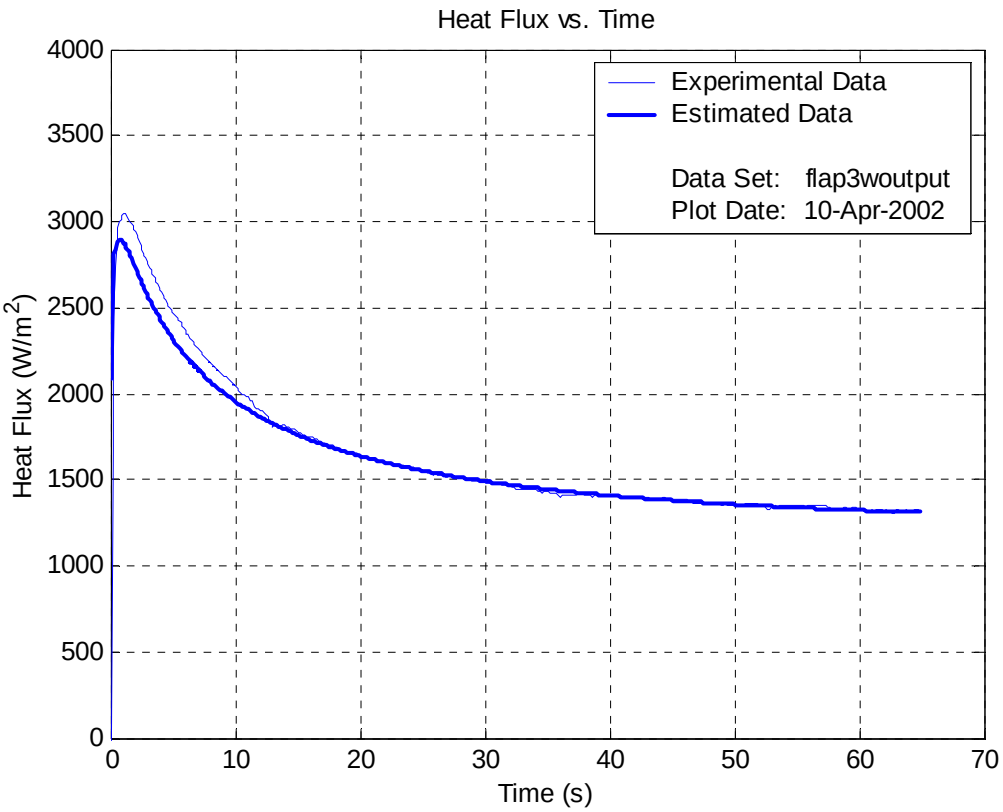
Heat Flux vs. Time
Experimental Data
Estimated Data
Data Set: flap3woutput
Plot Date: 10-Apr-2002
Heat Flux (W/m2)
Time (s)
0
500
1000
1500
2000
2500
3000
3500
4000
0
10
20
30
40
50
60
70

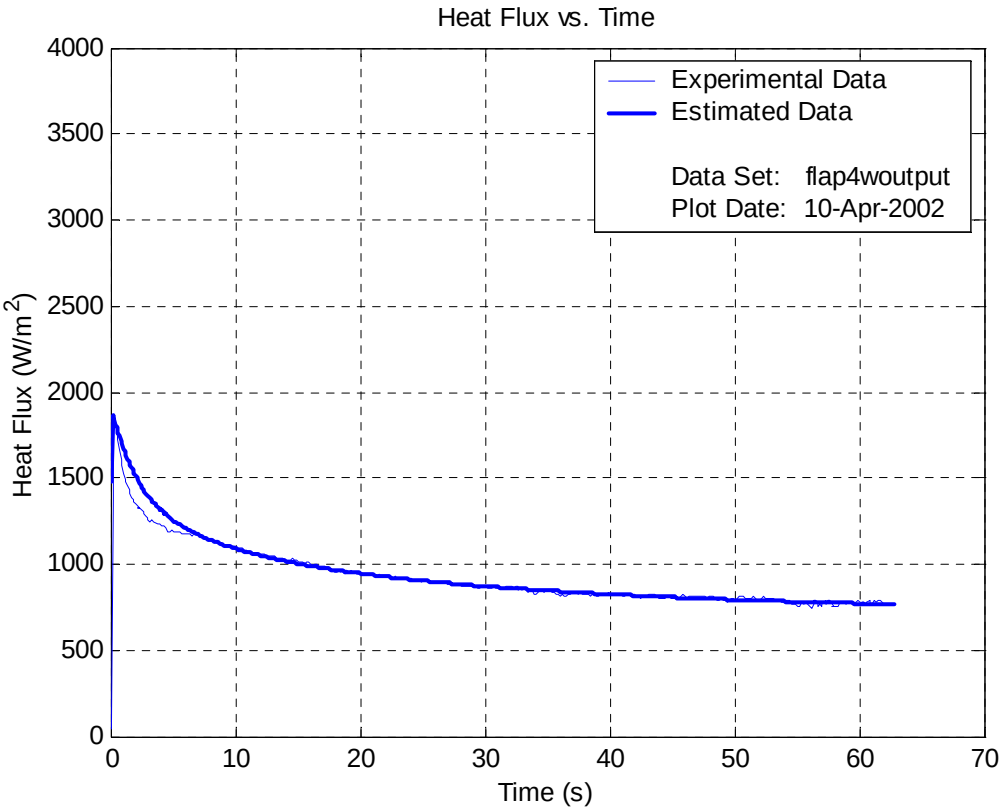
Heat Flux vs. Time
Experimental Data
Estimated Data
Data Set: flap4woutput
Plot Date: 10-Apr-2002
Heat Flux (W/m2)
Time (s)
0
500
1000
1500
2000
2500
3000
3500
4000
0
10
20
30
40
50
60
70

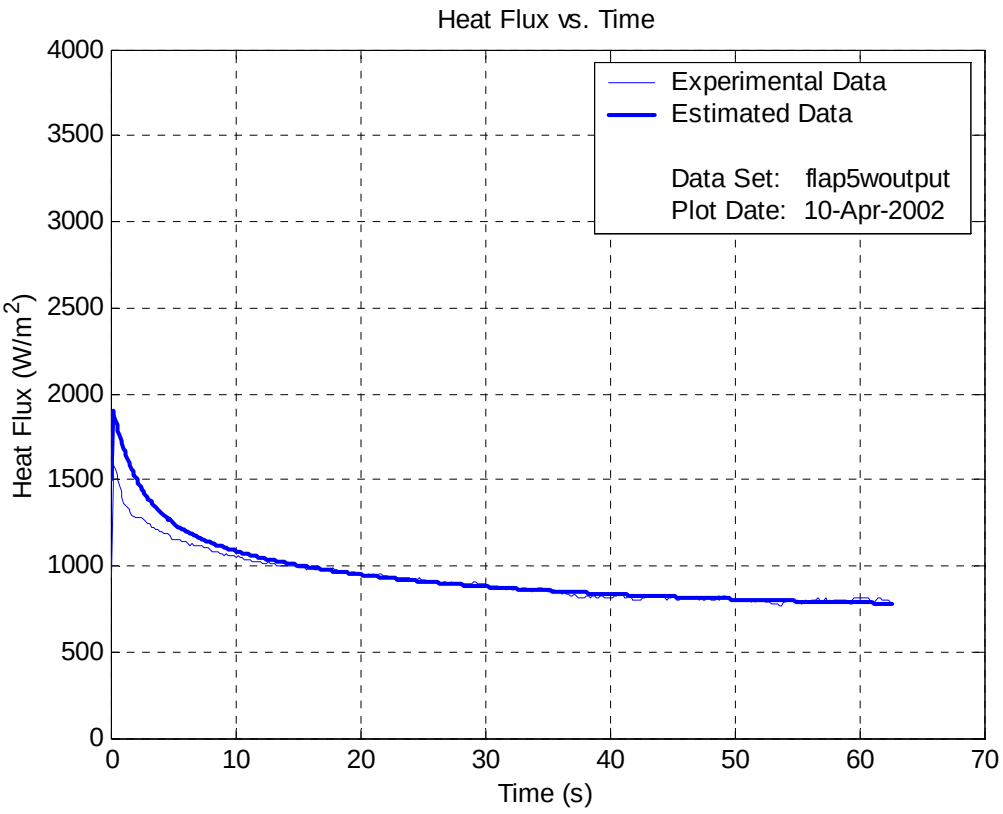
Heat Flux vs. Time
Experimental Data
Estimated Data
Data Set: flap5woutput
Plot Date: 10-Apr-2002
Heat Flux (W/m2)
Time (s)
0
500
1000
1500
2000
2500
3000
3500
4000
0
10
20
30
40
50
60
70

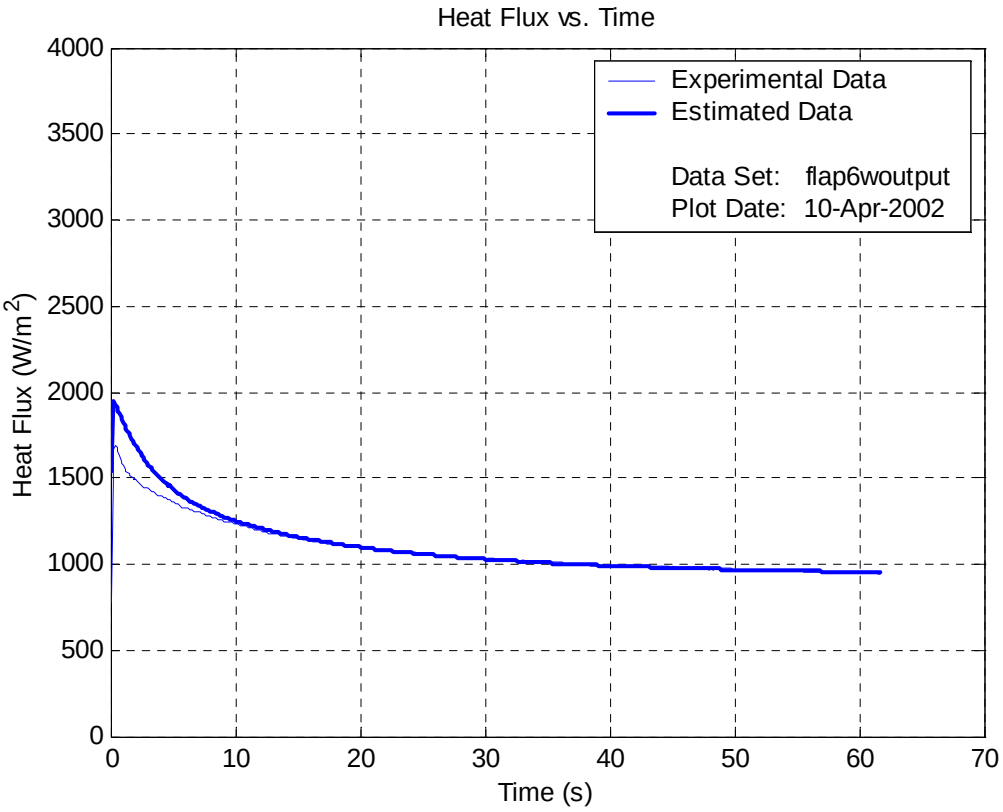
Heat Flux vs. Time
Experimental Data
Estimated Data
Data Set: flap6woutput
Plot Date: 10-Apr-2002
Heat Flux (W/m2)
Time (s)
0
500
1000
1500
2000
2500
3000
3500
4000
0
10
20
30
40
50
60
70

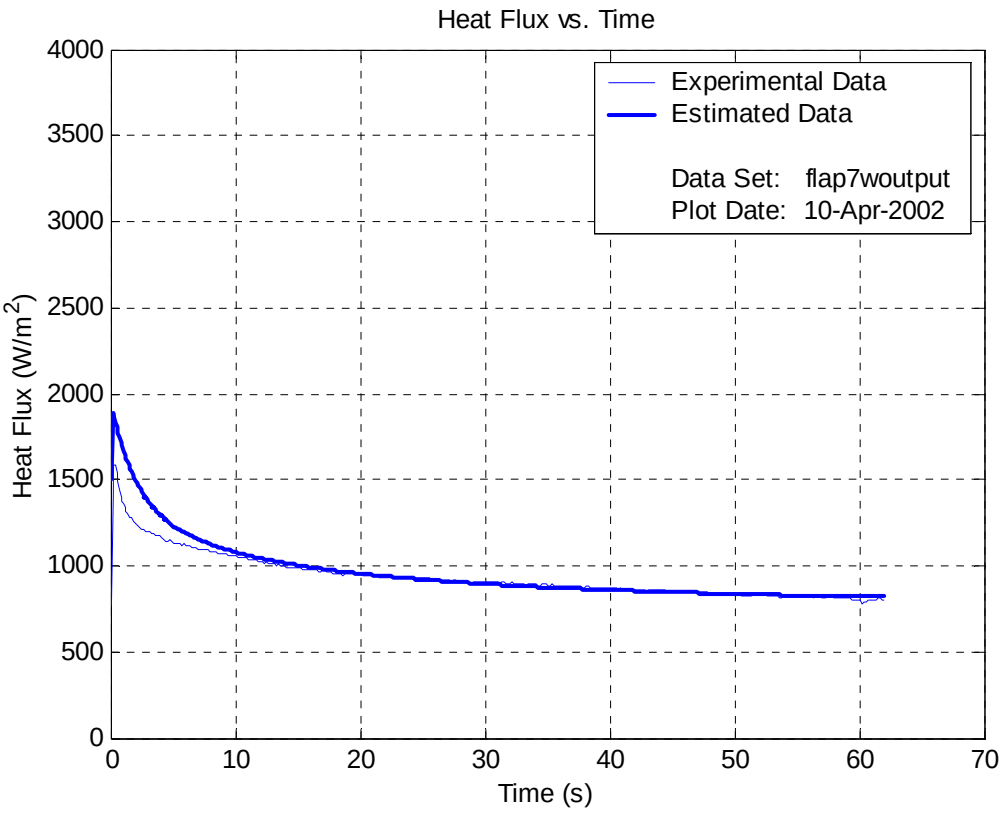
Heat Flux vs. Time
Experimental Data
Estimated Data
Data Set: flap7woutput
Plot Date: 10-Apr-2002
Heat Flux (W/m2)
Time (s)
0
500
1000
1500
2000
2500
3000
3500
4000
0
10
20
30
40
50
60
70

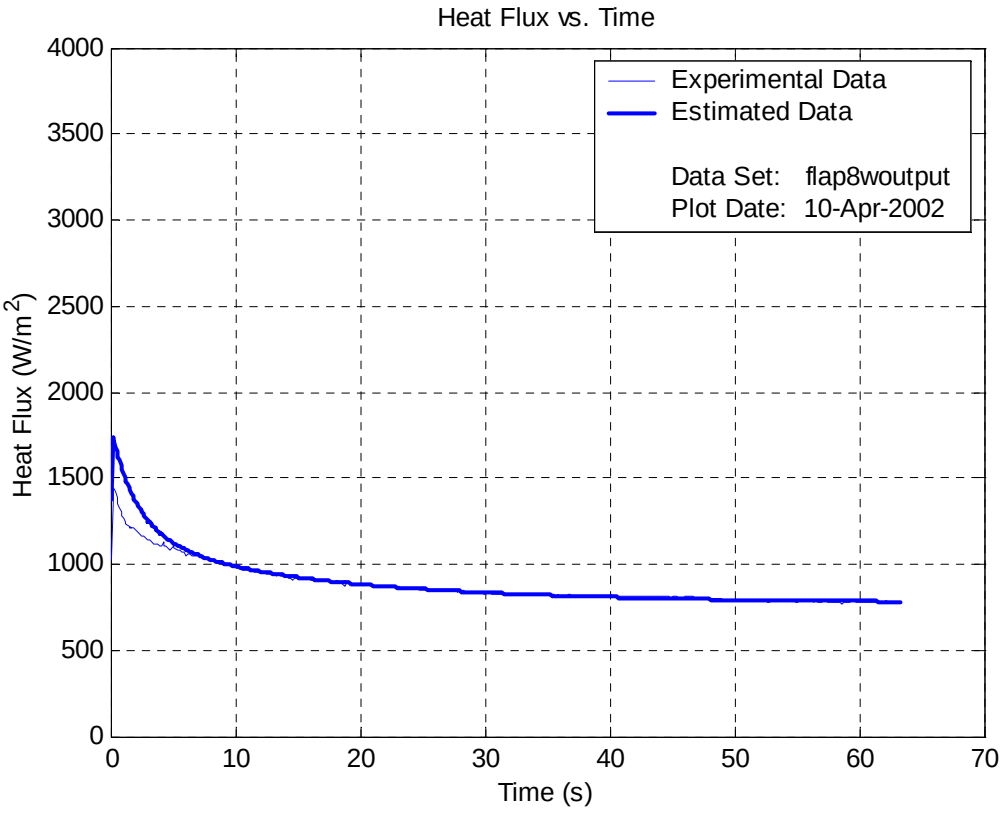
Heat Flux vs. Time
Experimental Data
Estimated Data
Data Set: flap8woutput
Plot Date: 10-Apr-2002
Heat Flux (W/m2)
Time (s)
0
500
1000
1500
2000
2500
3000
3500
4000
0
10
20
30
40
50
60
70

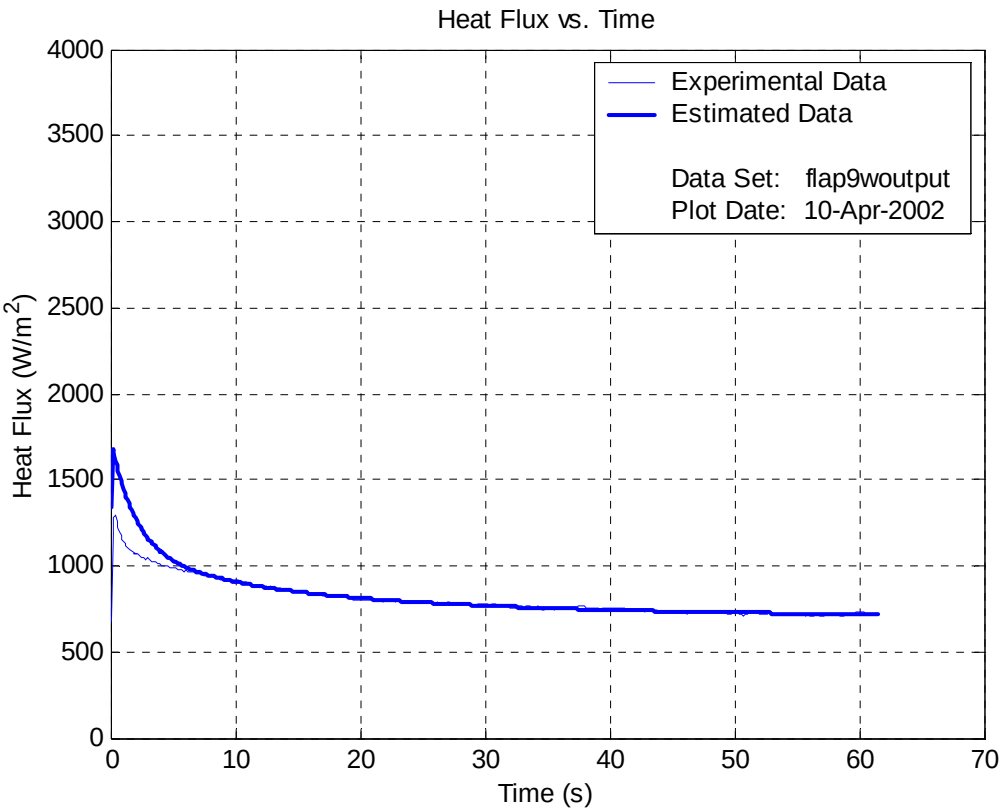
Heat Flux vs. Time
Experimental Data
Estimated Data
Data Set: flap9woutput
Plot Date: 10-Apr-2002
Heat Flux (W/m2)
Time (s)
0
500
1000
1500
2000
2500
3000
3500
4000
0
10
20
30
40
50
60
70

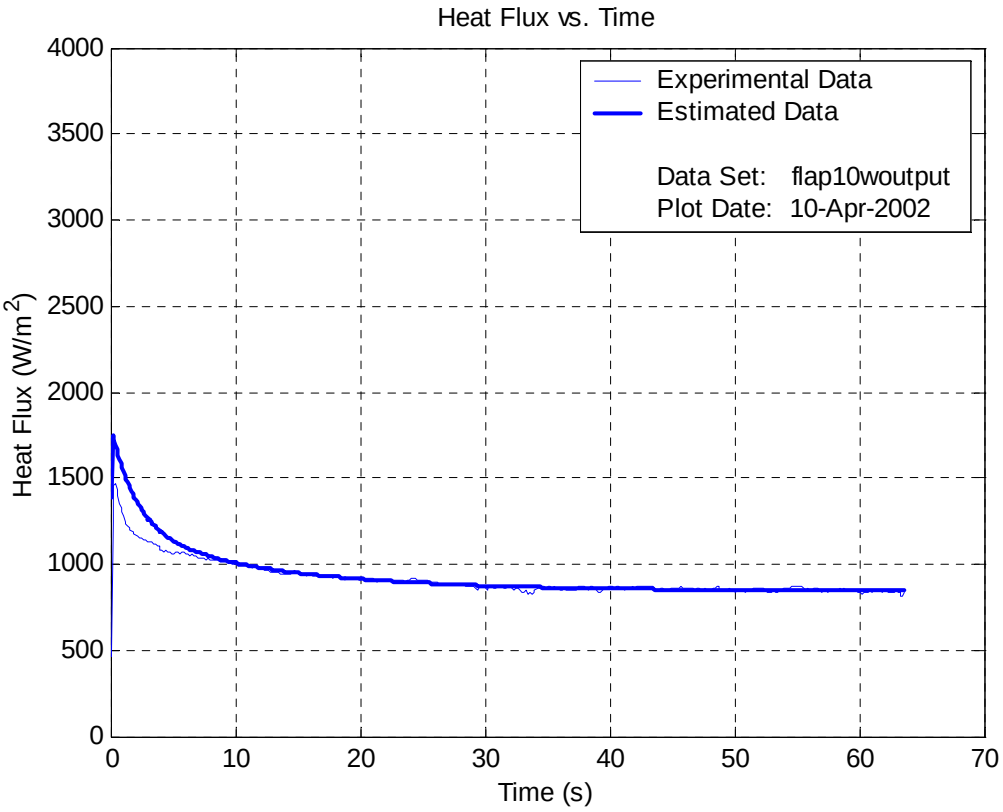
Heat Flux vs. Time
Experimental Data
Estimated Data
Data Set: flap10woutput
Plot Date: 10-Apr-2002
Heat Flux (W/m2)
Time (s)
0
500
1000
1500
2000
2500
3000
3500
4000
0
10
20
30
40
50
60
70

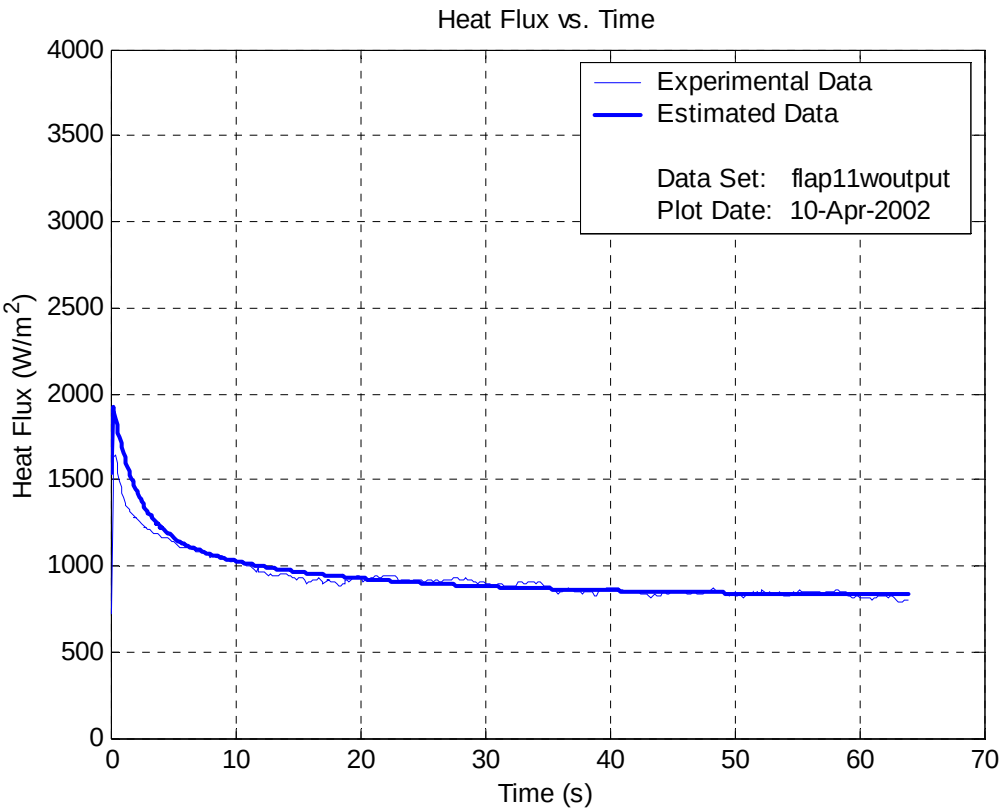
Heat Flux vs. Time
Experimental Data
Estimated Data
Data Set: flap11woutput
Plot Date: 10-Apr-2002
Heat Flux (W/m2)
Time (s)
0
500
1000
1500
2000
2500
3000
3500
4000
0
10
20
30
40
50
60
70

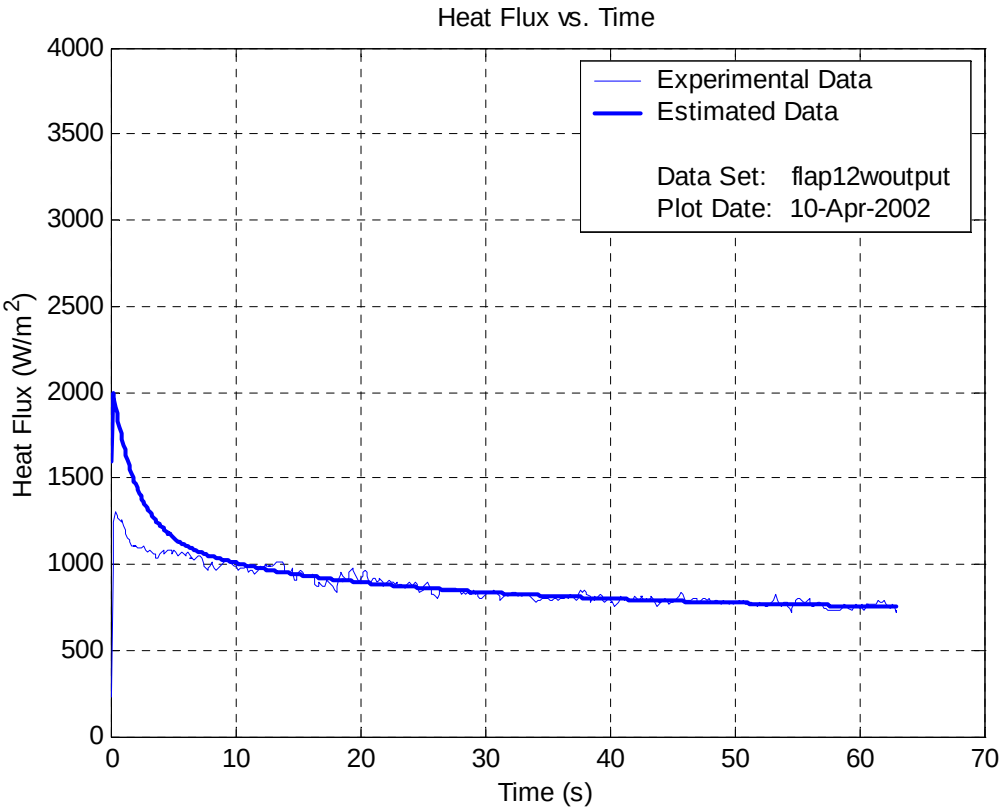
Heat Flux vs. Time
Experimental Data
Estimated Data
Data Set: flap12woutput
Plot Date: 10-Apr-2002
Heat Flux (W/m2)
Time (s)
0
500
1000
1500
2000
2500
3000
3500
4000
0
10
20
30
40
50
60
70

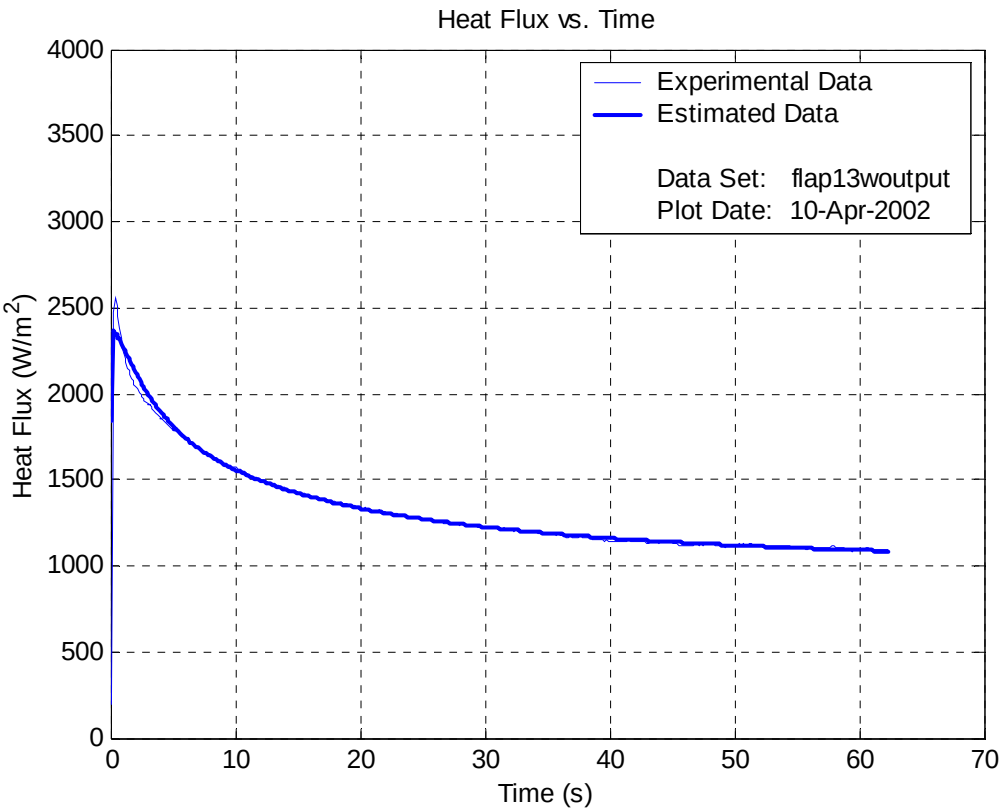
Heat Flux vs. Time
Experimental Data
Estimated Data
Data Set: flap13woutput
Plot Date: 10-Apr-2002
Heat Flux (W/m2)
Time (s)
0
500
1000
1500
2000
2500
3000
3500
4000
0
10
20
30
40
50
60
70

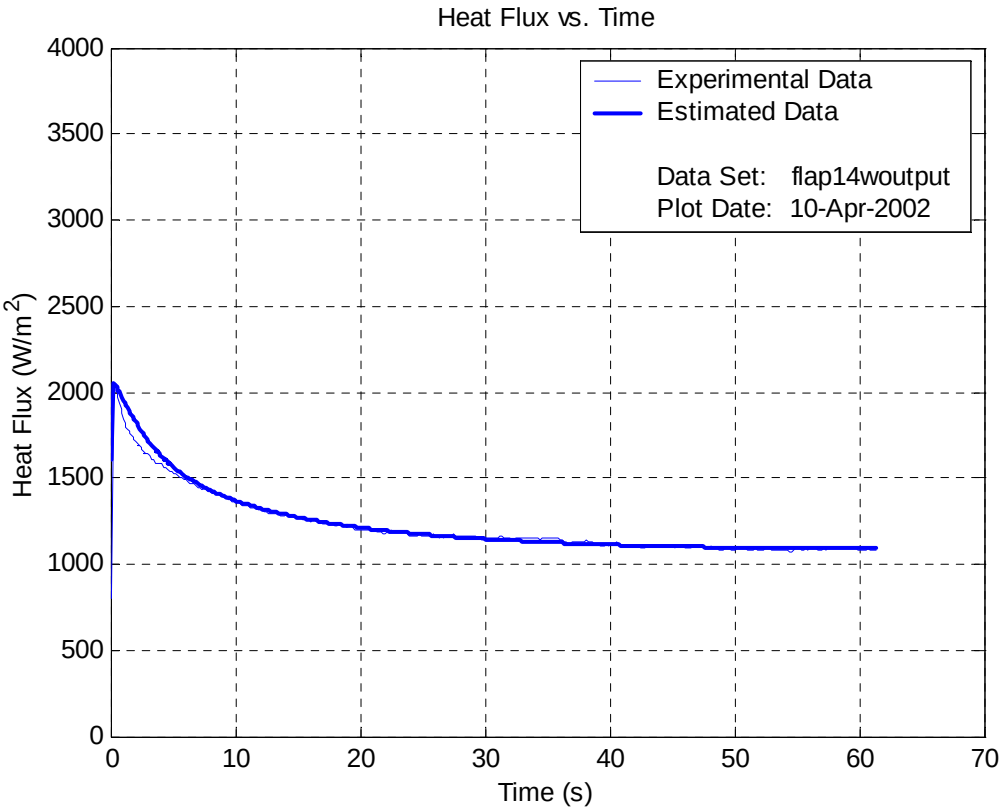
Heat Flux vs. Time
Experimental Data
Estimated Data
Data Set: flap14woutput
Plot Date: 10-Apr-2002
Heat Flux (W/m2)
Time (s)
0
500
1000
1500
2000
2500
3000
3500
4000
0
10
20
30
40
50
60
70

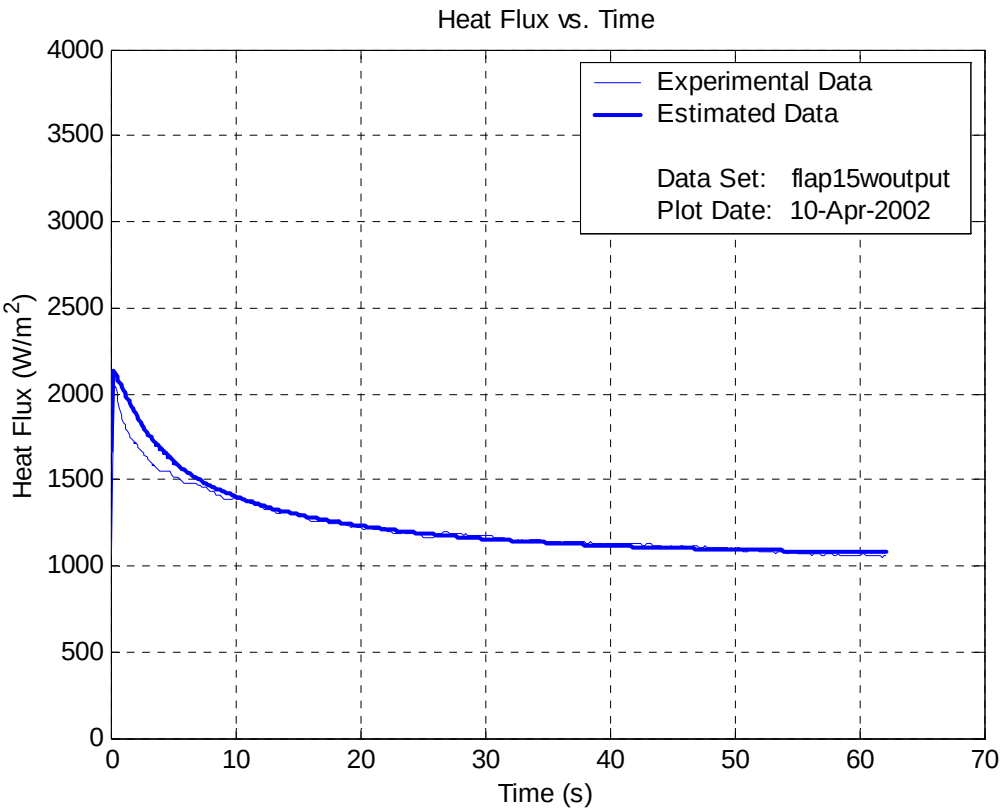
Heat Flux vs. Time
Experimental Data
Estimated Data
Data Set: flap15woutput
Plot Date: 10-Apr-2002
Heat Flux (W/m^2)
Time (s)
0
500
1000
1500
2000
2500
3000
3500
4000
0
10
20
30
40
50
60
70

B.4 Second Tissue Flap Results

This Appendix contains plots of the canine skin flap experiments outlined in Table 5.4. Each figure contains the experimentally recorded data plotted with the converged numerical solution for comparison. The data sets appear in the order they are listed below. The data file used to create the plot is noted in the legend of each graph. These figures were made using the estcomp.m Matlab program.

Data Sets

Data Set	Flap Condition	Time (min)	$T_{arterial}$ (°C)	T_{air} (°C)	T_{skin} (°C)	Bp (ml/ml/s)	Rc (m^2K/W)	SSY
bFlap1	Pre-Surgery	0	36.90	21.00	32.03	0.00830	0.00047	0.168
bFlap2		5	36.90	19.50	31.21	0.00653	0.00024	0.206
bFlap3		10	36.80	18.60	30.66	0.00663	0.00027	0.118
bFlap4		15	36.80	18.30	30.79	0.00691	0.00041	0.071
bFlap5		20	36.80	17.90	30.69	0.00770	0.00049	0.297
† bFlap6	Flap Excised No Occlusion	52	36.60	20.70	31.02	0.01748	0.00578	256.398
bFlap7		57	36.60	19.40	30.66	0.01309	0.00119	1.644
† bFlap8		62	36.60	18.90	30.61	0.01186	0.00187	28.731
bFlap9		67	36.60	18.60	30.56	0.01051	0.00081	0.297
† bFlap10		72	36.60	18.40	30.70	0.00850	0.00052	24.396
bFlap11	Flap Excised Occluded	78	36.60	18.50	30.20	0.00501	0.00094	2.737
† bFlap12		83	36.60	17.40	27.90	0.00525	0.00270	59.960
bFlap13		88	36.60	17.10	27.44	0.00467	0.00147	0.128
bFlap14		93	36.50	17.10	26.51	0.00518	0.00137	0.646
† bFlap15		98	36.50	16.90	26.57	No Convergence		

† These data sets have more variation than others same test. The cause of the added noise is unknown at this time, however it is important enough to call question to these data sets. Therefore, these data sets are regarded as being of questionable experimental accuracy.

Note: bFlap15 is not represented here because the data set did not converge in the parameter estimation routine.

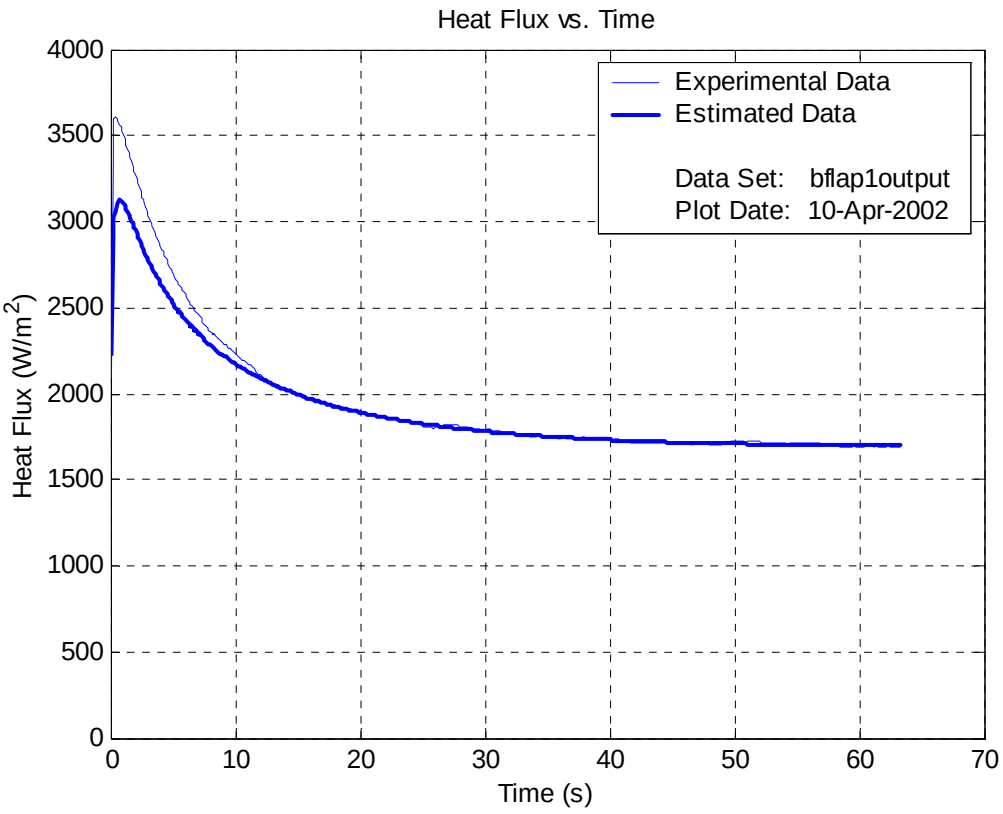
Heat Flux vs. Time
Experimental Data
Estimated Data
Data Set: bflap1output
Plot Date: 10-Apr-2002
Heat Flux (W/m2)
Time (s)
0
500
1000
1500
2000
2500
3000
3500
4000
0
10
20
30
40
50
60
70

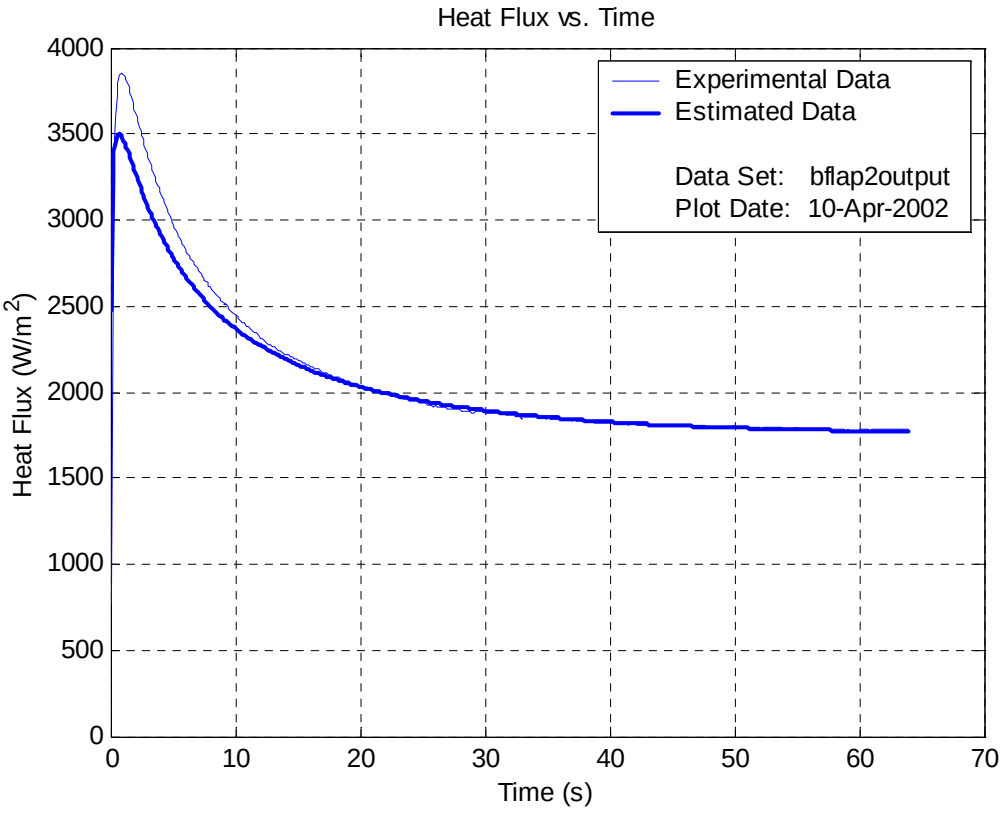
Heat Flux vs. Time
Experimental Data
Estimated Data
Data Set: bflap2output
Plot Date: 10-Apr-2002
Heat Flux (W/m2)
Time (s)
0
500
1000
1500
2000
2500
3000
3500
4000
0
10
20
30
40
50
60
70

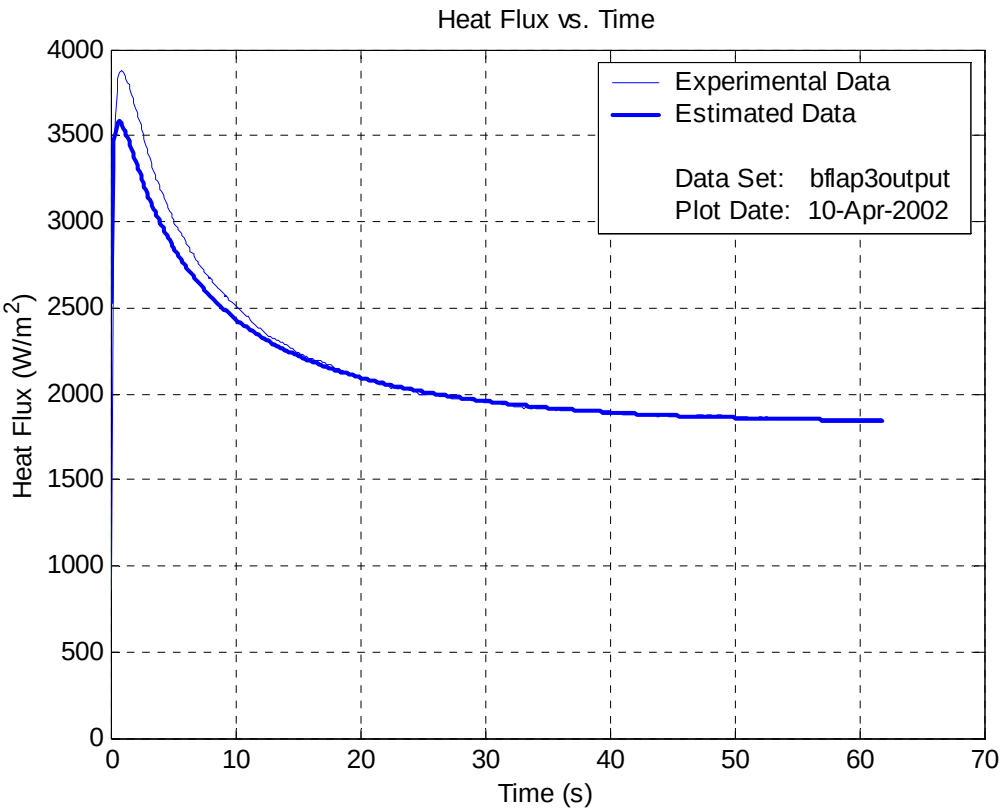
Heat Flux vs. Time
Experimental Data
Estimated Data
Data Set: bflap3output
Plot Date: 10-Apr-2002
Heat Flux (W/m2)
Time (s)
0
500
1000
1500
2000
2500
3000
3500
4000
0
10
20
30
40
50
60
70

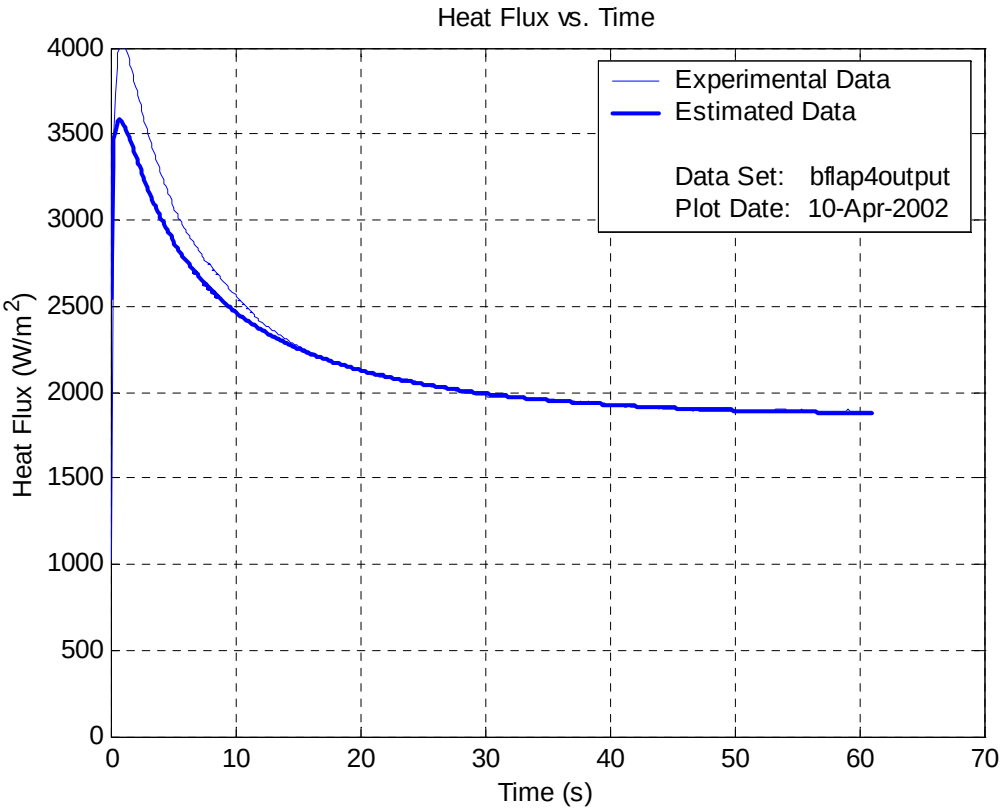
Heat Flux vs. Time
Experimental Data
Estimated Data
Data Set: bflap4output
Plot Date: 10-Apr-2002
Heat Flux (W/m2)
Time (s)
0
500
1000
1500
2000
2500
3000
3500
4000
0
10
20
30
40
50
60
70

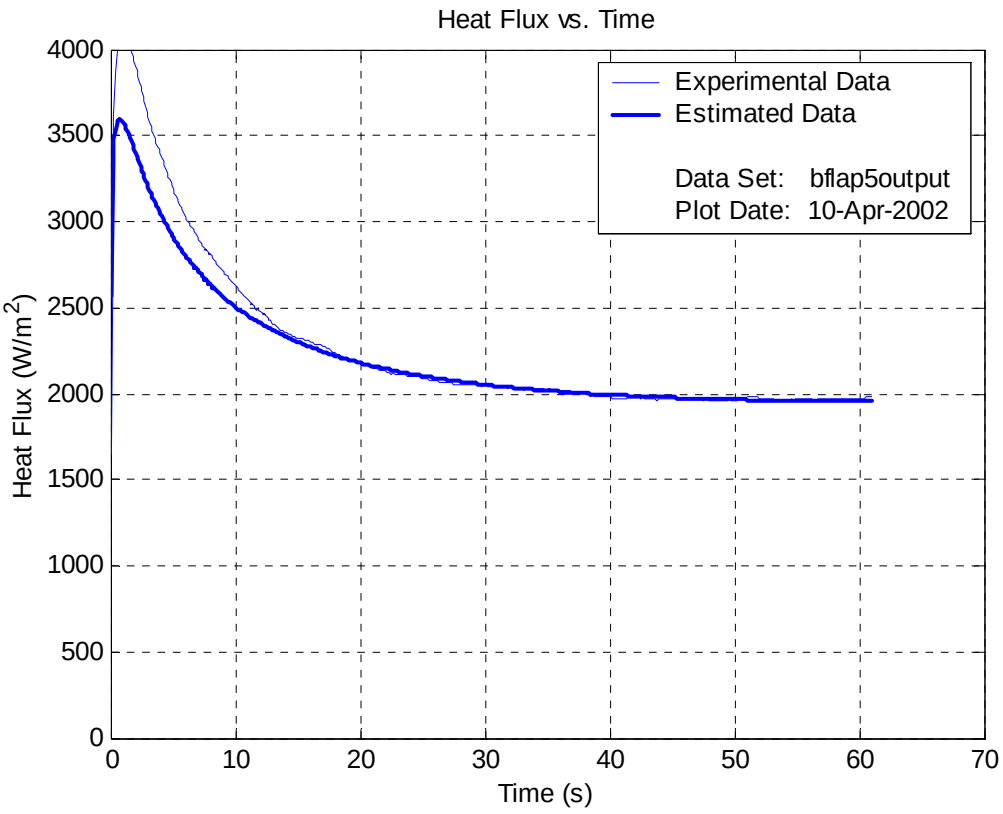
Heat Flux vs. Time
Experimental Data
Estimated Data
Data Set: bflap5output
Plot Date: 10-Apr-2002
Heat Flux (W/m2)
Time (s)
0
500
1000
1500
2000
2500
3000
3500
4000
0
10
20
30
40
50
60
70

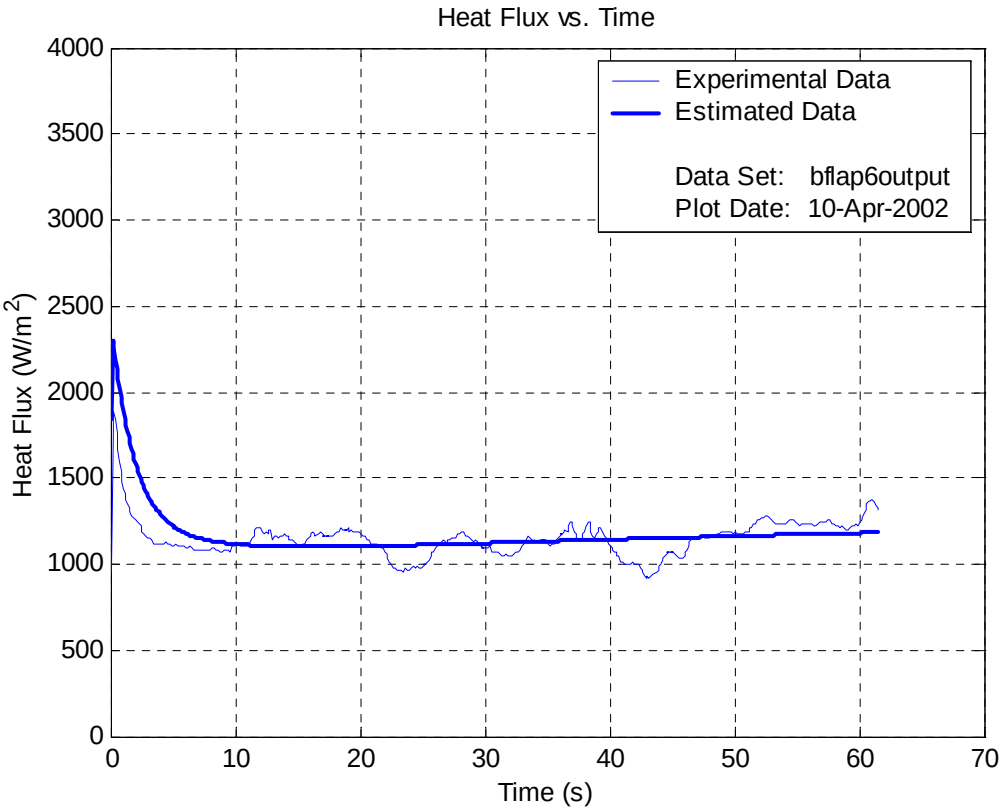
Heat Flux vs. Time
Experimental Data
Estimated Data
Data Set: bflap6output
Plot Date: 10-Apr-2002
Heat Flux (W/m2)
Time (s)
0
500
1000
1500
2000
2500
3000
3500
4000
0
10
20
30
40
50
60
70

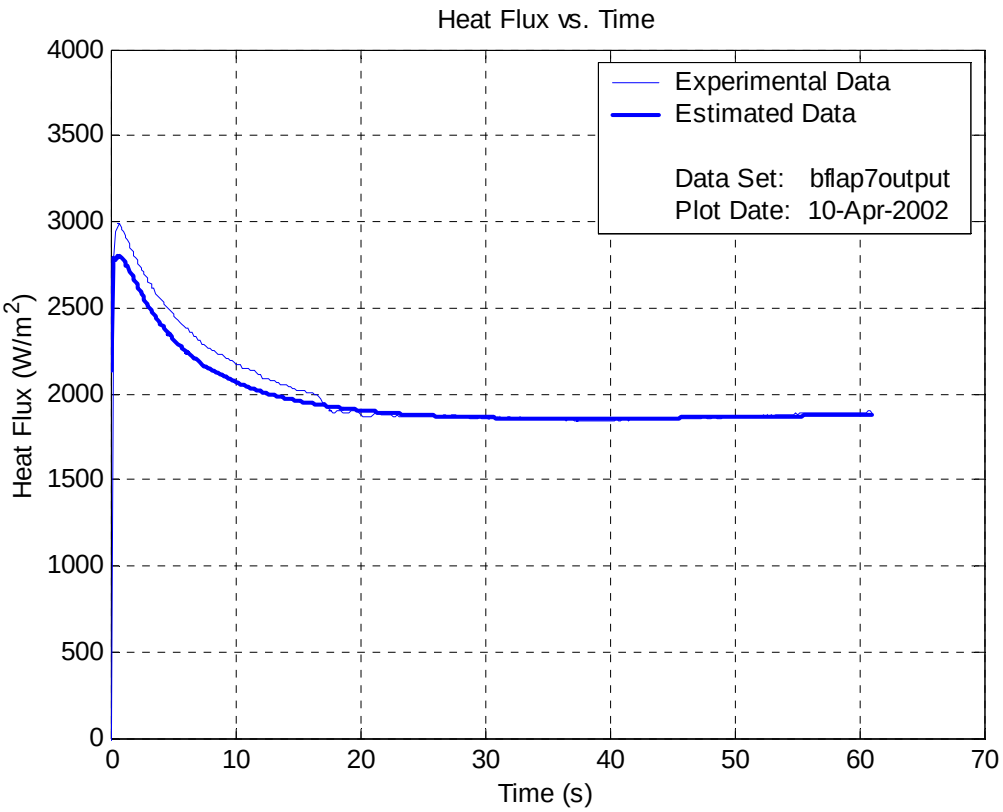
Heat Flux vs. Time
Experimental Data
Estimated Data
Data Set: bflap7output
Plot Date: 10-Apr-2002
Heat Flux (W/m2)
Time (s)
0
500
1000
1500
2000
2500
3000
3500
4000
0
10
20
30
40
50
60
70

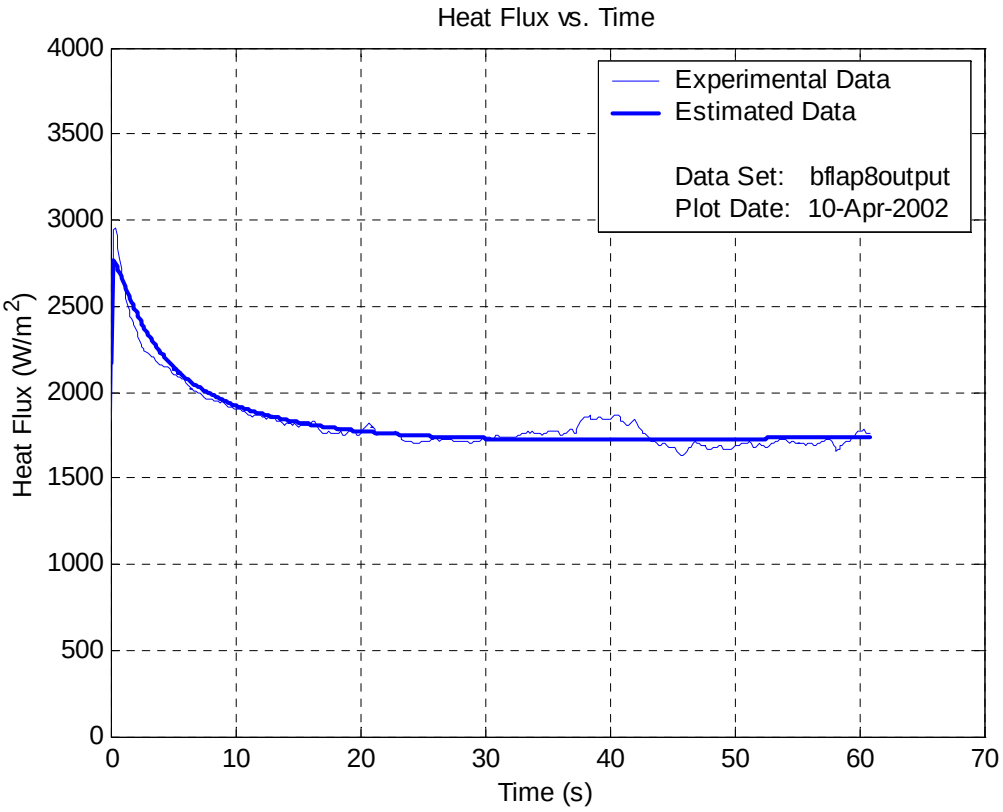
Heat Flux vs. Time
Experimental Data
Estimated Data
Data Set: bflap8output
Plot Date: 10-Apr-2002
Heat Flux (W/m2)
Time (s)
0
500
1000
1500
2000
2500
3000
3500
4000
0
10
20
30
40
50
60
70

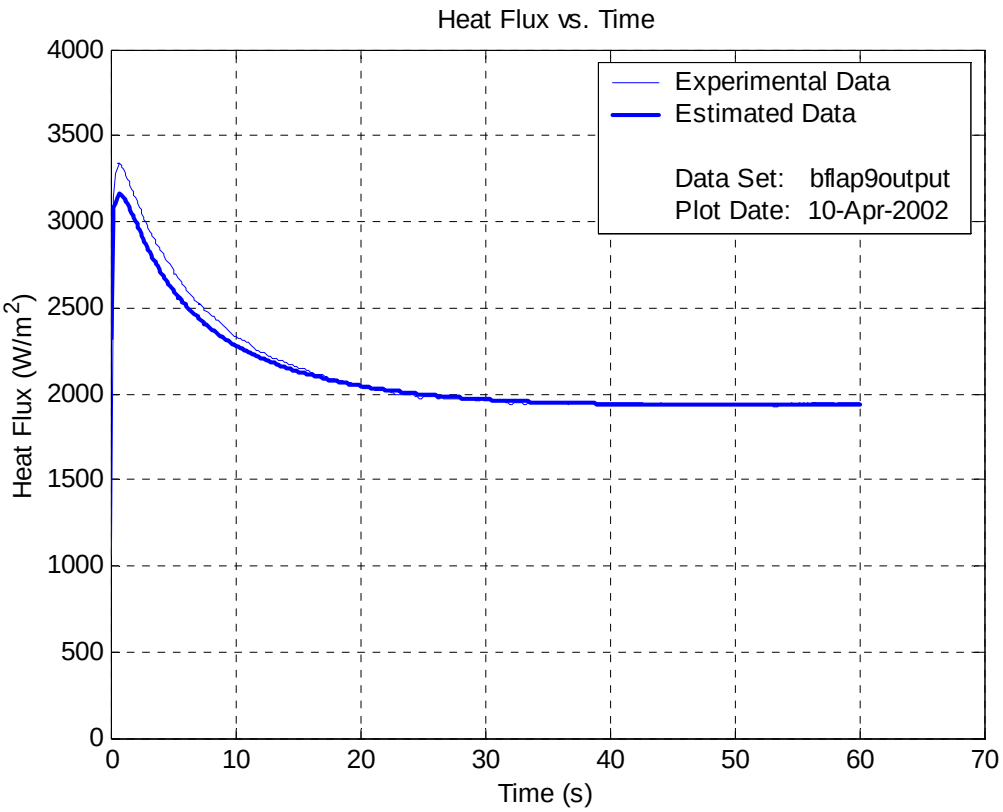
Heat Flux vs. Time
Experimental Data
Estimated Data
Data Set: bflap9output
Plot Date: 10-Apr-2002
Heat Flux (W/m2)
Time (s)
0
500
1000
1500
2000
2500
3000
3500
4000
0
10
20
30
40
50
60
70

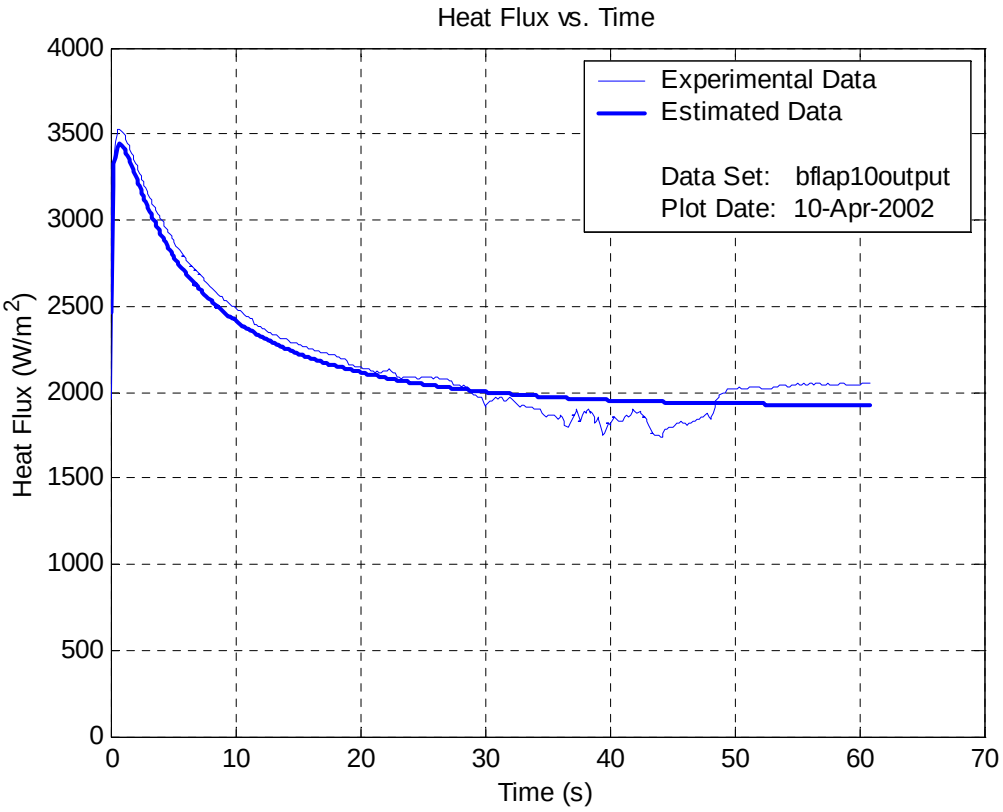
Heat Flux vs. Time
Experimental Data
Estimated Data
Data Set: bflap10output
Plot Date: 10-Apr-2002
Heat Flux (W/m2)
Time (s)
0
500
1000
1500
2000
2500
3000
3500
4000
0
10
20
30
40
50
60
70

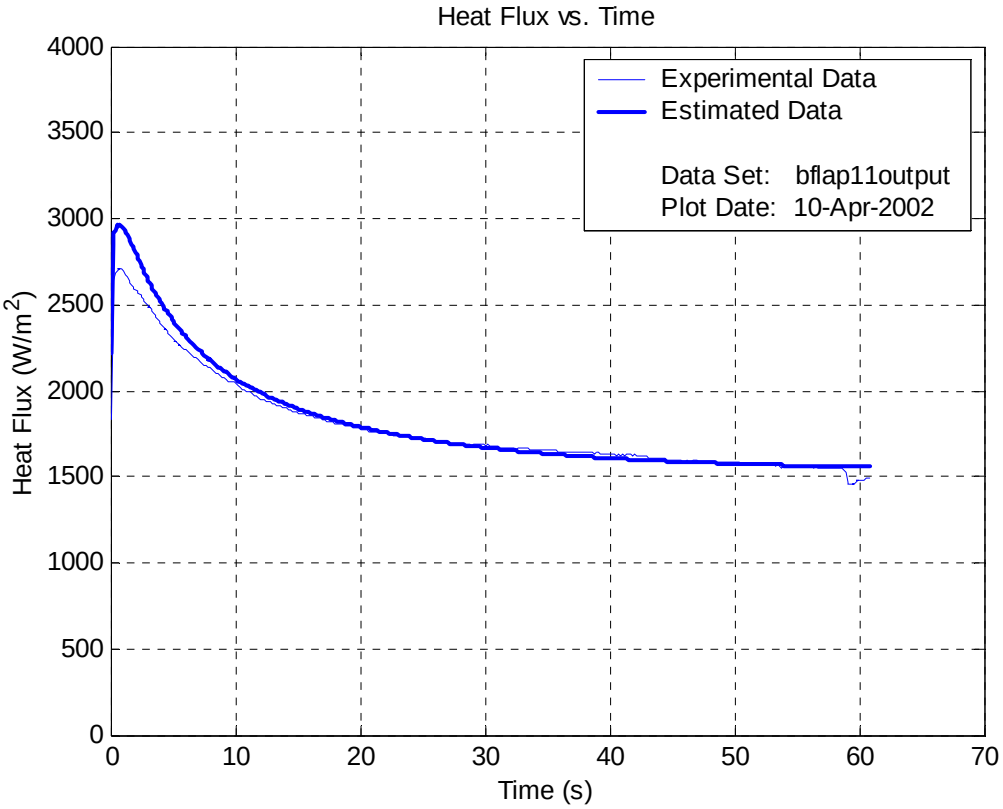
Heat Flux vs. Time
Experimental Data
Estimated Data
Data Set: bflap11output
Plot Date: 10-Apr-2002
Heat Flux (W/m2)
Time (s)
0
500
1000
1500
2000
2500
3000
3500
4000
0
10
20
30
40
50
60
70

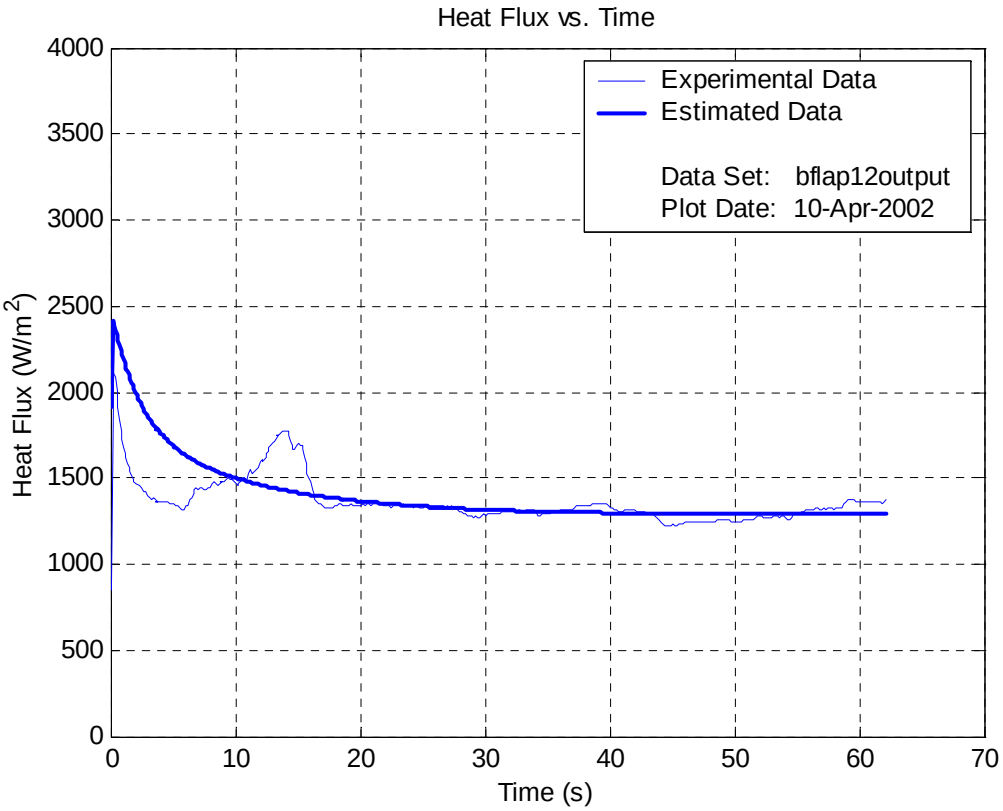
Heat Flux vs. Time
Experimental Data
Estimated Data
Data Set: bflap12output
Plot Date: 10-Apr-2002
Heat Flux (W/m2)
Time (s)
0
500
1000
1500
2000
2500
3000
3500
4000
0
10
20
30
40
50
60
70

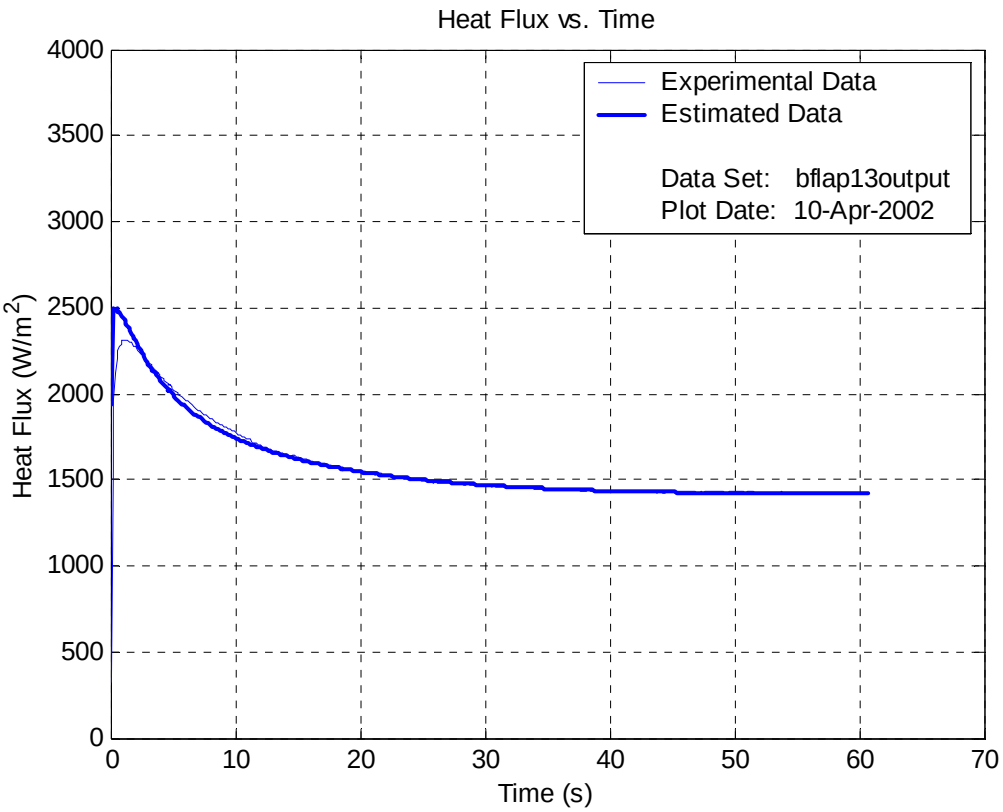
Heat Flux vs. Time
Experimental Data
Estimated Data
Data Set: bflap13output
Plot Date: 10-Apr-2002
Heat Flux (W/m2)
Time (s)
0
500
1000
1500
2000
2500
3000
3500
4000
0
10
20
30
40
50
60
70

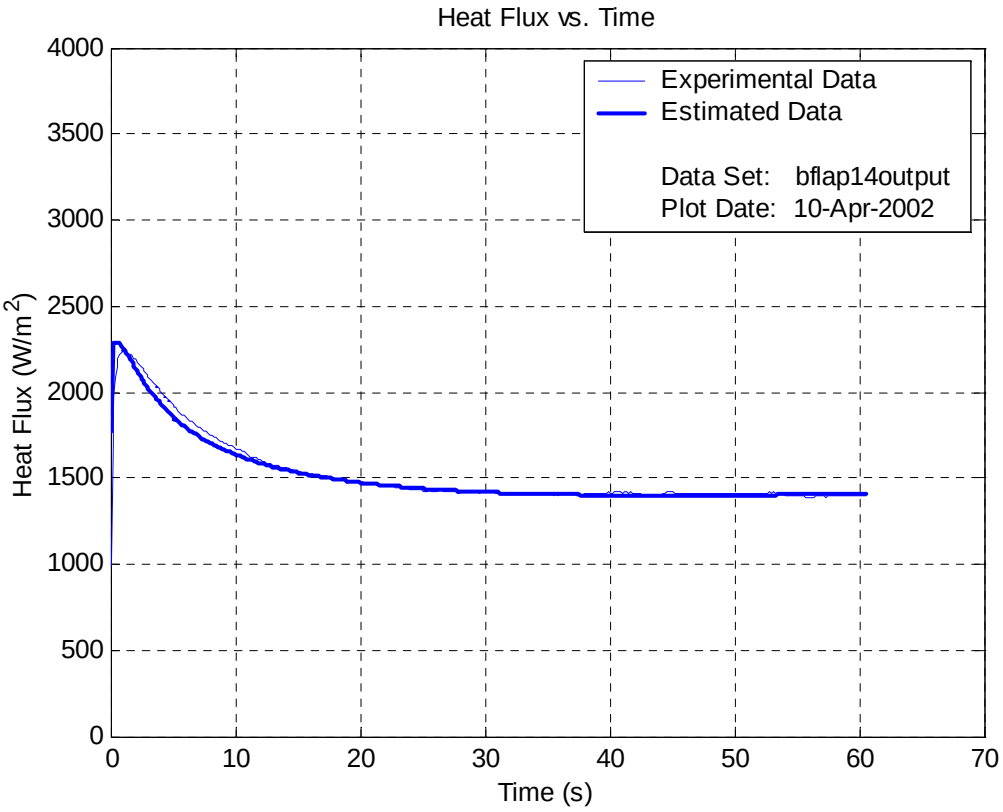
Heat Flux vs. Time
Experimental Data
Estimated Data
Data Set: bflap14output
Plot Date: 10-Apr-2002
Heat Flux (W/m2)
Time (s)
0
500
1000
1500
2000
2500
3000
3500
4000
0
10
20
30
40
50
60
70

Appendix C Procedures and Notes

C.1 Using the Parameter Estimation Code

General Use

The first part of the program asks the user to make a selection from the following choices:

1) ACCESS THE BIOMODEL
2) RUN THE PARAMETER ESTIMATION ROUTINE
3) MAP AN SSY FIELD

After this first selection, the program asks the user to input the names of an input file and two output files. The output files contain different data depending on which of the three routines is selected. The data in each of the output files is summarized in the table below.

Initial Selection	Output in File 1	Output in File 2
1	Full Heat Flux vs. Time data	No output
2	Estimation summary showing parameter guesses for each iteration	Full Heat Flux vs. Time data
3	File containing SSY map	No output

Each of the output files contains a header that summarizes the input information and shows which variables are being included in the file.

The program automatically creates a file called Debug that contains output from checkpoints throughout the program. This is a leftover from times of heavy program manipulation that may be of benefit to future users.

Variations on the Estimation Program

Currently, there are three different parameter estimation programs available to researchers that perform slightly different functions:

- **Parameter_Estimation.exe:** This is the standard parameter estimation program requiring the normal inputs for operation.
- **Airflow_Parameter_Estmation.exe:** This estimation program varies the convection coefficient on the top of the probe with time at the beginning of the data set. This is meant to approximate the increase in pressure that occurs when using the building air supply in Randolph Hall.
- **Low_Time_Step_Parameter_Estimation.exe:** This estimation program uses a much smaller time step (<1/400 s) to solve the biomodel so that stable a stable solution to the thru-probe heat flux is found. It is really only good for accessing the biomodel since the current bioprobe set up does not take data at that small of time intervals.

Each of these variations has its own FORTRAN file (.f) and Microsoft Developer Project Workspace file (.mdp), so any changes made to the biomodel should be made to all three programs. It would be possible, and very beneficial, to combine all three variations into the same program. It would require the addition of several more variables and inputs to take into account changes in airflow and time step size, but it could be easily done.

Input File Location

The input file being used with the parameter estimation routine should be located in the same folder as the executable file. Typically, this is the **Debug** folder associated with the Microsoft Developer Project Workspace file.

C.2 Input Files

Biomodel/Parameter Estimation Routine Input File Format

Below is a standard input file for the biomodel and parameter estimation code. First is a listing of the variables that are included in the input file as they appear in the biomodel/parameter estimation code. Then there is an example of the input file format using the variable names and one showing real data.

A standard input file contains two distinct areas: a header section and an experimental data section. The header section of the file contains information that controls aspects of the biomodel as well as some of the experimental conditions. The experimental data section contains the information recorded during an experiment.

To access the biomodel by itself, all that is needed is the header section of the input file. To run the parameter estimation routine, a full data file complete with the experimental data is required. An input file can be automatically created from a Test Point output file using the Matlab routine datasort.m.

Input Variables	
Variable	**Description**
N	number of data points in the experimental data
NP	number of parameters to be estimated
NI	number of independent variables
NEDGE	number of nodes in the r-direction in the probe
NNODES	total number of nodes in the r-direction
LEDGE	number of nodes in the z-direction in the probe
LNODES	total number of nodes in the z-direction
B(1)	blood perfusion guess
B(2)	contact resistance guess
airtemp	air temperature
artetemp	arterial temperature
skintemp	starting skin temperature
COUNTER	counter variable
Y	experimental heat flux array
VAR	variance of the experimental heat flux data set
T	experimentally recorded time

Symbolic File				Numeric File			
N NP NI				669 2 1			
NEDGE LEDGE NNODES LNODES				10 10 20 150			
B(1) B(2)				0.001 0.001			
airtemp artetemp skintemp				24.9 36.20 33.10			
COUNTER(1)	Y(1)	VAR(1)	T(1)	1	771.0537	181598.9234	0.1053
COUNTER(2)	Y(2)	VAR(2)	T(2)	2	1685.7457	181598.9234	0.2105
COUNTER(3)	Y(3)	VAR(3)	T(3)	3	2118.6051	181598.9234	0.3158
COUNTER(1)	Y(4)	VAR(4)	T(4)	4	2328.7156	181598.9234	0.4211
.	.	.	.	.	.	.	.
.	.	.	.	.	.	.	.
.	.	.	.	.	.	.	.
COUNTER(N)	Y(N)	VAR(N)	T(N)	669	1028.4360	181598.9234	70.4211